

## ABSTRACT

Title of Thesis: USING A HIGH RESOLUTION,  
MECHANISTIC MODEL OF FILTRATION,  
BIODEPOSITION, HYDRODYNAMICS, AND  
SEDIMENT BIODGEOCHEMISTRY IN  
ORDER TO UNDERSTAND THE DRIVING  
FORCES BEHIND NITROGEN DYNAMICS ON  
OYSTER REEFS

Kevin Kahover, Master of Science, 2022

Thesis Directed By: Professors Lora Harris, Jeremy Testa  
Marine-Estuarine-Environmental Sciences

The overarching goal of this work was to develop a modeling tool that can provide quantitative predictions of ecosystem services related to N removal and biomass production using oyster restoration metrics such as reef size and oyster planting densities. I expanded the predictive capability of an existing advection-diffusion model of particle capture on an oyster reef to incorporate oyster biodeposit production, transport, and relationship to nutrient cycling. The resulting oyster reef filtration, biodeposition, and ecosystem services model (ReeFBioDES) utilizes modeled or measured current velocities, temperature, salinity, and chlorophyll-a in a

given reef environment (reef length, oyster size and density) to predict spatial patterns of biodeposition production, transport, and denitrification. I applied the model at Little Neck Reef in Harris Creek (Choptank River) over an annual cycle for a range of oyster densities and found the model reproduced both the spatial dynamics of along-reef water-column concentrations of TSS, as well as generating rates of on-reef denitrification that are comparable to recently measured rates in experimental incubations of intact oyster clumps from Harris Creek. The model is now available for scenarios simulations to quantify ecosystem services associated with ongoing and future oyster restoration sites in Chesapeake Bay and other temperate coastal ecosystems that *C. virginica* occupies.

USING A HIGH RESOLUTION, MECHANISTIC MODEL OF FILTRATION,  
BIODEPOSITION, HYDRODYNAMICS, AND SEDIMENT BIOGEOCHEMISTRY IN  
ORDER TO UNDERSTAND THE DRIVING FORCES BEHIND NITROGEN DYNAMICS  
ON OYSTER REEFS

By

Kevin Kahover

Thesis submitted to the Faculty of the Graduate School of the  
University of Maryland, College Park, in partial fulfillment  
of the requirements for the degree of  
Master of Science  
2022

Advisory Committee:

Dr. Lora Harris, Co-Chair

Dr. Jeremy Testa, Co-Chair

Dr. Lawrence Sanford

© Copyright by

Kevin Kahover

2022

## Acknowledgements

I would like to thank the members of my thesis committee: Dr. Lora Harris, Dr. Jeremy Testa, and Dr. Larry Sanford for their endless patience and continual encouragement.

Additionally, I would like to thank Dr. Elizabeth North for providing the ROMS output for the model, as well as the field team from NOAA's Chesapeake Bay Office for providing exceptional support and allowing me to gather preliminary validation data.

Finally, I would like to thank everyone else who supported me during my time as a graduate student, especially Dr. Suzan Shahrestani, Dr. Katie Martin, Jessica Wingfield, Erin Crandall, Maggie, Zeke, and of course, Gail and Jim.

## Table of Contents

Acknowledgements .....	ii
List of Tables .....	iv
List of Figures .....	v
Introduction .....	1
Methods.....	12
1a. Overview: Major components .....	7
1b. Overview: Spatial Domain....	8
1c. Hydrodynamic Framework....	9
2. Oyster filtration and Biodeposition....	11
2a. Biodeposit Suspension.....	14
2b. Biodeposit Transport.....	18
2c. Model Validation Data.....	21
2d. Model Simulations.....	21
Results and Discussion.....	22
Model comparisons with field data.....	23
Initial model simulations.....	23
Impact of oyster density, reef length, and shell length on chlorophyll-a removal.....	24
Impact of current velocity and oyster density on biodeposit resuspension.....	25
Simulated nitrogen biogeochemistry.....	26
Conclusions and Future Improvements .....	28
Tables.....	31
Figures.....	35
Appendix A.....	51
References .....	97

## List of Tables

Table 1. A list of the primary variables used in each of the major model components. References are provided in the right-hand column for variables that are calculated using a method that was developed in a previous study.

Table 2: Scenarios of oyster reef length, oyster height, and oyster density.

Table 3: Nitrogen fluxes ( $\mu\text{mol m}^{-2} \text{h}^{-1}$ ) estimated for intact oyster communities in estuarine environments, including estimated oyster density (individuals per square meter). Estimates derived from this study are included from Figure 15.

## List of Figures

Figure 1. Conceptual Model of Nitrogen-Oyster Reef Dynamics Model, including the vertical grid for the advection-diffusion model. Model outputs include oyster biodeposition production rate (mass per time), deposition of biodeposits to sediments ( $\text{mg m}^{-2} \text{ d}^{-1}$ ), and rates of sediment-water fluxes of ammonium, oxygen, and nitrate and denitrification rates ( $\text{mg m}^{-2} \text{ d}^{-1}$ ) in both reef and sediment.

Figure 2. Box and arrow schematic diagram of the spatial domain and flows of material (chlorophyll-a, TSS) between the advection-diffusion model, the biodeposit transport model, and the sediment flux model.

Figure 3. (top panel) relationship of oyster density ( $\text{oysters m}^{-2}$ ) to roughness density (red lines) and % loss in shelter area (blue lines) over different oyster heights (in cm). (bottom panel) threshold oyster densities associated with a roughness density  $< 0.1$  and the onset of skimming flow as a function of oyster height (in cm).

Figure 4. Schematic describing design of user interface and connection to Chop-ROMS. Current velocities (in  $\text{cm/s}$ ), water temperature, and salinity are extracted from Chop-ROMS and assigned to the boundary of the chosen reef along with ambient chlorophyll-a concentrations, which then fuel an oyster filtration and biodeposit production model that then produces biodeposits that are processed in the sediment flux model.

Figure 5. (left) Map of substrate in Harris Creek, including subtidal sediment composition (sand, mud) and oyster reef, and (right) grid domain of the Chop-ROMS hydrodynamic model used for boundary conditions (green area indicates water cells).

Figure 6. Boundary conditions used as forcing functions for model simulations over the May-October period in 2010, including (top) salinity (blue lines) and water temperature (red lines) and (bottom panel) boundary chlorophyll-a concentrations measured via an in-situ sensor in Harris Creek by the Maryland Department of Natural Resources ([www.eyeonthebay.net](http://www.eyeonthebay.net)).



Figure 7. Montage of forcing functions and model dynamics in the oyster biodeposit transport model over a three week period in April on Little Neck Reef. (Left panels from top to bottom): Ambient, boundary conditions for chlorophyll-a, water velocity, and water temperature, (Right panels from top to bottom): Distribution of predicted chlorophyll-a over in the water column (top) and concentration of biodeposits in the reef subdomain (bottom). These two panels provide a snapshot of concentration at a single time step (April 15, 2010 1:00 AM). This figure shows how a boundary layer of water column Chl concentrations are easily during during periods of low velocities (such as those at slack tide). This is due to the fact that the extended residence time of water passing over the reef allows for a higher degree of chlorophyll uptake through oyster filtration. In fact, without significant horizontal advection, Chl removal at the upstream end of the reef is significant enough to prevent any biodeposit production in the downstream portions of the reef (i.e. TSS concentrations are below the minimum threshold for biodeposition).

Figure 8. Initial 3-day simulation output documenting changes in primary production, PAR, current velocity, chlorophyll-a and algal biomass in units of carbon.

Figure 9. Histograms representing the frequency at which different fractions of water-column chlorophyll-a were removed by model simulations at four oyster reefs with varying length, oyster density, oyster age, and location in Harris Creek. Reef A: (38.77309 N, -76.2823 W), <50 oysters m<sup>-2</sup>, 2.70 acres, Reef B: (38.76781 N, -76.2969 W), 150 oysters m<sup>-2</sup>, 20.24 acres, Reef C: (38.74 N, -76.31 W), <50 oysters m<sup>-2</sup>, 4.52 acres, Reef D: (38.71719 N, -76.3052 W), 50 oysters m<sup>-2</sup>, 70.50 acres.

Figure 10. Time-series of different fractions of water-column chlorophyll-a removal by model simulations at idealized oyster reefs with oyster density (top panel), reef length (middle panel), and oyster size (bottom panel).

Figure 11. Frequency of biodeposit suspension at varying current velocities at three representative oyster densities (25, 100, 300 oysters/m<sup>2</sup>).

Figure 12: Representative distribution of chlorophyll-a along Little Neck Reef in 2010, where blue colors indicate low chlorophyll-a (in bottom water at end of reef downstream of flow direction) and high chlorophyll-a in the near-surface waters.

Figure 13. (left panel) Little neck oyster reef. Circles indicate the five sampling locations, which are located along a transect that is oriented 47° from true north. (right panel) Optical backscatter (uncalibrated NTU) from transects taken on Little Neck Reef at maximum flood (top) and maximum ebb (bottom). OBS is a measure of particle concentration in the water so dark blue represents high particle concentrations.

Figure 14: Snapshot of 3-day simulation of nitrogen dynamics on Little Neck Reef, including (clockwise from the top left) sediment particulate carbon concentrations, rates of particulate N deposition to sediments, sediment-water rates of ammonia flux and denitrification under three scenarios of oyster densities (5, 50, and 100 oysters  $\text{m}^{-2}$ ).

Figure 15. Modeled sediment-water fluxes of ammonium (top), nitrate (middle), and dinitrogen gas (bottom) in Little Neck Reef under conditions of no oysters (0 oysters per  $\text{m}^{-2}$ ) versus 100 oysters per  $\text{m}^{-2}$ . The magnitude of all fluxes is greatly enhanced when oysters are present, especially for ammonium and denitrification.

## Introduction

The eastern oyster, *Crassostrea virginica*, is a reef-building bivalve that can be found throughout the coastal and estuarine waters of the eastern United States, as well as the Gulf of Mexico (Kennedy et al. 1996). As autogenic ecosystem engineers (Gutierrez et al 2003), eastern oysters create complex environments inhabited by fish, crustaceans, polychaetes, and other invertebrates (Rodney and Paynter 2006). A combination of overharvesting, habitat degradation, and disease has significantly reduced oyster stocks around the world (Roschild et al 1994, Beck et al 2011). In the Chesapeake Bay, oyster populations have declined to less than 1% of their estimated pre-industrial levels (Newell 1988, Wilberg et al 2011). This dramatic degeneration of a once-abundant fishery resource has also resulted in the subsequent loss of many of the ecosystem services that oyster reefs once provided (Coen et al 2007).

One of the ecological functions most commonly associated with oyster reefs is the removal of phytoplankton and suspended sediments through oyster filtration. An individual eastern oyster weighing 1 g DW can filter an average of 8.4-9.6 L of water per hour (Jordan 1987, Newell and Koch 2004). Almost all particles between 3-100  $\mu\text{m}$  are captured during filtration (Haven and Morales-Alamo 1970). Because they are able to efficiently capture particles from such a relatively large volume of water, oysters have the potential to control phytoplankton biomass as well as reduce suspended sediment concentrations.

Filtration occurs continuously; the constant pumping of lateral cilia creates feeding currents that deliver phytoplankton and other seston to the oyster's gills (Riisgard 1988, Newell and Kennedy 1996). The laterofrontal cirri on the surface of the gills filter out particles from the passing water, while frontal cirri transport the filtered material to labial palps, where additional sorting occurs (Silvester and Sleight 1984, Ward et al 1994). Material is either guided towards the

mouth for ingestion or incorporated into mucus and sent to the mantle margin. Larger particles that have settled out of the inhalant current naturally (Bernard 1974), as well as material rejected from the marginal food groove of the gill, are combined with the material exported from the labial palps to form mucus-coated aggregates called ‘pseudofeces’. The feces and the pseudofeces (collectively referred to as ‘biodeposits’), are exported out of the mantle either through ciliary action or forceful ejection (i.e. “shell-snapping”) (Newell and Kennedy 1996).

Rates of biodeposit production for *C. virginica* are highly variable (Jordan 1987). Results from early lab experiments on oysters from the Chesapeake Bay indicated an average production rate of 0.23 g d<sup>-1</sup> per individual oyster, with a maximum of 0.56 g d<sup>-1</sup> (Haven and Morales-Alamo 1966). Higgins et al (2013) measured a rate of 3.8– 15.9 ( $\pm$  1.1) g DW m<sup>-2</sup> d<sup>-2</sup> for aquaculture trays in St. Jerome Creek containing 286 oyster m<sup>-2</sup>, while Jordan (1987) reported a range of 1– 280 mg DW of biodeposits per g DW of oyster under normal conditions for the Choptank River. Variation in rates of biodeposition is primarily caused by changes in pseudofecal production, since the amount of pseudofeces produced by an oyster has been shown to scale proportionally to the concentration of the surrounding seston (Loosanoff and Engle 1947, Tenore and Dunstan 1973). Fecal production, on the other hand, is largely independent of seston concentration, although it can exhibit some seasonal variation (Haven and Morales-Alamo 1966).

Because bivalve biodeposits are mucus-bound aggregates, their sinking velocities are quite high (Kautsky and Evans 1987, Widdows et al 1998). Due to these high sinking rates, sedimentation from biodeposition can occur seven times faster than the ambient sedimentation of the surrounding seston (Giles and Pilditch 2004, Widdows et al 1998, Dame 1999). Oyster communities therefore have the capacity to significantly enhance organic matter deposition to the benthos (Hoellein and Zarnoch 2014, Holyoke 2008, Giles and Pilditch 2006). Biodeposition

from *C. virginica*, for example, was estimated to increase the sedimentation of organic matter in the lower Choptank River by 110% (Jordan 1987).

The nutritive quality of biodeposits generally depends on the nutritive quality of the seston, as well as the size of the phytoplankton being consumed, since small phytoplankton tend to have thicker, less digestible cell walls and lower proportions of esculent intracellular material (Hoellein et al 2015). Due to the preferential ingestion of nutritious particles, biodeposits have a much lower concentration of nutrients and organic matter when compared to the overlying seston (Jordan 1987, Deslous-Pauli et al 1992). Still, oysters are relatively inefficient at absorbing the particulate organic matter (PON) they capture during filtration, so the biodeposits they produce nonetheless contain a significant amount of labile nitrogen (Newell and Jordan 1983). Over time, the accelerated delivery of PON as a result of biodeposition can enhance the nutritive quality of the underlying sediments (Kaspar et al 1985, Deslous-Pauli 1992, Higgins et al 2013).

The overall effect of this nutritive enrichment is controlled by microbial processes in the underlying sediment. After being incorporated into the sediment, PON from biodeposits are used as substrate in a microbial-mediated oxidation reaction known as diagenesis.  $\text{NH}_4$ , which is a byproduct of this reaction, may be subject to further aerobic oxidation to produce  $\text{NO}_2^-$  and  $\text{NO}_3^-$  (Henriksen and Kemp 1988). The  $\text{NO}_2^-$  and  $\text{NO}_3^-$  that diffuses into the underlying anaerobic sediments can then undergo microbially mediated metabolic processes that result in the production of  $\text{N}_2$  gas, also known as denitrification. The resulting  $\text{N}_2$  gas, absent fixation, will rise through the water column and exit into the atmosphere, resulting in a net loss of N from the aquatic ecosystem (Seitzinger 1988).

The degree to which biodeposition alone actually alters sediment biogeochemistry is unclear, and tends to be location-specific (Carmichael et al 2012, Newell 2004). Studies

performed on oyster reefs *in situ* (Hoellein et al 2015), as well as in a laboratory setting (Newell et al 2002), have provided evidence linking *C. virginica* biodeposition to enhanced rates of  $N_2$  production. Conversely, Higgins et al (2013) found no pervasive indication that the forced addition of aquaculture-derived biodeposits to sediment cores significantly affected rates of either denitrification or annamox (the direct reduction of  $NH_4$  to  $N_2$  gas). Although several studies have shown that biodeposition increases the amount of  $NH_4$  released into the water column (Holyoke 2008, Higgins et al 2013, Giles and Pilditch 2006, Newell et al 2005, Jordan 1987, Jansen et al 2012), Hoellein and Zarnoch (2014) found no discernable effect of oyster biodeposition to N transformations of any kind. Overall, it appears that sediments respond to biodeposits differently based on the quality and quantity of the biodeposits being produced (Holyoke 2008).

The fate of the particulate nitrogen being deposited on an oyster reef, whether through biodeposition or other forms of sedimentation, is primarily influenced by three environmental factors: the amount of organic matter being produced, bottom-water oxygen concentrations, and the relative apposition of oxic and anoxic sediment zones. High loads of organic matter stimulate microbial respiration, causing  $O_2$  concentrations in the sediment to drop and the rate of ammonia production to increase (Tenore et al 1982). Because nitrifying bacteria use  $O_2$  as an electron acceptor, the aerobic conditions of the sediment pore water partially determine the extent to which the ammonia produced in the surface sediments undergoes nitrification. Since nitrate must first diffuse into anaerobic sediments before use by denitrifying bacteria, a close pairing of oxic and anoxic sediment zones is needed in order for the generation of  $N_2$  gas to occur (Kristensen 1988). On oyster reefs, a close proximity between nitrifying and denitrifying bacteria has been

used to explain the low efflux of  $\text{NO}_3$  and high rate of denitrification simultaneously observed over reef sediments (Newell et al 2002).

Although organic matter deposition is an important part of *C. virginica*'s overall influence on the surrounding ecosystem, there are other processes through which a reef can affect nutrient dynamics. Top-down control on phytoplankton biomass through oyster filtration, for example, may facilitate nitrogen removal, since water-column  $\text{NO}_3$ , which would have otherwise been used to fuel phytoplankton growth, can instead diffuse into the sediments and be delivered to nitrogen-reducing bacteria (Newell et al 2002). The unique structural complexity of reef sediments has also been thought to enable accelerated rates of nitrogen removal (Hoellein et al 2015). Biodeposit production increases the deposition of fine-grained ( $1\text{--}3\ \mu\text{m}$ ) sediments (Damas 1935, Haven and Morales-Alamo 1966), which are favored by bioturbating organisms. Since bioturbation increases the surface area-to-volume ratio of the sediment, more space (habitat) is made available for oxic and suboxic processes, such as nitrification and denitrification, to occur (Welsh and Castadelli 2004). The increased spatial complexity of the sediment also accelerates the transport of oxygen, as well as other oxidants and reductants, to porewater microbes (Kristensen 1988, Owens 2009). It is therefore unsurprising that fine-grained, bioturbator-rich sediments have been shown to produce elevated rates of coupled nitrification-denitrification (Sundback et al 2002).

The physical presence of the oysters themselves may also facilitate the removal of nitrogen. Welsh and Castadelli (2004) discovered a significant and direct association between potential nitrification rates (PNR's) and the surface of benthic invertebrates, including the bivalve filter-feeders *Mytilus galloprovincialis* and *Tapes philippinarum*. Since their experiments were performed on a taxonomically and functionally diverse group of benthic invertebrates, the

authors suggest that the colonization of invertebrate surfaces by nitrifying bacteria may be a widespread phenomenon. Oysters, which themselves greatly increase the surface area and rugosity of a seabed, also provide habitat for a wide range of macrofaunal and epiphytic organisms (Rodney and Paynter 2006, Kellogg et al 2013); therefore, it is possible that an oyster reef and its corresponding menagerie of inhabitants may offer ample space for nitrifier colonization.

Although several mechanisms have been proposed to explain how oyster reefs could help facilitate coupled nitrification-denitrification, a clear consensus regarding the extent to which oysters actually remove nitrogen from an ecosystem has not been reached. Since dissolved constituents of N are both simultaneously consumed and released by oyster reefs (Dame et al 1989), under certain conditions, oysters may simply recycle the standing stock of N in an ecosystem (Newell et al 2005). There is also ample evidence that the combined effects of faunal excretion and microbial-driven ammonification can release of large amounts of dissolve nitrogen to the water column (Dame et al 1984, Asmus and Asmus 1991, Dame et al 1992, Dame and Libes 1993, Nelson et al 2004, Kellogg et al. 2013, Peterson et al 2014). For example, Dame et al (1989) found that 66% of the total nitrogen taken up by an intertidal oyster reef was regenerated in the form of  $\text{NH}_4$ , resulting in a net annual release of  $125 \text{ g N m}^{-2} \text{ yr}^{-1}$ .

Perhaps the most direct evidence of enhanced denitrification related to the presence *C. virginica* was found by Kellogg et al (2013), who performed incubations of sediment trays equilibrated *in situ* on a restored oyster reef located in a Chesapeake Bay tributary. The values of denitrification they observed, which ranged seasonally from  $0.3 - 1.6 \text{ mmol N}_2\text{-N m}^{-2} \text{ h}^{-1}$ , were exceptionally high, given that denitrification rates for Chesapeake Bay soft sediments have rarely been recorded above  $0.18 \text{ mmol N}_2\text{-N m}^{-2} \text{ h}^{-1}$  (Kemp et al 2005). Newell et al (2002) found that



additions of simulated biodeposits (algal pellets) to reef sediments under aerobic conditions promoted net nitrogen removal and resulted in the nitrification of ~20% of the total N added.

This study focused on developing conceptual and numerical models of a restored oyster reef with the capacity to combine both coupled physical-biological processes (filtration and impact on particle availability) with formulations to describe the production of biodeposits and interaction of these biodeposits with the overlying water column and physical conditions. Finally, an existing diagenetic model of sediment microbial processes describing nitrogen cycling was coupled to these formulations in order to evaluate a conceptual model describing oyster reef nitrogen dynamics. This thesis is focused on describing the model and model formulations and providing preliminary simulations that explore model function and aspects of nitrogen cycling.

## **Methods**

The main objective of this study was to develop a mechanistic approach to modeling nitrogen dynamics on an oyster reef. To accomplish this, I constructed a time-iterative model that includes fundamental reef processes such as oyster filtration, biodeposition, hydrodynamic transport, and sediment biogeochemistry to characterize the exchange of organic nitrogen across the phytoplankton-oyster-microbial food web. The model was designed to operate at high spatial and temporal resolution; the forcing functions of the model were updated at hourly time steps, and numerous spatial partitions were used to discretize the model domain.

### **1a. Overview: Major components**

The model rests on a two-dimensional, discretized advection diffusion scheme, which was used to simulate the transport of chlorophyll and biodeposits over an oyster reef. The basic

2-D hydrodynamic formulations were coupled to an oyster filtration model in order to account for the impact of oyster feeding on the resulting particle distribution (Forsyth 2014). The filtration rate formulation (Ehrich and Harris 2015) models the removal of particles from the water column as a function of salinity, temperature, and the concentration of total suspended solids. I advanced the model of Forsyth (2014) by including mechanistic details related to nitrogen cycling that focused on the production and fate of biodeposits on the reef, as well as explicitly modeling biogeochemical processes in the underlying sediments.

By concentrating organic matter through the process of bio-filtration, the oysters then pass that organic material on to the crevices and three-dimensional spaces that make up an oyster reef. The oysters themselves also disrupt flow, which leads to shear stress that acts to affect biodeposit availability through potential resuspension. A detailed biodeposition transport model incorporated oyster morphology with hydrodynamic functions to simulate sinking and suspension of biodeposits across the model domain. These processes were first described in detailed conceptual models (Figure 1-2), and then numerical integrated into the model workflow. The resulting accumulations of biodeposits provided substrate for the sediment biogeochemical model, which was used to address the central research questions of this project regarding the impact on nitrogen by oyster reefs. A full list of model parameters is provided in Table 1, and the complete model Matlab code is included in Appendix A.

### **1b. Overview: Spatial Domain**

The spatial domain of the model represents a two-dimensional cross-section of subtidal oyster reef and the water-column it inhabits. The horizontal dimension ( $x$ ) of the domain extends across the entire length of the reef, while the vertical dimension of the domain ( $z$ ) extends from the surface of the water column down to a depth of 10 cm below the sediment-water interface

(Figure 2). For simplicity, the governing equations of the model were restricted to describing mass/momentum transfer in the  $x$ - and  $z$ -dimensions; transport across the minor axis ( $y$ ) of the reef was not considered. For model calculations involving variables with a transverse length component, a nominal reef width of 1m was assumed.

The model domain was composed of three contiguous subdomains: the water column, the reef, and the underlying sediments. In order to simulate reef process in a spatially-explicit manner, each of these subdomains were partitioned into grids. The dimensions of the two-dimensional water column grids were largely determined by the stability constraints of the governing transport equations being applied to them. For example, for simulation scenarios designed to describe the Little Neck reef (300 m reef, 6 m deep), the water-column advection-diffusion domain included ~0.5 m vertical grid resolution, while the sediment biogeochemical model included mm to cm vertical resolution. Details of each model subdomain are described below.

### 1c. Hydrodynamic Framework

The equations that were used to model transport of suspended matter in the water column were derived from the standard conservation and continuity laws governing the motion of viscous fluids. It is important to note, however, that several simplifying assumptions regarding the nature of the flow were made. For example, the Navier-Stokes equation of fluid motion states that for incompressible flows (where  $\nabla \cdot \mathbf{u} = 0$ ):

$$\rho \frac{D\mathbf{u}}{Dt} = -\nabla P + \rho \hat{\mathbf{F}} + 2\mu \nabla^2 \mathbf{u}$$

Here,  $\mathbf{u}$  is the velocity vector,  $\rho$  is density,  $P$  is pressure,  $\mu$  is the dynamic viscosity, and  $\hat{\mathbf{F}}$  is the sum of the external body forces acting on the liquid. The final term,  $\mu \nabla^2 \mathbf{u}$ , denotes the viscous

stress acting on the fluid (Kundu and Cohen 2002, Chanson 2004). For two-dimensional flow along the  $xz$  axis, Eqn. 1a becomes:

$$\rho \left( \frac{\partial u}{\partial t} + u \frac{\partial u}{\partial x} + w \frac{\partial u}{\partial z} \right) = -\hat{F}_x \frac{\partial z}{\partial x} - \frac{\partial P}{\partial x} + \mu \left( \frac{\partial^2 u}{\partial x^2} + \frac{\partial^2 u}{\partial z^2} \right)$$

where  $u$  and  $w$  are the  $x$  and  $z$  components of  $\mathbf{u}$ .

To avoid the effects of reef-scale pressure gradients, topographic structures such as reef crests and mounds, though typical of some mature reefs, were ignored. The reef was therefore treated as a flat bed. Changes in elevation due to bed slope were also ignored, as were changes in water depth due to the presence of surface gravity waves. These conditions, along with the assumption of a homogenous density in the water column, allow us to drop the gravity term  $\hat{F}_x$ .

Velocity profiles for a given hourly time step were derived by treating the flow within that hour as both fully developed ( $\partial u / \partial x = 0$ ) and steady-state ( $\partial u / \partial t = 0$ ). The diffusive terms of the momentum equation also needed to be modified in order to account for the shear stress caused by the presence of the oysters. Under conditions of rough, turbulent flow ( $Re_\tau > 55$ ), viscous forces are negligible outside of the thin viscous sublayer. In the larger, logarithmic portion of the boundary layer, turbulent forces dominate. The apparent shear stress caused by turbulence can be described as a function of the shear strain ( $du/dz$ ) and the eddy viscosity  $\nu_e$ :

$$\bar{\tau} = -\nu_e \frac{du}{dz}$$

By applying Prandtl's mixing length method,  $\nu_e$  can be approximated as:

$$\nu_e = \kappa u_* z$$

where  $\kappa$  is the Von Karman constant ( $\kappa=0.4$ ),  $u_*$  is the friction velocity, and  $z$  is the height above the bed. The vertical velocity profile can be achieved by equating the turbulent stress to the shear stress at the bed surface, then taking the integral:

$$\rho u_*^2 = \rho \kappa u_* z \frac{du}{dz}$$

$$\int \frac{du}{dz} = \int \frac{u_*}{\kappa z}$$

$$\frac{u}{u_*} = \frac{1}{\kappa} \ln(z) + c$$

For fully rough flows, the constant of integration is absorbed into the roughness height  $z_o$ , giving the standard equation:

$$\frac{u_z}{u_*} = \frac{1}{\kappa} \ln \left[ \frac{z}{z_o} \right]$$

The governing mass transfer equation used to model the movement of Chlorophyll-a and suspended biodeposits across the reef domain, was derived in a similar fashion to the momentum equation, except that turbulent flux was described using the turbulent diffusivity constant  $K_z$ :

$$\frac{\partial \text{Chl}}{\partial t} + u \frac{\partial \text{Chl}}{\partial x} + w \frac{\partial \text{Chl}}{\partial z} = \frac{\partial}{\partial z} \left( K_z \frac{\partial \text{Chl}}{\partial z} \right)$$

For depth-limited flows,  $K_z$  is given as:

$$K_z = \kappa u_* z \left( 1 - \frac{z}{h} \right)$$

## 2. Oyster filtration and Biodeposition

The amount of phytoplankton removed from the water column was estimated using the oyster filtration model presented in Forsyth (2014) and Ehrich and Harris (2015). Filtration was modeled as an allometric function of oyster weight. In order to capture the oyster's physiological responses to different environmental conditions, a series of environmental limitation factors were also included in the equation. These factors, which are normalized to produce fractions between

0 and 1, were multiplied by the weight-based filtration formulation to produce the following equation for filtration rate  $FR_i$  ( $\text{m}^3 \text{ oyster}^{-1} \text{ day}^{-1}$ ):

$$FR_{(x)} = 0.17 \times W^{0.75} \times f(T) \times f(S) \times f(TSS)$$

Here,  $W$  is the dry weight of the oyster (normalized by 1g DW), and 0.17 is a constant representing the maximum filtration rate. The remaining terms ( $f(T)$ ,  $f(S)$ , and  $f(TSS)$ ) are the limitation factors relating to temperature ( $T$ ), salinity ( $S$ ), and the concentration of total suspended solids ( $TSS$ ), respectively (Forsyth 2014, Ehrich and Harris 2015).

$$f(T) = e^{(-0.006(T-27)^2)}$$

$$f(S) = \begin{cases} 0 & S < 5 \\ 0.0926 \cdot S - 0.139 & 5 \leq S \leq 12 \\ 1 & S > 12 \end{cases}$$

$$f(TSS) = \begin{cases} 0.1 & TSS < 4 \text{ mg L}^{-1} \\ 1 & 4 \leq TSS \leq 25 \text{ mg L}^{-1} \\ 10.364 \cdot \ln(TSS)^{-2.0477} & TSS > 25 \text{ mg L}^{-1} \end{cases}$$

The distribution of chlorophyll (Chl-a) over the reef was modeled using a variation version of the advection-diffusion equation (see Forsyth 2014, Fr  chette et al 1989, Butman et al 1994),

$$u \frac{\partial Chl}{\partial x} = \frac{\partial}{\partial z} \left( K_z \frac{\partial Chl}{\partial z} \right) + R$$

where  $C$  is the chlorophyll concentration and  $R$  is the removal of chlorophyll due to oyster filtration. Current velocity at height  $z$  ( $u_z$ ) is controlled by boundary layer parameters as stated in Forsyth (2014).  $R$  is best given as:

$$R = -Chl_{x,1} \left( \frac{FR_x}{\partial z} \right)$$

where  $\partial z$  is the difference in height between the depth nodes of the water column subdomain. By solving the spatially discretized advection diffusion equation across the water column subdomain, the model was able to produce a two dimensional profile of Chl-a concentrations along the primary reef axis.

Biodeposition  $\left(\frac{\text{mg}}{\text{gDW}_{\text{oyster}} \cdot \text{h}}\right)$  was modeled as a function of temperature ( $T$ ) and TSS, using a relationship developed by Jordan (1987):

$$\log_{10}(B) = -0.7459 + (0.1478 \cdot T) + (-4.21 \times 10^{-3} \cdot T^2) + (2.55 \times 10^{-4} \cdot T^2 \cdot \text{TSS}) + (-5.21 \times 10^{-6} \cdot T^2 \cdot \text{TSS}^2)$$

The values of TSS that were used in this formulation were determined by multiplying the near-bottom chlorophyll concentrations of the previous time step by a Chla:TSS conversion factor of  $1.9 \times 10^6 \text{ mg TSS mg}^{-1} \text{ Chl cm}^{-3}$  (based on observations made at Harris Creek). This approach to estimate biodeposit production effectively disconnects the filtration formulations from the biodeposition rate. In effect, it assumes that biodeposition is a function of the overlying water chlorophyll-a, but that there is no mass balance constraint on the weight of biodeposits produced. Future modeling efforts using bioenergetics formulations for oyster growth will allow a relaxation of these assumptions. The total amount of biodeposits produced over the course of an hour was found by multiplying the biodeposition rate  $B$  ( $\text{mg gDW}_{\text{oyster}} \text{ h}^{-1}$ ) by the specified population density of the reef (oysters  $\text{m}^{-2}$ ) and the average oyster dry weight ( $g$ ). Since oyster filtration can result in a downstream depletion in seston concentration, it was important to model biodeposition in a spatially-explicit manner. In order to do so, a separate one dimensional layer (the reef subdomain) was used to track the decay and accumulation of across the reef.

## 2a. Biodeposit Suspension

An exponential decay function was used to simulate the transformation of biodeposits within the reef subdomain from ribbon-like to a simple particle form. The coefficients of this function were chosen so that the majority of the biodeposit mass would be lost over the course of three days, which is the general amount of time it takes for biodeposits to completely lose their ribbon-like structure (L. Sanford personal communication). The ‘decayed’ portion of the biodeposit mass served as a source of PON/POC for the sediment flux model, while the remaining mass in the reef subdomain remained available for potential suspension.

When calculating whether biodeposit suspension/transport would occur, it was important to account for the hydrodynamic consequences of small-scale reef topography. For example, as water flows around an oyster shell, an adverse pressure gradient forms between the upstream and downstream faces of the oyster. This imbalance, known as form drag, can cause the flow to separate, resulting in an increased level of turbulence just downstream of the oyster. The increased turbulence reduces the shear stress (skin friction drag) acting on the biodeposits that have accumulated behind the oyster, thereby reducing the chance that these biodeposits will undergo saltation or resuspension. It is therefore the unique shielding effect of neighboring oysters that ultimately controls the suspension of the biodeposits that have settled in the interstitial spaces of the reef. I completed a comprehensive evaluation of different formulations to represent oyster reefs as a form of drag, and a description and comparative analysis of these methods is included in Appendix B, which can be accessed here:

<https://drive.google.com/drive/folders/1xtZHjUQiDu4GOQ2SjyiLIan7SeJIY8bR?usp=sharing>.

The final formulations I chose are described below.



Since skin drag is the mechanism responsible for the suspension of biodeposits, the model must first calculate the shear stress attributed to skin friction by partitioning total stress contributing components. To accomplish this, I chose to adopt the stress partitioning method outlined in Shao and Yang 2005, where total drag force ( $\tau_{total}$ ) is partitioned into three components: form drag ( $\tau_f$ ), skin drag on the underlying surface ( $\tau_g$ ), and the skin drag acting on the roughness elements ( $\tau_{re}$ ):

$$\tau_{total} = \tau_f + \tau_g + \tau_{re}$$

The Shao and Yang method is a modified version of the partitioning scheme presented in Raupach 1992, which was developed using existing atmospheric field data, as well as ~~and~~ wind-tunnel experiments performed on sparse roughness arrays<sup>[LH1]</sup>. The Raupach model is based on the concepts of effective shelter area ( $A$ ), which is used to parametrize the reduction in shear stress that occurs within the turbulent wake of an isolated roughness element, as well as the effective shelter volume ( $V$ ), which is used to describe effect that a roughness element has upon the drag forces of its neighboring elements. The effective shelter area is defined as

$$A = c \frac{\Lambda A_{ref}}{N} \frac{\bar{U}}{u_*}$$

Here,  $N$  is the number of roughness elements,  $A_{ref}$  is the reference unit of ground area,  $\bar{U}$  is the depth averaged velocity,  $u_*$  is the friction velocity, and  $c$  is a constant of integration ( $\sim 0.37$ ). The roughness density ( $\Lambda$ ) is given as:

$$\Lambda = \frac{N A_f}{A_{ref}}$$

where  $A_f$  is the projected surface area of an individual roughness element normal to the flow.

After incorporating  $A$  and  $V$  into calculations of  $\tau_f$  and  $\tau_g$ , Raupach 1992 arrived at the following partitioning function:

$$\frac{\tau_s}{\tau_{total}} = \frac{1}{1 + \beta\Lambda}$$

where  $\beta$  is a dimensionless ratio defined as:

$$\beta = \frac{C_R}{C_G}$$

In the current model,  $C_g$  is treated as the drag coefficient related to the surface of the interstitial reef sediments, and  $C_r$  is the drag coefficient of a single roughness element (an oyster) in unobstructed flow.

This partitioning scheme is only valid for values of  $\Lambda < 0.1$ . As outlined in Figure 3, this condition is only met for assemblages of oysters that are either very small or have very low densities. To apply the principles of this method to roughness arrays with values of  $\Lambda > 0.1$ , Shao and Yang 2005 introduced an additional shape parameter: the skin area index ( $\varphi$ ),

$$\varphi = \frac{NA_s}{A_{ref}}$$

where  $A_s$  is the projected area of the oysters transverse to flow. The two shape parameters ( $\Lambda, \varphi$ ) can be combined to produce an ‘effective’ frontal area index  $\Lambda_e$  (i.e. the percentage of the total frontal area that actually generates sheltering):

$$\Lambda_e = \frac{\Lambda}{(1 - \varphi)^n} \exp\left[-\frac{a\Lambda}{(1 - \varphi)^n}\right]$$

Here, and  $a$  and  $n$  are constants. Using the default values from Shao and Yang 2005,  $a$  and  $n$  were assigned values of 6 and 0.1, respectively.

Using  $\Lambda_e$  and  $\sigma$ , the modified stress partitioning equation becomes:

$$\frac{\tau_s}{\tau_{total}} = \left(1 - \frac{\beta\Lambda_e}{1 + \beta\Lambda_e}\right) \exp(-b_s\varphi)$$

where  $b_s$  is an empirically-derived constant. Following Shao and Yang 2005,  $b_s$  was assigned a value of 5.

The total shear stress ( $\tau_{total}$ ) acting on the reef at any given time step was calculated as

$$\tau_{total} = \rho u_*^2,$$

where

$$u_* = U \left[ \frac{1}{\kappa} \ln \left( \frac{z_{ref}}{z_0} \right) \right]^{-1}.$$

$U$  is the depth-integrated velocity, and  $z_{ref}$  is the reference height (0.3 m). For model runs involving small sized oysters and/or oyster densities ( $A \leq 0.25$ ), the roughness equation suggested in Theurer 1973 was used:

$$\frac{z_0}{\eta} = 1.6A(1 - 1.67\varphi).$$

where  $\eta$  is the maximum height of an oyster shell. It is important to note the variable  $\eta$  is different than the oyster shell length  $h$ ; since the oysters on subtidal reefs often have some degree of vertical orientation (see Grinnell 1974),  $\eta = h$  only when the oysters are perfectly upright (i.e. the elevation angle ( $\theta$ ) is  $90^\circ$ ). Therefore,  $\eta$  is a function of both  $h$  and  $\theta$ . For this study, an arbitrary  $\theta$  of  $45^\circ$  was used, resulting in a value of  $\eta$  that is roughly equal to  $h[\sin(45^\circ)]$  (For further detail on how the oyster shape parameters were calculated in the model, see Appendix B).

For model runs involving moderate-large sized oysters and/or oyster densities ( $A > 0.25$ ), the approach of Styles (2015) is used, where the turbulent boundary layer over an oyster reef is parameterized using a simple function of the average oyster height. For reefs that lack columnar morphology, like those being modeled in this study, Styles (2015) gives:

$$z_0 = \frac{c \eta}{30}$$

Where  $c$  is constant between 3.5-7. Although this equation was derived from data collected over beds of oysters with a primarily prostrate orientation, a median value of  $c$  gives estimates of  $z_0$  that agree reasonably well with roughness heights derived from reefs with more vertical orientations (Reidenbach 2013); therefore, a value of  $c = 5$  was used.

In order to calculate  $\beta$ ,  $C_R$  was assumed to have a value of 0.3. This is a reasonable approximation, given its similarity to drag coefficients values reported for isolated hemispheres and bivalves of similar shape (Denny 1988). The sediment drag coefficient  $C_G$  was found by calculating the friction velocities that would occur from unobstructed flow over the underlying reef bed:

$$C_G = \frac{u_{*grain}^2}{U^2}$$

In this model, the non-erodible portion bed sediments were assumed to be composed of decayed biodeposits. Therefore, a sediment roughness height of  $z_{o(sed)} = 0.002$  was used to calculate the necessary friction velocities. This value of  $z_o$  is within the typical range reported on mud flats, whose sediments share the general smooth, cohesive, and mucous qualities of deteriorated biodeposits accumulations.

Suspension occurred whenever the shear stress acting on the biodeposits ( $\tau_s$ ) was greater than or equal to a critical value of  $\tau_{crit} = 0.05$  Pa. This value for  $\tau_{crit}$  was chosen based on the biodeposit erosion experiments of Holyoke (2008).

## **2b. Biodeposit Transport**

When hydrodynamic conditions favored suspension ( $\tau_s \geq \tau_{crit}$ ), newly created biodeposits were not delivered directly to the reef subdomain, but were instead subjected to

advective transport both across and off the reef. This was achieved by employing time-domain version of the discretized advection diffusion equation:

$$\frac{\partial C}{\partial t} + u \frac{\partial C}{\partial x} = \frac{\partial}{\partial z} \left( K_z \frac{\partial C}{\partial z} \right) + w_s \frac{\partial C}{\partial z}$$

Expanding the vertical diffusivity term:

$$\frac{\partial C}{\partial t} + u \frac{\partial C}{\partial x} = K_z \frac{\partial^2 C}{\partial z^2} + \frac{\partial K_z}{\partial z} \frac{\partial C}{\partial z} + w_s \frac{\partial C}{\partial z}$$

Here,  $\partial C / \partial t$  is the change in biodeposit concentration ( $\text{mg m}^{-2}$ ) over time,  $u(\partial C / \partial x)$  and  $w_s(\partial C / \partial z)$  are the horizontal and vertical advection terms, respectively. The vertical components of the transport equations were solved implicitly, while the horizontal advection terms were solved explicitly. Vertical diffusivity was assumed to be negligible.

A central finite differencing scheme was used to solve the transport equation between two time steps ( $n$ ):

$$\begin{aligned} \frac{C_{x,z}^{n+1} - C_{x,z}^n}{\Delta t} = & \frac{K_z}{\Delta z^2} [C_{x,z+1}^{n+1} - 2C_{x,z}^{n+1} - C_{x,z-1}^{n+1}] \\ & + \frac{\Delta K_z}{\Delta z^2} [(1 - \gamma)C_{x,z}^{n+1} + \gamma C_{x,z+1}^{n+1} - (1 - \gamma)C_{x,z-1}^{n+1} - \gamma C_{x,z}^{n+1}] \\ & + \frac{w_s}{\Delta z} [(1 - \gamma)C_{x,z}^{n+1} + \gamma C_{x,z+1}^{n+1} - (1 - \gamma)C_{x,z-1}^{n+1} - \gamma C_{x,z}^{n+1}] \\ & - \frac{u}{\Delta x} [(1 - \phi)C_{x,z}^n + \phi C_{x+1,z}^n - (1 - \phi)C_{x-1,z}^n - \phi C_{x,z}^n] \end{aligned}$$

where:  $\gamma = \begin{cases} 0 & \text{if } w_s + \frac{\partial K_z}{\partial z} < 0 \\ 1 & \text{if } w_s + \frac{\partial K_z}{\partial z} \geq 0 \end{cases}$        $\phi = \begin{cases} 0 & \text{if } u > 0 \\ 1 & \text{if } u < 0 \end{cases}$

Here,  $w_s$  is the fall velocity of the biodeposits, which was calculated as a function of their equivalent spherical diameter ( $ESD$ ). The relationship between shell length  $h$ ,  $ESD$ , and  $w_s$  was derived from data collected at an oyster aquaculture site (L. Sanford, unpublished):

$$ESD (\mu\text{m}) = 266.7h - 117.74$$

$$w_s(\text{m s}^{-1}) = 0.0334 \cdot ESD^{0.8153} \cdot 1e^{-3}$$

To solve the  $C^{n+1}$  implicitly, the discretized transport equation can be rearranged as:

$$aC_{x,z+1}^{n+1} + bC_{x,z}^{n+1} + cC_{x,z-1}^{n+1} = r$$

where  $a, b, c$  are coefficients containing the advection and diffusivity terms while  $r$  corresponds to the terms on right hand side of the equation. The resulting system of linear equations was used to construct a tridiagonal matrix, which could be solved after solving  $r$  using known values of  $C^n$ .

Boundary conditions are as follows:

$$\text{Reef/bottom: } f_i = r - c(C_i^n + \text{input}_{\text{biodeposits}})$$

$$\text{Surface: } f_i = r - a(0)$$

The transport model operated on one second internal time steps. The advection-diffusion grid that was used to spatially partition the water column had a cell dimensions of ( $dx = 30 \text{ cm}$ )  $\times$  ( $dz = 6.7$ ). These values were chosen to satisfy stability constraints imposed by the fall velocity  $w_s$ . Biodeposits were considered ‘settled’ when they reached the bottom of the reef domain. The nitrogen component of the biodeposits, which was determined to be an average of 4.8 mg N per g biodeposits for oyster in the Choptank River, MD (Jordan 1987), was served as PON input into the sediment flux model, which was also spatially explicit.

It is important to note that only a portion of the total biodeposit mass in the sublayer is delivered to SFM—this is the amount calculated from the biodeposit exponential decay function. This function was based on observations made during his study at the Merinetics oyster farm (L. Sanford unpublished data), which showed that biodeposits completely lose their ribbon-like structure within 3 days. For the purposes of this study, the physical degradation of the biodeposits is assumed to be caused by microbial-driven diagenesis, so that the loss of biodeposit mass in the reef sublayer directly coincides with its delivery as a source of PON into SFM . I

therefore chose decay rate constant of  $\zeta = -0.064$ , which ensured that the majority of the biodeposit mass would be removed from the reef sublayer over the course of 3 days.

## **2c. Model Validation Data**<sup>[LH2]</sup>

During the summer of 2017 extensive sampling of variables relevant for the model occurred at Little Neck Reef, a restored oyster reef in Harris Creek, MD. The goal of this field effort was to obtain data to validate the oyster filtration model. Little Neck Oyster Reef was selected as our study site due to its ideal location in Harris Creek, the predominance of along-axis flow, and its relatively high oyster density. Oyster plantings have occurred on this site since 2012, making this high-density reef an ideal reference for the model. In collaboration with the field operations team at NOAA's Chesapeake Bay Office and the R/V Potawaugh, sampling of the oyster reef occurred continuously over the course of 12 hours. This sampling scheme enabled us to observe changes in the vertical distribution of phytoplankton (chlorophyll-a) and seston (TSS) for the duration of a complete tidal cycle. Five sampling stations were distributed equidistant along the major axis of the reef. At each station, a profile of the water column was taken with a CTD equipped with a laser in-situ scanning transmissometer (LISST) and an optical backscattering sensor (OBS). At three of the five stations, water samples were taken at four discrete depths. These samples were filtered and later analyzed for TSS, TSV, and Chl-a concentrations. An Acoustic Doppler Profiler (ADP) was also deployed on the reef to gather information on the current velocities and tidal height.

## **2d. Model Simulations**

A key goal for this model was to move towards a modeling framework that is accessible to others. In this implementation that included procuring forcing functions describing the hydrodynamic, bathymetric, temperature, and salinity for reefs located in Harris Creek, located

in the Choptank River, a tributary of Chesapeake Bay, MD where oyster restoration efforts have been ongoing. A programming framework was created for end users to enter latitude and longitude coordinates for the reef of interest and query available Chop-ROMS data to provide forcing functions for model runs as pictured in Figures 4-5. Additional forcing functions describing substrate and chlorophyll-a, salinity, and temperature (Figure 6) were also drawn from regionally available databases for the Choptank Tributary ([www.eyesonthebay.net](http://www.eyesonthebay.net)).

After thorough exploration and debugging of the model code, a series of model simulations were performed. Initially, short 3-5 day synoptic simulations and longer fortnightly simulations (Figure 7, 8) were carried out to determine basic characteristics and performance of the model during spring and summer conditions. These simulations allowed for visualization of chlorophyll and biodeposit distributions for a given set of forcing conditions (Figure 7). Following this effort, longer simulations were performed exploring various configurations of oyster densities, height, and reef lengths as described in Table 2.

## **Results and Discussion**

A significant product from this work is the model code itself, which is included as Appendix A and available in this google drive repository:

<https://drive.google.com/drive/folders/1xtZHjUQiDu4GOQ2SjyiLIan7SeJIY8bR?usp=sharing>

Coding used a modular approach in Matlab and includes annotation and plotting routines. Table 1 provides a detailed list of model parameters and variables described for each model module. The remainder of the results are focused on describing simulated output, evaluating the biodeposition model, examining N dynamics, and comparing simulated dynamics with a limited



available validation dataset. A comprehensive literature review of oyster feeding, ecosystem effects, hydrodynamic impacts, and effects on nutrient cycling are included in Appendix C.

### **Model comparisons with field data**

Before reporting critical output describing biodeposit transport and nitrogen cycling that were the primary goal of this modeling exercise, it is important to evaluate how well the model matches field data. Field measurements on the restored Little Neck Reef would suggest a clear signature of oyster filtration (i.e., depressed particle distributions) at the maximum flood and ebb tides (Figure 13), and provide a snapshot of how water clarity may be enhanced by filtering bivalves. At both stages of the tidal cycle, both suspended solids and particle volume concentrations decreased over the reef in the direction of the tide, suggesting that particles were gradually depleted from the water-column as water passed over the reef. Snapshots of model-simulated chlorophyll-a distributions qualitatively reflect this same pattern over space (Figure 12). Prior investigations reported that mean uptake rates of POC on flood tides (e.g.,  $1.87 \text{ g C m}^{-2} \text{ h}^{-1}$ ) were considerably higher than the filtration rate of  $0.34 \text{ g C m}^{-2} \text{ h}^{-2}$  they indirectly estimated from literature values for an annual temperature of  $20^{\circ}\text{C}$  (Dame and Patten 1981). This observation suggests that some other processes, such as physical sedimentation, may be important on the reef. Although we did not quantify the individual contributions of filtration and roughness-induced physical biodeposition at this time, future simulations can quantify these effects.

### **Initial model simulations**

Model runs clearly demonstrate that all components of the coupled model provide a mechanistically-based, coupled modeling tool that represents realistic conditions around oyster reefs in Chesapeake Bay. The model Matlab interface (Figure 7) illustrates the forcing condition of the model (chlorophyll-a, temperature, current velocity) over a snapshot fortnightly period, and includes chlorophyll-a removal rates over the reef and associated spatial patterns of biodeposit accumulation. Figure 8 shows simulation output from a 3-day model run documenting available light (PAR), current velocities, and the chlorophyll-a concentrations at the most southern end of Little Neck Reef in Harris Creek. The fully coupled model clearly documents the removal of chlorophyll over Little Neck Reef, with minimum concentrations occurring at the far end of the reef with respect to water movement (Figure 12). These patterns align with field data documenting particle distributions through the water column (Figure 13). Associated with this chlorophyll-a removal is an accumulation of biodeposits along the reef, with highest biodeposit thickness occurring on the near end of the reef (Figure 7). Thus, as chlorophyll-a is filtered from the water within the first 100-150 meters of reef, high biodeposit accumulations occur in parallel. The magnitude of chlorophyll-a removal by the reef generally varies between 0 and 50%, with the majority of time during April to October simulating 0-20% chlorophyll-a removal (Figure 10). Although these removal fractions are not very large, they do represent non-trivial chlorophyll-a filtering by the reef and enough carbon and nitrogen mass to reveal substantial biodeposit production. The roughly 100 hours when >50% of chlorophyll-a was removed would represent a substantial loss term for ambient phytoplankton material.

### **Impact of oyster density, reef length, and shell length on chlorophyll-a removal**

Model simulations representing the range of scenarios/conditions described in Table 2 were successful in demonstrating the impact of individual oyster and oyster reef characteristics on

chlorophyll-a removal (Figure 9,10). In the first example (Figure 9), the frequency of various fractions of chlorophyll-a removal rates are displayed at individual reefs in Harris Creek with varying size and oyster density. These simulations revealed a skewing of the histogram to the right for the two largest reefs (panel B and D; Figure 9), where more model timesteps induce removal rates that exceeded 20%. In contrast, the two smallest reefs (panels A and C in Figure 9) show that the majority of timesteps include removal rates of less than 10%. In the second example exploring these relationships (Figure 10), chlorophyll removal rates of varying reef characteristics are documented, which clearly show that larger oyster densities, longer reef lengths, and larger individual oysters induce higher removal rates (Figure 10). These impacts are especially apparent in the summer months, with impacts of shell length exhibiting nonlinear responses (diminishing removal impact with larger oysters; e.g. from 8 cm to 10 cm) as predicted by the allometric formulation used to model filtration rates. These results are similar to those reported by Forsyth (2014). The critical result from the new model formulations described here are to understand how these processes translate to biodeposition and how the biodeposit module serves as a transition point for organic material from the water column to reef and sediment scale biogeochemistry.

### **Impact of current velocity and oyster density on biodeposit resuspension**

For open sediment beds lacking large immobile bed roughness, the initiation of sediment transport is directly related to the shear stresses that are exerted on the sediment bed by wave energy or horizontal advection. In contrast, three-dimensional benthic structure of oyster reefs, with its substantial roughness, also promotes greater turbulence, thus putting more of the water column in contact with the reef. One consequence of this dynamic is that in systems with tidally driven currents, depletion of seston above beds of benthic suspension feeders has been

demonstrated both in the field (Frechette et al 1989, Muschenheim and Newell 1992) and in flume studies (Butman et al 1994, O’Riordan et al 1995). Figure 11 examines the role of current velocity and interactions with oyster density on the potential for deposition and resuspension.

Because of the model formulation focuses on critical thresholds around shear stress, this modeling framework is needed to understand when suspension of the biodeposits might happen.

Model simulations show that a smaller fraction of time-steps include resuspension at higher oyster densities (Fig. 13). The change in suspension timesteps is most substantial between 250 and 400 oysters/m<sup>2</sup> (Figure 13), indicating a potential non-linear effect oyster density on resuspension. This pattern illustrates how higher oyster densities effectively shield the biodeposits, preventing resuspension, while lower density conditions result in more frequent suspension events. Wright et al. (1990) showed some of the earliest quantitative evidence of greater friction induced by oysters, reporting that friction for oyster shells was nearly 3 times that reported for sand beds. By extension, I conclude that the enhanced friction provided by oyster reefs decreased the resuspension potential of biodeposits.

### **Simulated nitrogen biogeochemistry**

Due to the tight coupling between benthic and pelagic systems in nearshore ecosystems, oyster-reef associated sediment fluxes (resulting from biodeposition) can have significant impacts on the nutrient dynamics of the whole ecosystem and affect primary production (Tenore et al 1982, Porter et al 2004). When populations of suspension-feeding bivalves are dense, particulate matter is deposited at rates several times what would be suspected by natural seston settling (Lund 1957a, Haven and Morales-Alamo 1966a). Indeed, simulated oyster reef biodeposition in the model resulted in substantially elevated nitrogen deposition rates to sediments (Figure 14). Consequently, clear patterns emerged from the deposition of these

biodeposits and the subsequent processing of nitrogen on the reef. When compared to baseline simulations without oysters, the production of ammonium changed from nearly zero to in excess of  $25 \text{ mmol N m}^{-2} \text{ d}^{-1}$ , which is on the same order of magnitude of ammonium fluxes from mid-Bay anoxic sediments (Fig. 15). Although nitrate fluxes were not altered by the presence of oysters and associated biodeposit production, denitrification rates in the  $100 \text{ oysters m}^{-2}$  simulations indicated rates three times background levels (Fig. 15). This pattern is consistent with elevated denitrification rates observed in intact oyster reefs (Kellogg et al. 2013, Humphries et al. 2016, Jackson et al. 2020), although the magnitude predicted in the model is somewhat lower than observed (Table 3).

Interestingly, the rate of increase of ammonium was not overcome by denitrification fluxes, indicating that in a mass balance context oysters produce a net release of nitrogen from biodeposits back to the water column. This is ~~an~~ important because it has been suggested that nutrient regeneration from bivalve biodeposits may counterbalance the removal of phytoplankton biomass by stimulating new phytoplankton blooms (Doering et al 1986, Asumus and Asmus 1991). Kellogg et al. (2013) reported high rates of ammonium release associated with oyster reefs, consistent with the fact that oyster excretion and microbial biodeposit remineralization will both lead to high rates of ammonification. Several other studies have shown that the organic N that is deposited by bivalves in aquaculture situations is remineralized and leads to increases in ammonium in the water column, changing the N from non-reactive to reactive forms (Porter et al. 2004, Gibbs et al. 2005, Dame 2012). Therefore, it is clear that enhanced organic matter delivery to the sediments through biodeposition stimulates  $\text{NH}_4$  production, yet the degree at which this enhanced ammonification either hinders or facilitates further N transformations is likely dependent on structure/community of the reef as a whole. For example, numerous studies

have demonstrated that the presence of burrow-forming, benthic macrofauna stimulates rates of nitrification and/or coupled nitrification/denitrification (Piehler and Smyth 20115, Carmichael et al 2012). The structure complexity of oysters reefs and shell surface also provide microhabitats and anoxic microsites, which have the ability to allow for further N transformation (Jenkins and Kemp 1984, Guitierrez et al 2003, Brandes and Devol 1995, Kellog et al 2013) Thus, although all nutrient cycling processes are expected to be enhanced on an oyster reef, the relative changes in the net nitrogen removal as a function basic reef properties such as of oyster height and density need to be further studied.

These nitrogen removal rates are relevant when placed in the context of empirical observations. Cornwell et al. (2020), extrapolated N removal rates estimated to be 57 lbs. N acre<sup>-1</sup> y<sup>-1</sup> for low oyster biomass (< 75 g DW m<sup>-2</sup>), which translates to an estimated annual N removal of ~20,000 lbs. of N in the 350 acres of restoration in Harris Creek. The simulations reported here estimated N removal of 160 lbs. N acre<sup>-1</sup> yr<sup>-1</sup> for oyster densities of 100 m<sup>-2</sup>. In both cases, nitrogen removal rates were higher for oyster reef communities relative to adjacent sediments unoccupied by oyster reefs. These findings are consistent with the fact that denitrification rates on oyster reefs are expected to be highest for reefs in oxic, relatively aphotic waters (like deeper regions of Harris Creek) where denitrifying bacteria don't need to compete with benthic algae for nitrogen and where reduced oxygen levels do not inhibit coupled nitrification-denitrification (e.g., Kemp et al. 1990). As such, other investigators in mid-Atlantic region and the northeast coast of the United States have reported similarly high rates of denitrification in intact oyster communities (Table 3).

## **Conclusions and Future Improvements**

In conclusion, it is clear that biodeposit production and remineralization within oyster reefs leads to enhanced nitrogen cycling (both removal and recycling processes), and the model developed in this proposal represents those effects. The model is thus ready to be applied to simulate a range of oyster reef sizes and densities at restoration sites within Harris Creek and other Chesapeake Bay restoration sites. In order for this model to be used more widely in the community there are a few remaining steps to be completed. For example, a future research question will focus on understanding whether the combined action of reducing phytoplankton concentrations via oyster filtration with the recycling capacity of the reef ultimately results in a whole ecosystem enhancement of nitrogen use efficiency or whether overall productivity is reduced.

There are also numerous details of oyster reef biodeposit dynamics and associated nitrogen cycling effects that could be better addressed in future studies. ~~Although the potential number of these questions is larger,~~ I will summarize a few key processes here that I recommend as starting points. First, predicting times or sites where denitrification is driven by the C and N species originating from oyster biodeposits remains a challenge under eutrophic conditions. While the model presented in this Thesis and several prior studies have estimated N cycling rates on local reef communities (Kellogg et al. 2013, Humphries et al. 2016), the potential for reef-derived particulates to be exported off the reef to support denitrification is poorly understood, and more spatially-expansive models are required to address this. Indeed, Coen and Luckenbach (2000) argued that system level effects of oyster filtration have been poorly quantified, especially as they might relate to any specific restoration project, and this challenge remains. Secondly, the fate of biodeposits between the time when they are produced and when they are delivered to a location where denitrification can occur is poorly understood. In this thesis, I used an idealized

exponential decay function to characterize biodeposit breakdown prior to deposition, but few studies defining mineralization rates for biodeposits exist. Prior studies, such as for mussel biodeposits, identified that temporal or spatial variability is unknown (Giles and Pilditch 2006; Carlsson et al 2010) and no studies have defined the specific effects of temperature of biodeposit composition on biodeposit mineralization rates. Third, the model I developed does not include dynamic estimates of oyster growth, thus there is a basic lack of mechanistic coupling (both conceptually and quantitatively) between filtration, oyster metabolism, and biodeposit production. Future work could consider mortality rates because as oysters die, their tissues decompose and release N and P sequestered in their soft tissues back into the water column and/or substrate, or how dynamic changes in oyster size and associated feeding and roughness effects would influence the conclusions described here. Finally, it is well established that various environmental factors affect the feeding behavior of suspension-feeding bivalves in general (e.g., temperature, salinity, food availability/quality) and given that the natural environment is typically much more variable than is practical to simulate in the laboratory settings where model formulations derive from (Judge et al 1993), a better accounting for filtration effects associated with new types of environmental data (real-time algal identification, particle size estimates) will improve oyster filtration and growth models.



Table 1. A list of the primary variables used in each of the major model components. References are provided in the right-hand column for variables that are calculated using a method that was developed in a previous study (Additional variables that appear in this table are defined in Appendix A).

Symbol	Description	Units	References
<b><i>Oyster and Reef Parameters</i></b>			
$g$	weight of an individual oyster	g	
$h$	oyster length	cm	
$L$	reef length	m	
$N$	oyster density	oyster m <sup>-2</sup>	
$W$	reef width	m	
$\eta$	vertical height of oyster	cm	
$\lambda$	average distance between oysters	cm	
$\theta$	vertical orientation of oysters on the reef (0-90°)	---	
$s$	streamwise length of oyster	cm	
$b$	spanwise length of oyster (transverse to flow)	cm	
$\phi$	Wooding's shape parameter	----	
$Ar_{bio}$	frontal area of oyster	cm <sup>2</sup>	
$A_f$	projected surface area normal to flow	cm <sup>2</sup>	
$A_s$	windward wetted surface area	cm <sup>2</sup>	
$S_{ref}$	area of smooth surface (w/o roughness)	cm <sup>2</sup>	
$\lambda$	roughness concentration	---	
$\lambda_e$	effective roughness concentration	---	
$SA_{bio}$	total surface are of roughness element	cm <sup>2</sup>	

### Environmental Variables

$d$	depth of water column	m	
$S$	hourly-averaged salinity	ppt	
$T$	hourly-averaged temperature	°C	
$\bar{U}$	hourly-averaged, depth-integrated velocity	m s <sup>-1</sup>	
$U_z$	hourly-averaged, depth-specific velocity	m s <sup>-1</sup>	
$\rho$	water density	kg m <sup>-3</sup>	Millero and Poisson 1981
$\mu$	dynamic viscosity	kg m <sup>-1</sup> s <sup>-1</sup>	Sharqawy et al 2010
$\nu$	kinematic viscosity ( $\mu/\rho$ )	m <sup>2</sup> s <sup>-1</sup>	

### Biodeposition Production

$S$	hourly-averaged salinity	ppt	
$T$	hourly-averaged temperature	°C	
$BD_{prod}$	biodeposition rate	mg g <sup>-1</sup> DW <sub>oyster</sub> h <sup>-1</sup>	Jordan 1987
$fTSS$	filtration rate modifier as a function of seston concentration		Fulford et al 2007
$w_2$	sedimentation velocity	cm d <sup>-1</sup>	DiToro 2001
$PON_i$	concentration of PON in reactivity class $i$	mmol N m <sup>-2</sup>	DiToro 2001
$kPON_i$	first-order reaction rate coefficient	d <sup>-1</sup>	DiToro 2001
$H_2$	depth of the anaerobic layer	cm	DiToro 2001
$\theta_{PONi}$	temperature coefficient for diagenesis	---	DiToro 2001
$J_{PON}$	depositional flux of PON from the overlying water column to the sediment	g N m <sup>-2</sup> d <sup>-1</sup>	DiToro 2001
$fPON$	fraction of $J_{PON}$ in the $i^{th}$ reactivity class	---	DiToro 2001

### Biodeposition Transport

$a_1$	empirical constnat	----	
$BD_{x,m}$	mass of biodeposits in deposition sub-grid	mg	
$BD_{x,r}$	biodeposition rate	mg g <sup>-1</sup> DW <sub>oyster</sub> <sup>-1</sup> h <sup>-1</sup>	Jordan 1987
$B$	intercept of log-wall equation for a smooth wall	---	
$C$	constant of integration for fully rough flows (determined empirically) (=8.5)	----	
$C_D$	drag coefficient		
$D_{50}$	median grain size of biodeposits	m	
$d_h$	distance of the zero velocity plane from the top of the roughness elements	m	
$ESD$	equivalent spherical diameter of the biodeposits	m	
$g$	acceleration due to gravity	m s <sup>-2</sup>	
$k$	apparent hydraulic roughness	m	
$k_s$	equivalent sand grain roughness (of biogenic roughness)	m	
$k_{grain}$	equivalent sand grain roughness (of biodeposits)		
$Re$	Reynolds number		
$Re_*$	Reynold's roughness (due to sandgrain roughness/skin friction)		
$Re_\tau$	Reynold's roughness (due to roughness element)		
$Re_\tau (smooth/rough)$			

$u$	threshold Reynold's roughness for smooth or/fully rough flows	$\text{m s}^{-1}$	
$u_{* \text{ grain/form}}$	velocity at reference height $z$ above bottom friction velocity due to skin friction ( $u_{* \text{ grain}}$ ) or form drag ( $u_{* \text{ total}}$ )	$\text{m s}^{-1}$	
$u_{* \text{ total}}$	total friction velocity (form and skin)	$\text{m s}^{-1}$	
$w_s$	fall velocity of biodeposits	$\text{m s}^{-1}$	
$Y$	Bronlie's explanatory variable for Shield's curve	---	
$X$	distance from leading edge of reef	$\text{m}$	
$Z_{\text{ref}}$	reference height	$\text{m}$	
$z_o$	roughness height of oyster	$\text{m}$	Frechette 1989,
$\gamma'$	specific weight of the biodeposits	$\text{N m}^{-3}$	
$\delta_x$	height of boundary layer at $x$	$\text{m}$	
$\lambda_{A,k}$	shape/density roughness parameters	----	
$\theta_{\text{crit}}$	critical Shields parameter	----	
$\theta_o$	dimensionless Shield's parameter	----	
$\rho_s$	biodeposit density	$\text{kg m}^{-3}$	
$\kappa$	von Karmen constant	----	
$\tau_{\text{grain/total}}$	shear stress due to skin friction or form drag	$\text{N m}^{-2}$	
$\chi_{\text{bio}}$	composite roughness parameter	---	
$\Omega_{\text{bio}}$	composite roughness parameter	---	

Table 2: Scenarios of oyster reef length, oyster height, and oyster density.

Scenarios	Density (N)	Oyster height	Reef length
Group 1	0, 25, 100, 250	8	300
Group 2	100	4,8,10	300
Group 3	100	8	50, 100, 300

Table 3: Nitrogen fluxes ( $\mu\text{mol m}^{-2} \text{h}^{-1}$ ) estimated for intact oyster communities in estuarine environments, including estimated oyster density (individuals per square meter). Estimates derived from this study are included from Figure 15.

Method	Oyster density	NH <sub>4</sub> flux	NO <sub>23</sub> flux	N <sub>2</sub> flux	Source
Model	0	2	1.6	33	This study
Model	100	145	8	75	This study
Incubation	54			581.9	Humphries et al.2016
Incubation		450	80	600	Jackson et al. 2018
Incubation		351	183	159	Kellogg et al. 2013

# Nitrogen-Oyster Dynamics Model

The diagram illustrates the Nitrogen-Oyster Dynamics Model, which consists of three main components:

- Oyster Filtration Model:** A grid-based model showing the advection and diffusion of water and nutrients. The grid is defined by spatial coordinates  $C_{x,z}$ ,  $C_{x+1,z}$ , and  $C_{x+2,z}$  and vertical velocity  $U_z$ . The model shows water flowing through the oyster column, with arrows indicating the direction of flow. The oyster column is represented by a series of oyster shells, and the water column is divided into layers (Aerobic Layer, Anaerobic Layer).
- Biodeposition Model:** A model showing the process of biodeposition, where oysters filter water and deposit organic matter (biodeposits) on the sediment. The model includes arrows for "Resuspension" and "Biodeposits".
- Sediment Flux Model:** A model showing the flux of nitrogen through the sediment. It includes the following processes:
  - Nitrification:**  $\text{NH}_4^+ \rightarrow \text{NO}_3^-$
  - Denitrification:**  $\text{NO}_3^- \rightarrow \text{N}_2$
  - Diagenesis (Ammonification):**  $\text{PON} \rightarrow \text{NH}_4^+$
  - Denitrification:**  $\text{NO}_3^- \rightarrow \text{N}_2$The model also shows the flux of  $\text{NH}_4^+$  and  $\text{NO}_3^-$  between the water column and the sediment, and the final fate of nitrogen as  $\text{N}_2$  gas or buried in the sediment.

35

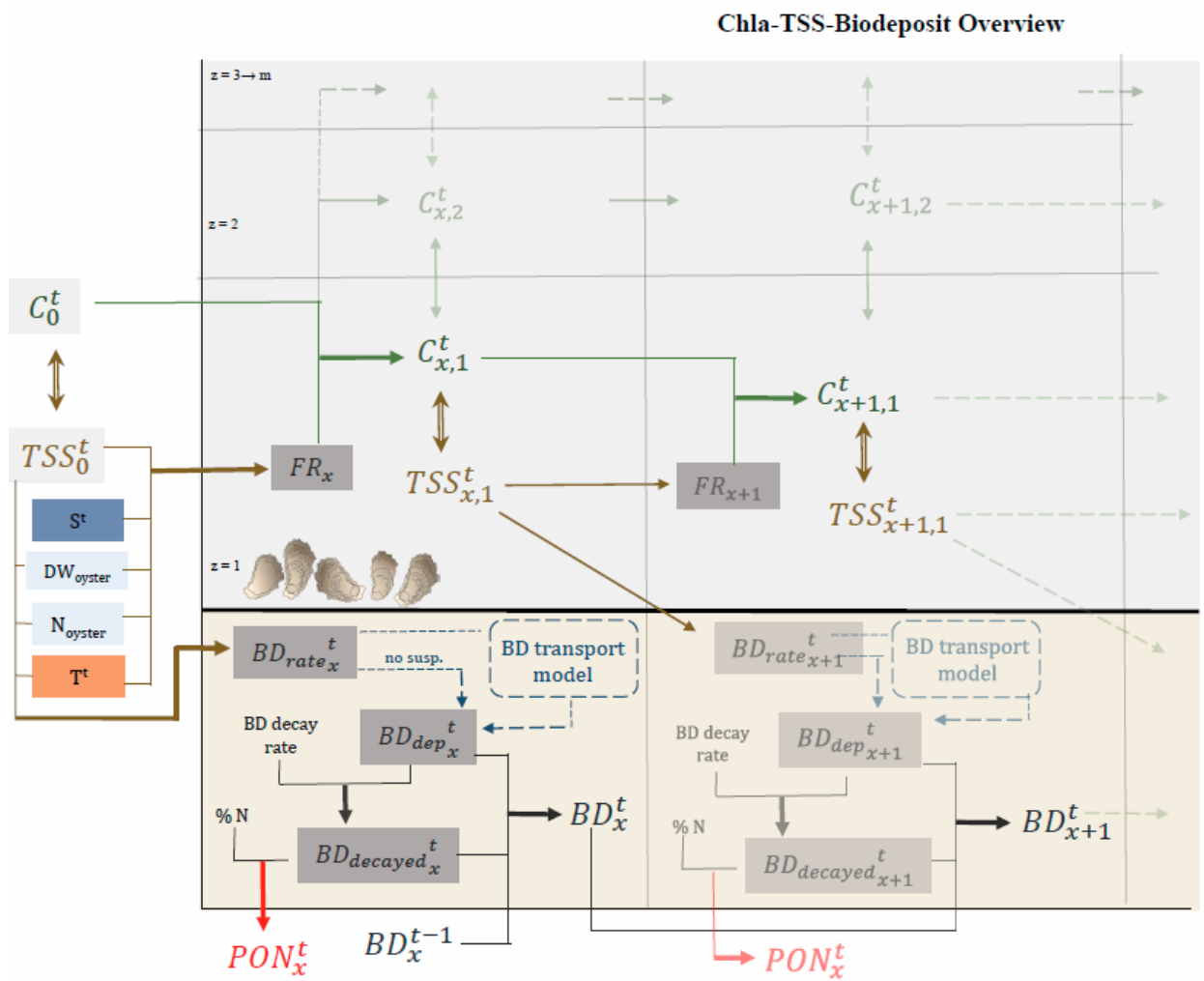


Figure 2. Box and arrow schematic diagram of the spatial domain and flows of material (chlorophyll-a, TSS) between the advection-diffusion model, the biodeposit transport model, and the sediment flux model.

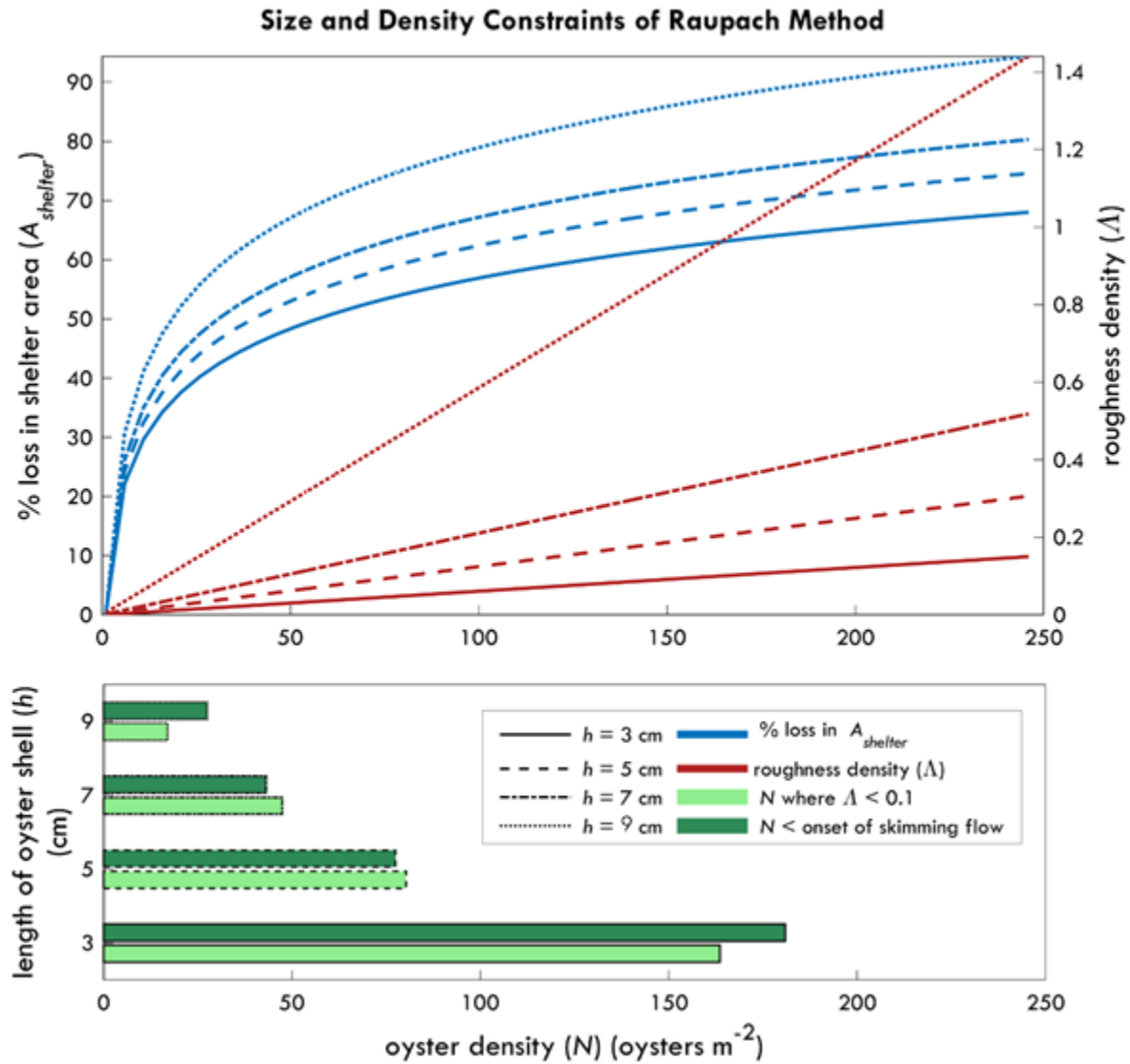


Figure 3. (top panel) relationship of oyster density ( $\text{oysters m}^{-2}$ ) to roughness density (red lines) and % loss in shelter area (blue lines) over different oyster heights (in cm). (bottom panel) threshold oyster densities associated with a roughness density  $< 0.1$  and the onset of skimming flow as a function of oyster height (in cm).

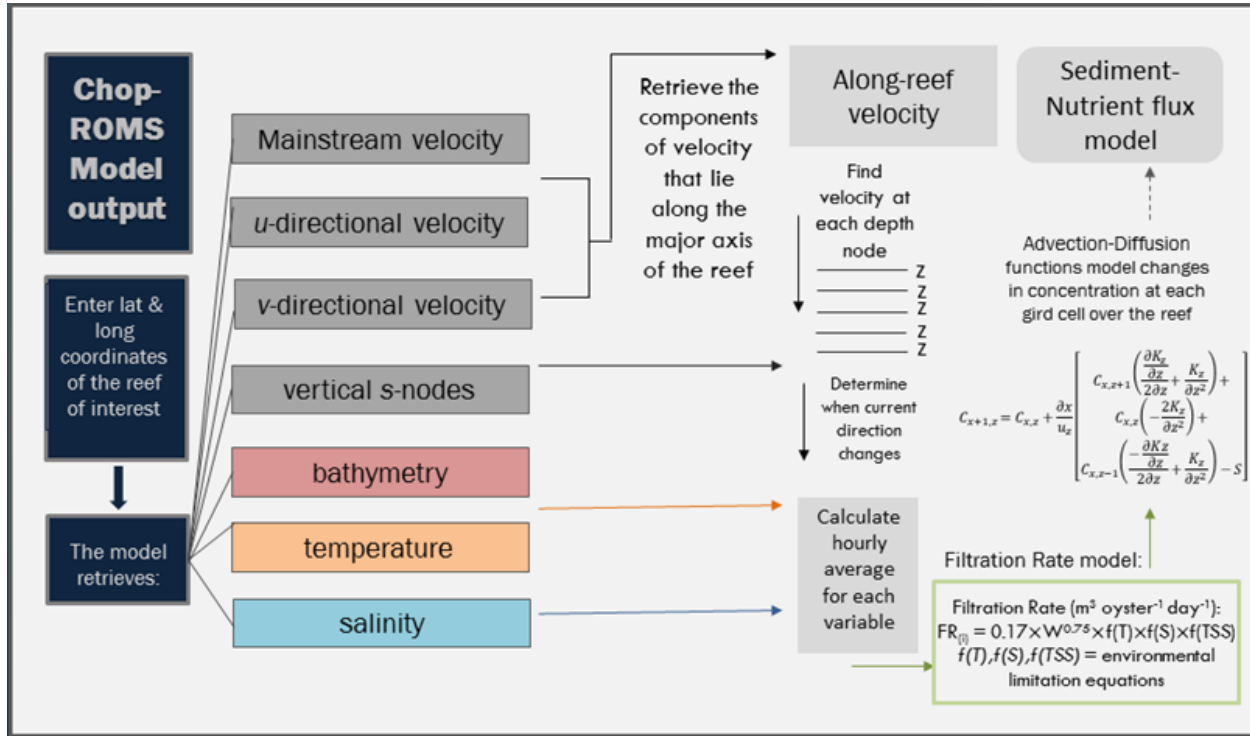


Figure 4. Schematic describing design of user interface and connection to Chop-ROMS. Current velocities (in cm/s), water temperature, and salinity are extracted from Chop-ROMS and assigned to the boundary of the chosen reef along with ambient chlorophyll-a concentrations, which then fuel an oyster filtration and biodeposit production model that then produces biodeposits that are processed in the sediment flux model.



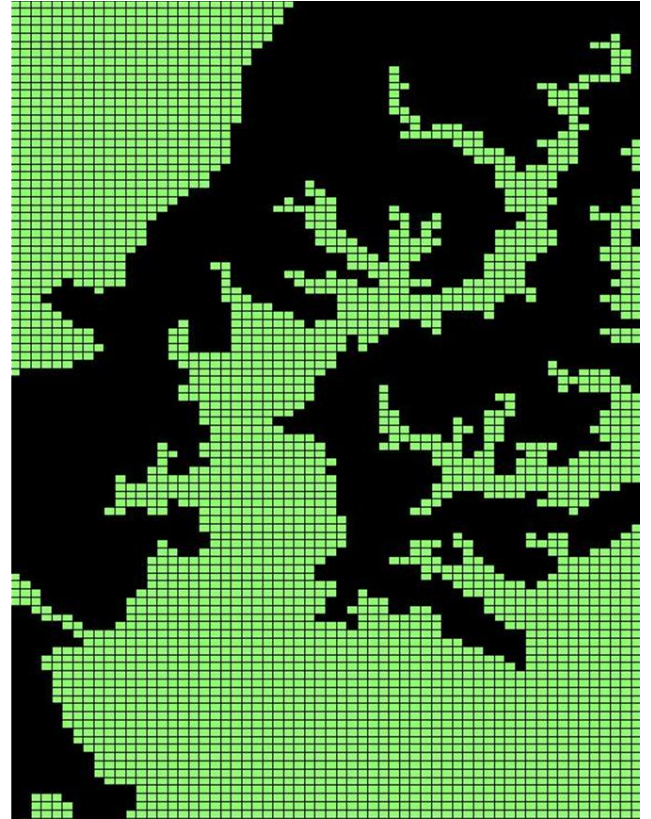
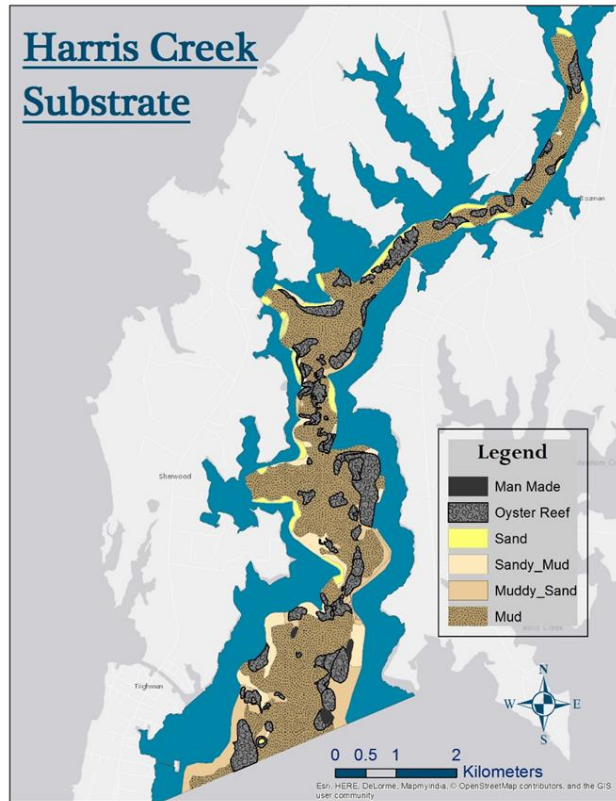


Figure 5. (left) Map of substrate in Harris Creek, including subtidal sediment composition (sand, mud) and oyster reef, and (right) grid domain of the Chop-ROMS hydrodynamic model used for boundary conditions (green area indicates water cells).

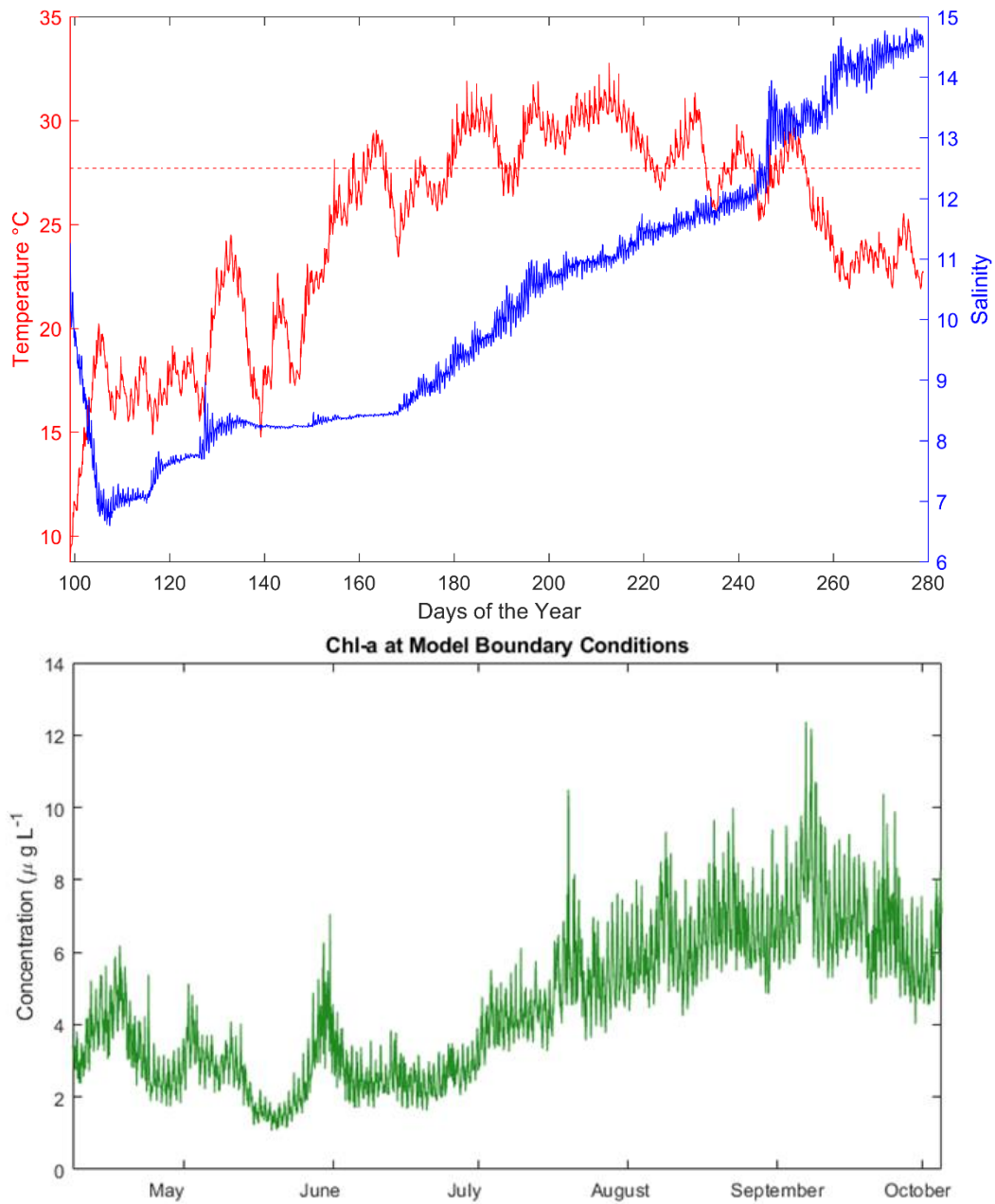


Figure 6. Boundary conditions used as forcing functions for model simulations over the May-October period in 2010, including (top) salinity (blue lines) and water temperature (red lines) and (bottom panel) boundary chlorophyll-a concentrations measured via an in-situ sensor in Harris Creek by the Maryland Department of Natural Resources ([www.eyeonthebay.net](http://www.eyeonthebay.net)).

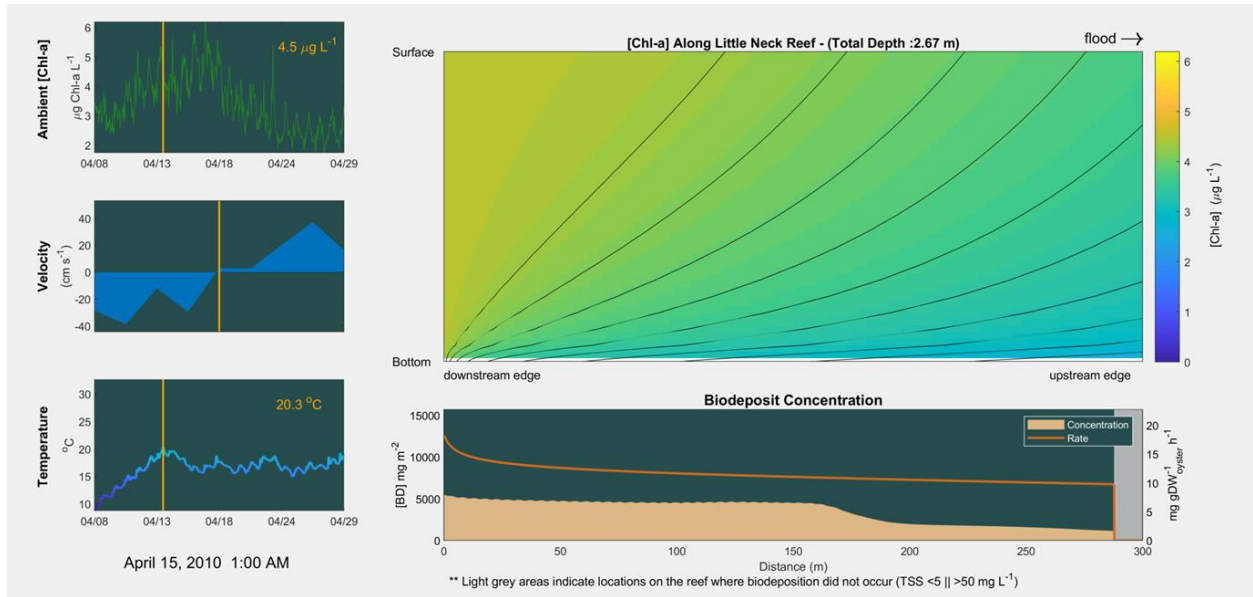


Figure 7. Montage of forcing functions and model dynamics in the oyster biodeposit transport model over a three week period in April on Little Neck Reef. (Left panels from top to bottom): Ambient, boundary conditions for chlorophyll-a, water velocity, and water temperature, (Right panels from top to bottom): Distribution of predicted chlorophyll-a over in the water column (top) and concentration of biodeposits in the reef subdomain (bottom). These two panels provide a snapshot of concentration at a single time step (April 15, 2010 1:00 AM).

This figure shows how a boundary layer of water column Chl concentrations are easily during during periods of low velocities (such as those at slack tide). This is due to the fact that the extended residence time of water passing over the reef allows for a higher degree of chlorophyll uptake through oyster filtration. In fact, without significant horizontal advection, Chl removal at the upstream end of the reef is significant enough to prevent any biodeposit production in the downstream portions of the reef (i.e. TSS concentrations are below the minimum threshold for biodeposition).

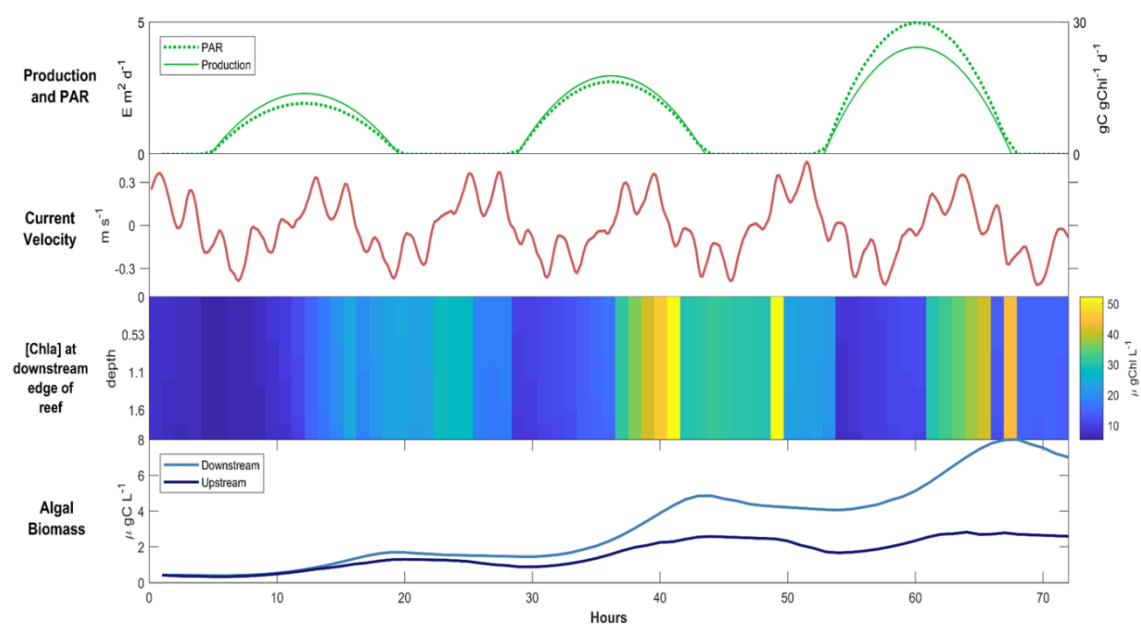


Figure 8. Initial 3-day simulation output documenting changes in primary production, PAR, current velocity, chlorophyll-a and algal biomass in units of carbon.

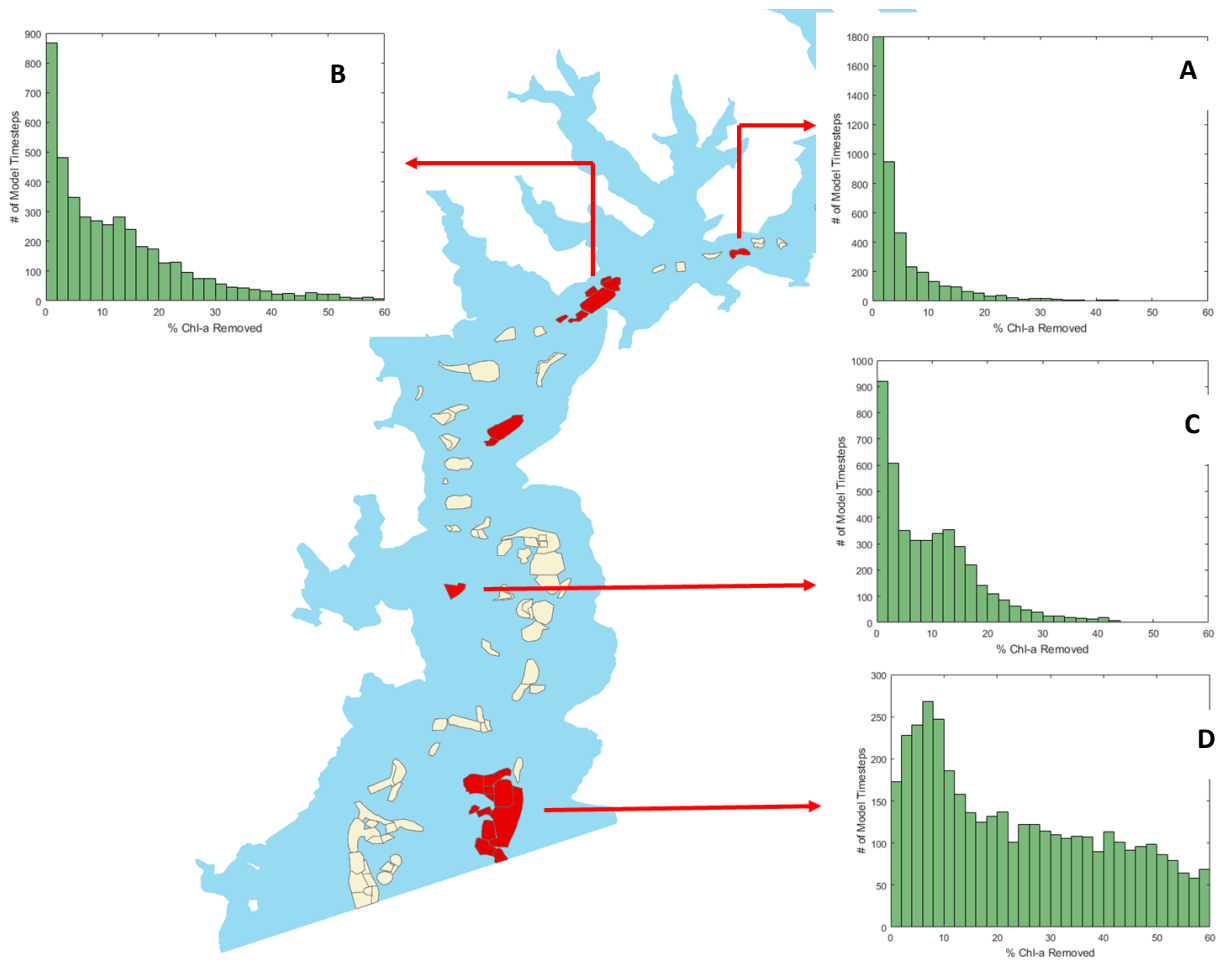


Figure 9. Histograms representing the frequency at which different fractions of water-column chlorophyll-a were removed by model simulations at four oyster reefs with varying length, oyster density, oyster age, and location in Harris Creek. Reef A: (38.77309 N, -76.2823 W), <50 oysters  $\text{m}^{-2}$ , 2.70 acres, Reef B: (38.76781 N, -76.2969 W), 150 oysters  $\text{m}^{-2}$ , 20.24 acres, Reef C: (38.74 N, -76.31 W), <50 oysters  $\text{m}^{-2}$ , 4.52 acres, Reef D: (38.71719 N, -76.3052 W), 50 oysters  $\text{m}^{-2}$ , 70.50 acres.

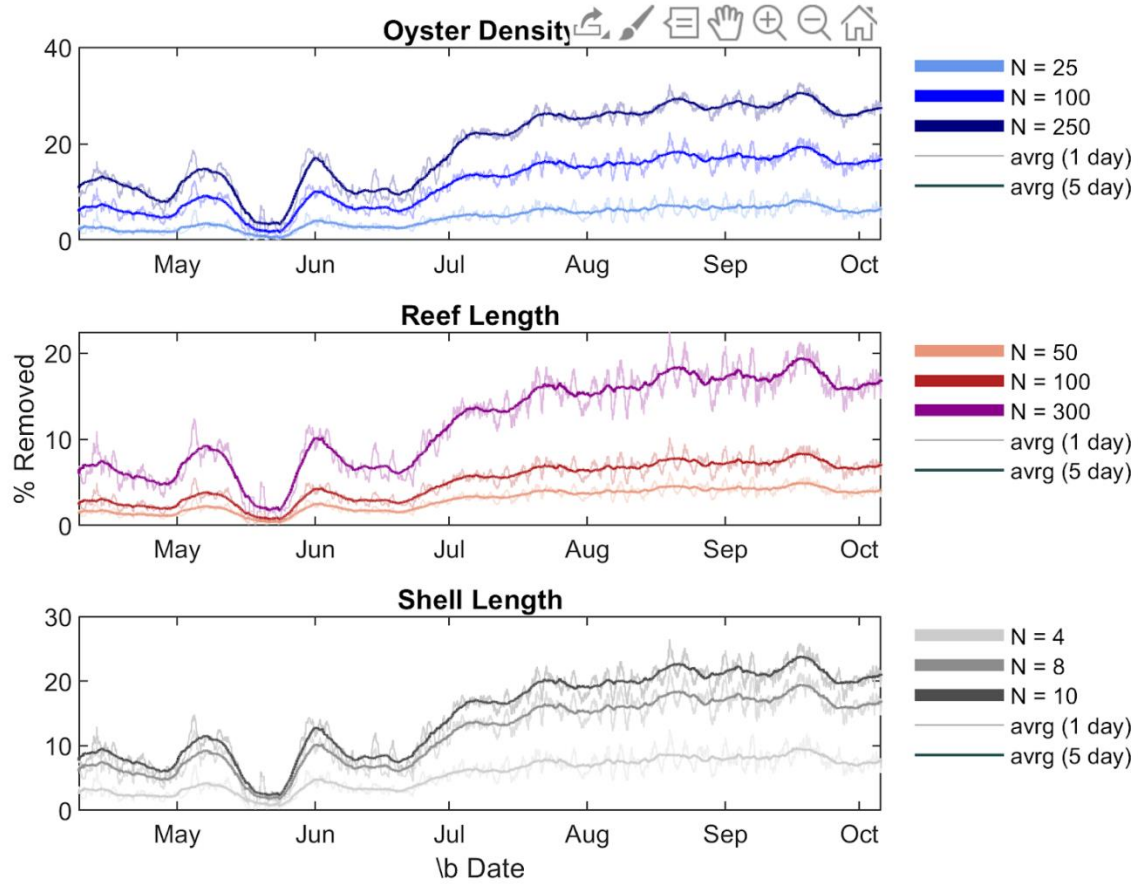


Figure 10. Time-series of different fractions of water-column chlorophyll-a removal by model simulations at idealized oyster reefs with oyster density (top panel), reef length (middle panel), and oyster size (bottom panel).

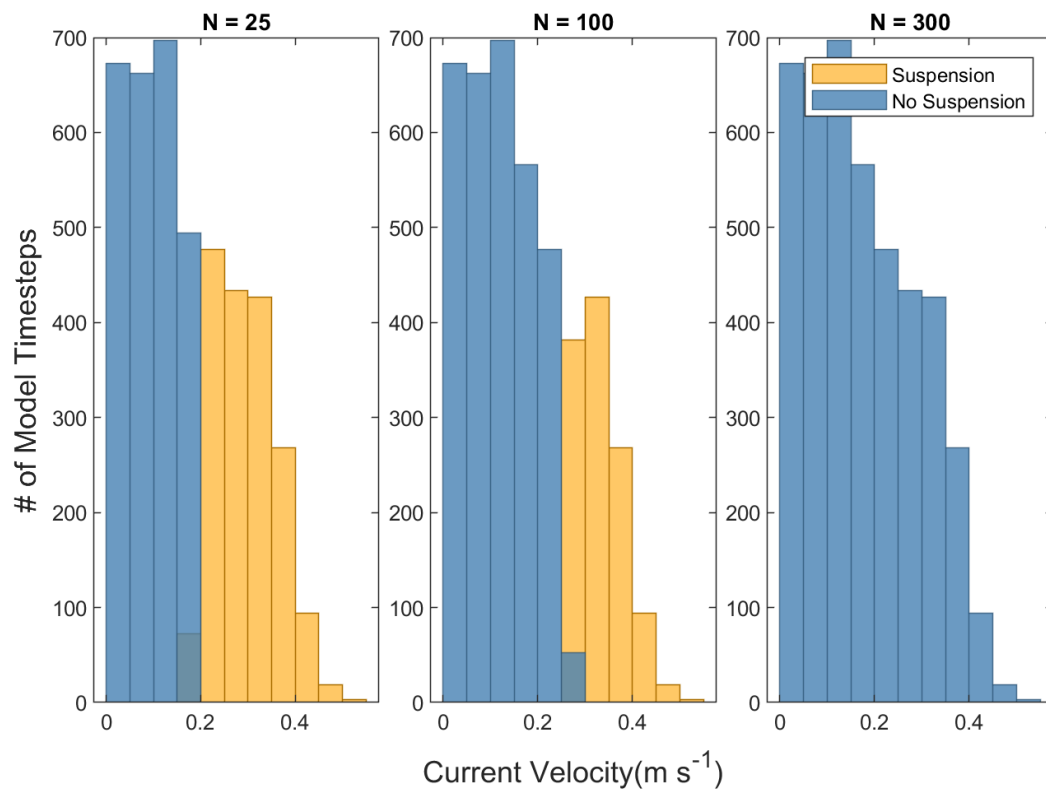


Figure 11. Frequency of biodeposit suspension at varying current velocities at three representative oyster densities (25, 100, 300 oysters/m<sup>2</sup>).

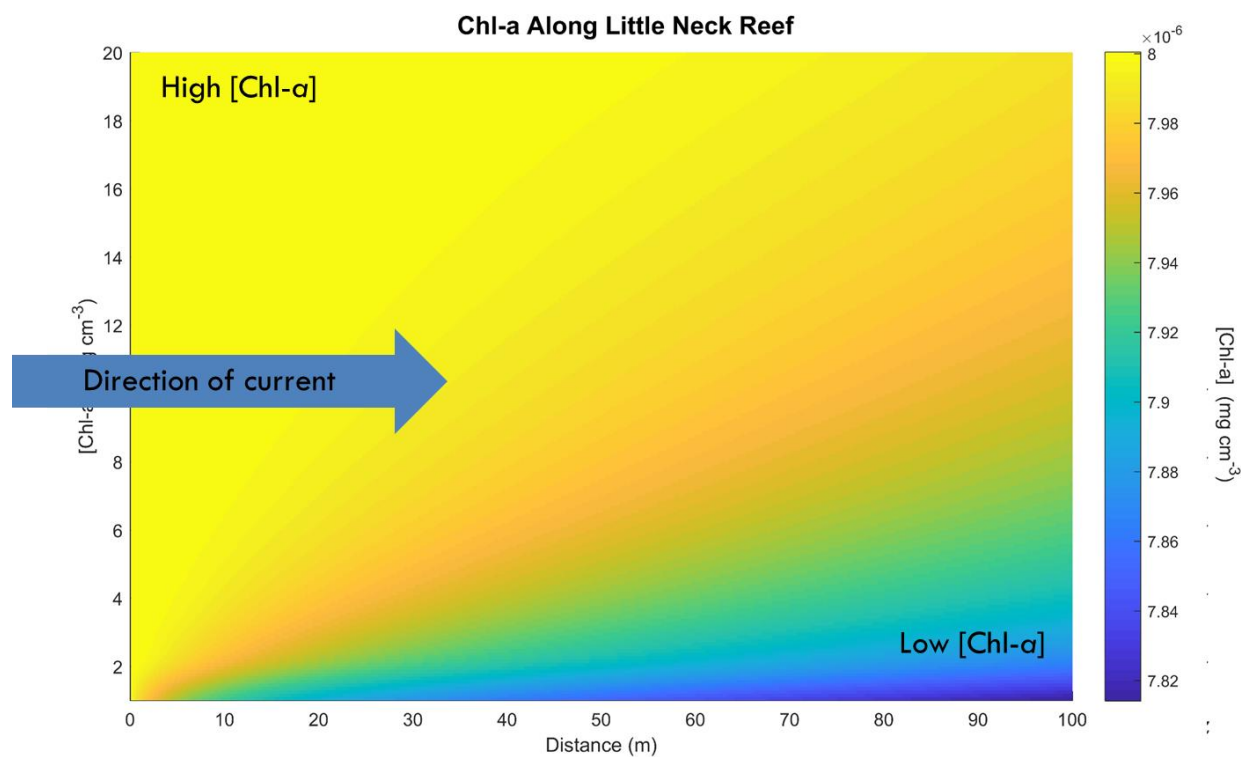


Figure 12: Representative distribution of chlorophyll-a along Little Neck Reef in 2010, where blue colors indicate low chlorophyll-a (in bottom water at end of reef downstream of flow direction) and high chlorophyll-a in the near-surface waters.



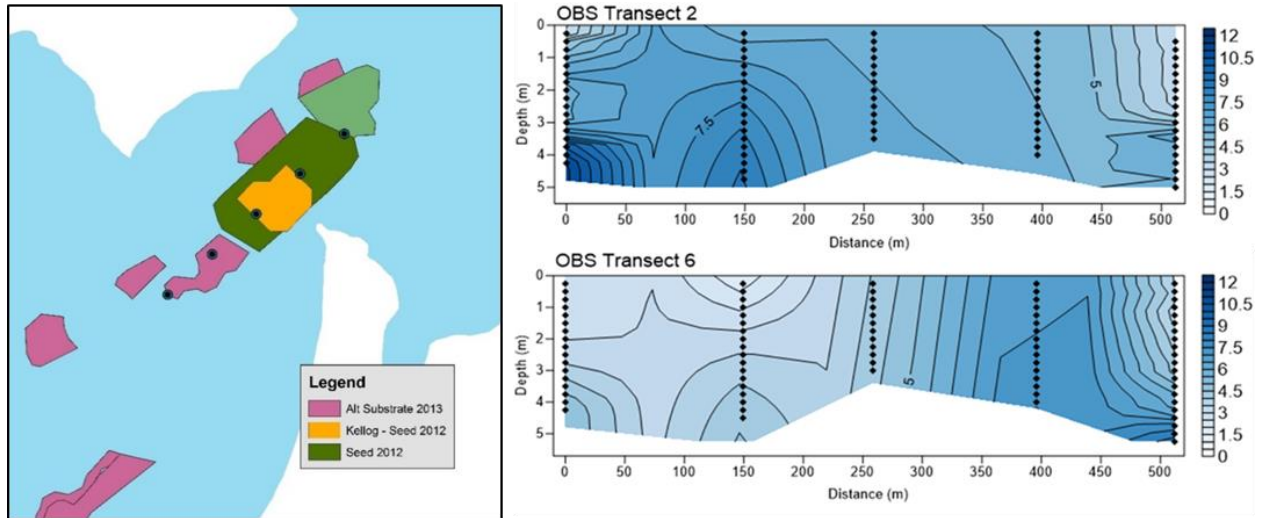


Figure 13. (left panel) Little neck oyster reef. Circles indicate the five sampling locations, which are located along a transect that is oriented  $47^\circ$  from true north. (right panel) Optical backscatter (uncalibrated NTU) from transects taken on Little Neck Reef at maximum flood (top) and maximum ebb (bottom). OBS is a measure of particle concentration in the water so dark blue represents high particle concentrations.

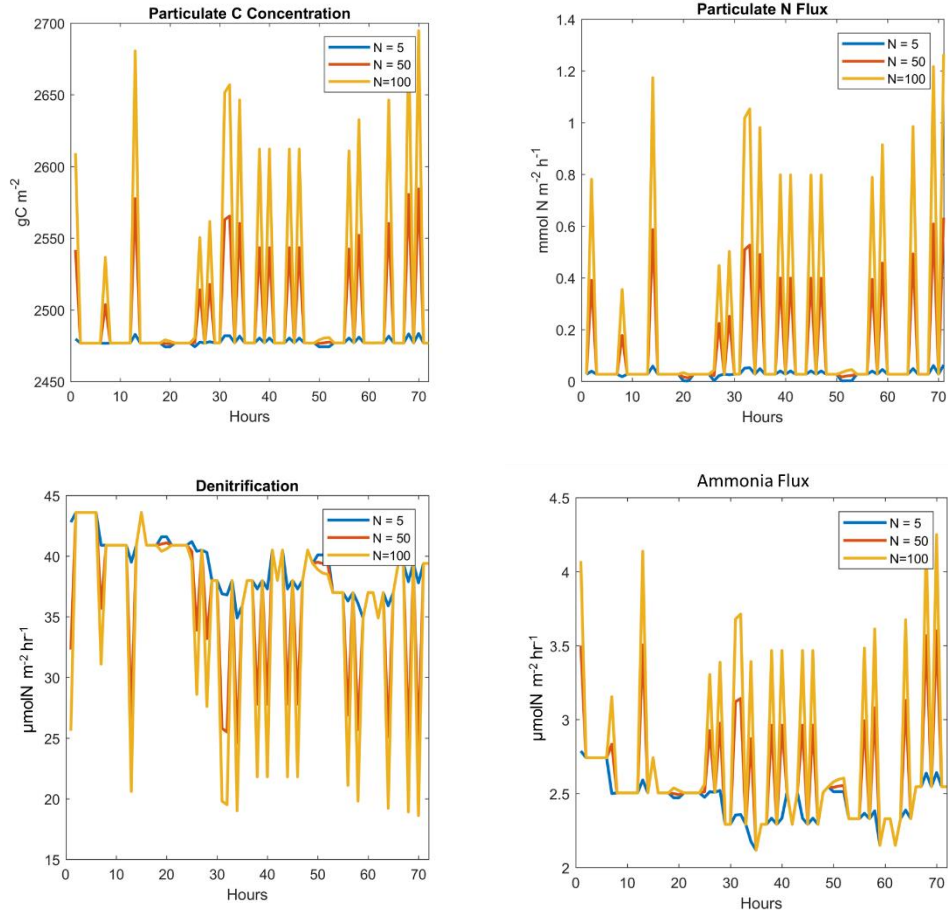


Figure 14: Snapshot of 3-day simulation of nitrogen dynamics on Little Neck Reef, including (clockwise from the top left) sediment particulate carbon concentrations, rates of particulate N deposition to sediments, sediment-water rates of ammonia flux and denitrification under three scenarios of oyster densities (5, 50, and 100 oysters m<sup>-2</sup>).

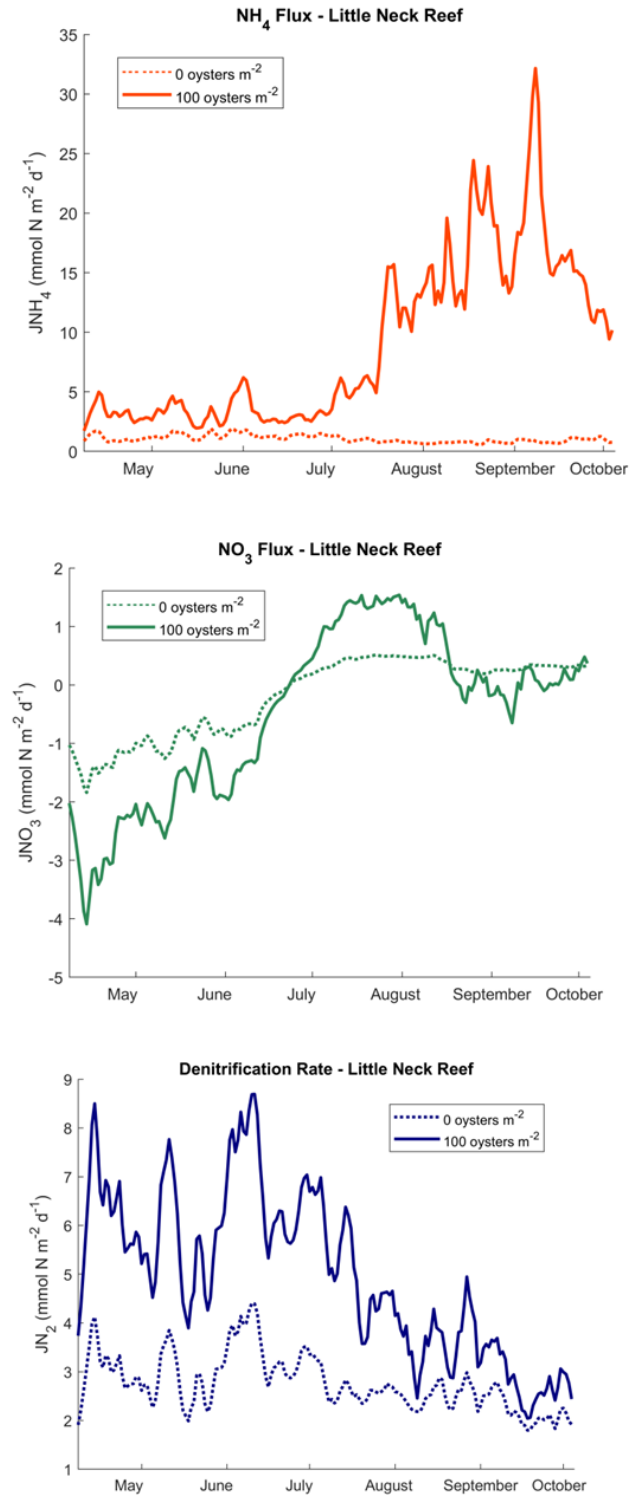


Figure 15. Modeled sediment-water fluxes of ammonium (top), nitrate (middle), and dinitrogen gas (bottom) in Little Neck Reef under conditions of no oysters (0 oysters per m<sup>-2</sup>) versus 100 oysters per m<sup>-2</sup>. The magnitude of all fluxes is greatly enhanced when oysters are present, especially for ammonium and denitrification.

## Appendix A

The following pages provide the Matlab code that I developed for the model. All scripts are available for download:

<https://drive.google.com/drive/folders/1xtZHjUQiDu4GOQ2SjyiLlan7SeJIY8bR?usp=sharing>.

A directory listing the various the scripts is given below.

### I. Primary Routine

- i. *Master\_Script\_NODM.m*
- ii. *run\_NODM.m*

### II. Primary Initialization Scripts

- iii. *getROMS\_data.m*
- iv. *setupSFM.m*
- v. *initialize\_NODM.m*
- vi. *Virtual\_Oyster\_Reef.m*

### III. Biodeposit Hydrodynamics

- vii. *Biodeposit\_Suspension.m*
- viii. *Biodeposit\_Transport.m*

### IV. Sediment Flux Model

- ix. *run\_SFM.m*
- x. *createsfmolwctvf\_alg.m*
- xi. *createsedinput.m*
- xii. *createsfmcontrol*
- xiii. *initialize\_OLWC.m*

### V. ROMS Integration

- xiv. *chopROMS\_NODM.m*
- xv. *time\_chopROMS.m*
- xvi. *locateReef\_ChopROMS.m*

## MASTER\_SCRIPT\_NODM.m

```
%% Nitrogen-Oyster Dynamics Model (NODM) %%%%%%%%%%%%%%%%%%%%%%%%%%%%%%%%%%%%%%%%%%%%%%%%%%%%%%%%%%%%%%%%%%%%%%%%%%
clear

%% Load base ROMS variables: -----

% Retrieve environmental parameters (salinity, velocity, depth, temperature)
from ROMS netCDF file(s):
if exist(netCDF_input.mat,'file') == 2
    load netCDF_input.mat
else
    getROMS_data
end

%% Primary input parameters: -----

% Reef parameters:
Reef_length = 300; %reef length in meters
N = 50; %oyster density (oysters/m^2)

% Oyster parameters
% --> Define oyster size by either shell length ('oysterheight') or dry
%      weight ('oysterweight'):
oysterheight = 8; %cm
oysterweight = []; %dry weight of individual oyster (g)
% **Note: All additional parameters can be changed in 'initialize_NODM.m'**

%% Options for the model run: -----

% Choose spatial resolution of the biogeochemical model:
% 0 = Average values among gridcells and use the averaged values as input to
%     the SFM and reef-layer biogeochemical models
% 1 = Apply calculations separately for each grid cell
SFM_resolution = 0;

% Choose whether or not to include oysters:
% 0 = no oysters (N=0)
% 1 = include oysters (density = N)
oysters_include = 1;

% Include biodeposit transport?
BD_AdvD_include = true;

% Run SFM?
run_SFM = true;

%% Designate output directory -----

%Primary output:
dir_1 = 'C:\...'; %where the primary output will be saved to
%Secondary output:
dir_2 = 'C:\...'; %where all additional output will be saved

%% Run Model -----
```

```

% Prime SFM to initialize cell arrays and establish stable biogeochemical
conditions:
if run_SFM
    [SFM_input,SFM_output,SFM_prime] = setupSFM_NODM;
end

% Construct the model domain, define additional parameters, and initialize
model arrays:
initialize_NODM

% Run the model:
run_NODM

```

## run\_NODM.m

```

%% Run Model -----

for I = 1:model_length_hours
%% Chl-a/TSS Advection-Diffusion Eqns, Biodeposition %%%%%%%%%%%%%%%

    if UX_dir_switch_hourly(i)==1
        revx = 1;
        revx_dx = 1;
    else
        revx=Boxnum;
        revx_dx = -1;
    end
    outChla = chla_avrgs(i)/1e6; %(mg/cm^3)
    outTSS = outChla*fraction;
    Fr = nan(1,Boxnum); %oytser filtration (cm^3/cm^2/hr)
    C = zeros(Boxnum,nDepth_nodes); % Hourly [Chl-a] across model domain
                                     %(mg/cm^3)
    BD_input_inst_m2 = zeros(1,Boxnum); %instantaneous (hourly) biodeposit
                                     % production mg/m2
    biodep_rate = zeros(1,Boxnum);

%% Calculate Chl-a concentrations -----

% Determine hourly filtration rate:
    %Temperature limitation factor:
    fT=exp(-0.006*(TEMP_avrg(i)-27)^2);

    %Salinity limitation factor:
    if (SAL_avrg(i)<5)
        fS=0;
    elseif (SAL_avrg(i)>=5) && (SAL_avrg(i)<=12)
        fS=(0.0926*SAL_avrg(i))-0.139;
    else
        fS=1;
    end

    %TSS-limitation factor:
    fTSS = nan(1,Boxnum);
    if (outTSS>50)
        fTSS(1) = 0; %Jordan 1987
    elseif (outTSS>25) %f(TSS)
        fTSS(1)=10.364*(log(outTSS))^-2.0477;
    elseif (outTSS<4)
        fTSS(1)=0.1;
    elseif (outTSS>=4) && (outTSS<=25)
        fTSS(1)=1;
    end

    %Find retention/filtration efficiency of algal cells based on their
    size distribution:
    reten_eff_matrix = part_size_distr;
    sz_classes = size(reten_eff_matrix);
    for ijk = 1:sz_classes(1)
        if reten_eff_matrix(ijk,1) < 3 || ...
            reten_eff_matrix(ijk,1) > 100
            reten_eff_matrix(ijk,2) = 0;
        end
    end
end

```

```

elseif reten_eff_matrix(ijk,1) <=5.7
    reten_eff_matrix(ijk,2) = ...
        (14.78*reten_eff_matrix(ijk,1) + 15.56)/100;
        %Riisgard 1988
else
    reten_eff_matrix(ijk,2) = 1;
end
end
max_retention = part_size_distr(:,2);
real_retention = reten_eff_matrix(:,2);
retention_efficiency = max_retention.*real_retention;

%Final filtration rate:
Fr(1) = Frmax*fT*fS*fTSS(1)*sum(retention_efficiency)*100;
        %(cm^3 * cm^-2 * hr^-1)

%First find bottom left gridcell: -----
%Chl-a after filtration
C(1,1)=outChla+(dx/u{1}(i))*(outChla*((dkdz{i}(1)/(2*dz))...
    +(K{i}(1)/(dz^2)))+outChla*(-2*K{i}(1)/(dz^2))+outChla... *(-
    dkdz{i}(1)/(2*dz)+K{i}(1)/(dz^2))-(Fr(1)*outChla/dz));
if C(1,1) < 0 %correct for error when velocity is very near zero
    C(1,1) = 0;
end
TSS{i} = zeros(1,Boxnum);
TSS{i}(1,revx)=outTSS; %starting bottom (left/right) gridcell [TSS] =
    %outTSS

%Biodeposition
if TSS{i}(1,revx) < 5 || TSS{i}(1,revx)> 50
    biodep_rate(1,revx) = 0;
else
    log10_biodep_rate = -0.7459+(0.1478*TEMP_avrg(i))+...
        (-4.21e-3*(TEMP_avrg(i))^2)...
        + (2.55e-4*(TEMP_avrg(i))^2*outTSS)...
        + (-5.21e-6*(TEMP_avrg(i))^2*outTSS^2);
        %(Jordan 1987)
    biodep_rate(1,revx) = 10^log10_biodep_rate;
        %(mg * gDWoyster^-1 * h^-1)
end
BD_input_inst_m2(1,revx) = N * g * biodep_rate(1,revx);
        %(mg m^-2 h^-1)

%Next, find rest of water collumn above bottom left gridcell:
for z=2:nDepth_nodes
    C(1,z)=outChla+(dx/u{z}(i))*(outChla*((dkdz{i}(z)/(2*dz))...
        +(K{i}(z)/(dz^2)))+outChla*(2*K{i}(z)/(dz^2))...
        + outChla*(-dkdz{i}(z)/(2*dz)+K{i}(z)/(dz^2)));
end

%Now find the rest of the gridcells: -----
for x=1:Boxnum-1
    TSS{i}(1,revx+revx_dx)=C(x,1)*fraction; %TSS is equal to previous
        %grid cells.
    %Chla after filtration (bottom grid cells):
    C(x+1,1)= C(x,1)+(dx/u{1}(i))*(C(x,2)*((dkdz{i}(1)/...
        (2*dz)))+(K{i}(1)/(dz^2)))+...

```



```

        C(x,1)*(-2*K{i}(1)/(dz^2))+C(x,1)*...
        (-dkdz{i}(1)/(2*dz)+K{i}(1)/(dz^2))-...
        (Fr(x)*C(x,1)/dz));
if C(x+1,1) < 0
    C(x+1,1) = 0;
end
if (TSS{i}(revx)>50)
    fTSS(x+1) = 0;
elseif (TSS{i}(revx)>25)
    fTSS(x+1)=10.364*(log(TSS{i}(revx))).^-2.0477;
elseif (TSS{i}(revx)<4)
    fTSS(x+1)=0.1;
elseif (TSS{i}(revx)>=4)&&(TSS{i}(revx)<=25)
    fTSS(x+1)=1;
end
Fr(x+1) = ...
    Frmax*fT*fS*fTSS(x+1)*sum(retention_efficiency)*100;

%Biodeposition
if TSS{i}(1,revx) < 5 || TSS{i}(1,revx)>50
    biodep_rate(1,revx+revx_dx) = 0;
else
    log10_biodep_rate = -0.7459+(0.1478*TEMP_avrg(i))...
        +(-4.21e-3*(TEMP_avrg(i))^2)...
        +(2.55e4*(TEMP_avrg(i))^2*TSS{i}(1,revx))...
        +(-5.21e6*(TEMP_avrg(i))^2*(TSS{i}(1,revx))^2);
                                                                    %(Jordan 1987)
    biodep_rate(1,revx+revx_dx) = 10^log10_biodep_rate;
                                                                    %(mg * gDWoyster^-1 * h^-1)
end
BD_input_inst_m2(1,revx+revx_dx)=
    N * g * biodep_rate(1,revx+revx_dx);

%Find top grid:
C(x+1,nDepth_nodes)=
    C(x,nDepth_nodes)+(dx/u{nDepth_nodes}(i))*...
    (C(x,nDepth_nodes)*((dkdz{i}(nDepth_nodes)/(2*dz))...
    +(K{i}(nDepth_nodes)/(dz^2)))+ C(x,nDepth_nodes)...
    *(-2*K{i}(nDepth_nodes)/(dz^2))+...
    C(x,(nDepth_nodes-1))*(dkdz{i}(nDepth_nodes)/...
    (2*dz)+K{i}(nDepth_nodes)/(dz^2)));
if C(x+1,nDepth_nodes) < 0
    C(x+1,nDepth_nodes) = 0;
end
%Find the rest of the vertical gridcells:
for z=2:(nDepth_nodes-1)
    ....C(x+1,z)=C(x,z)+(dx/u{z}(i))*...
    (C(x,z+1)*((dkdz{i}(z)/(2*dz))+(K{i}(z)/(dz^2)))+...
    C(x,z)*(-2*K{i}(z)/(dz^2))+C(x,z-1)*...
    (-dkdz{i}(z)/(2*dz)+K{i}(z)/(dz^2)));
    if C(x+1,z) < 0
        C(x+1,z) = 0;
    end
end
revx = revx+revx_dx;
end

```

```

%Daily change indicator:
if i < model_length_hours
    if intg_day_of_ts(i+1)~=intg_day_of_ts(i)
        END_DAY = true;
    end
else
    END_DAY = true;
end

%% Update daily ROMS values: -----
if hr_i == 1
    inday_indx = intg_day_of_ts == intg_day_of_ts(i);
    ROMS.sal_daily(dv_trckr) = mean(SAL_avrg(inday_indx));
    ROMS.temp_daily(dv_trckr) = mean(TEMP_avrg(inday_indx));
    ROMS.DO_daily(dv_trckr) = mean(DO_avrgs(inday_indx));
    SFM_output.olwc.sal(dv_trckr) = ROMS.sal_daily(dv_trckr);
    SFM_output.olwc.temp(dv_trckr) = ROMS.temp_daily(dv_trckr);
    SFM_output.olwc.do(dv_trckr) = ROMS.DO_daily(dv_trckr);
end

%% Biodeposit suspension and transport -----

if oysters_include == 1
    Biodeposit_Suspension
end

%% Determine amount filtered: -----

FILTRATION.upstreamCHLA(:,i) = C(1,:).*1e6;
FILTRATION.downstreamCHLA(:,i) = C(Boxnum,:).*1e6;
%ug/L Chl-a exiting the reef domain

%% Update output arrays: -----

CHLA{i} = C';
FILTRATION.rate{i} = Fr/N;
FILTRATION.rate_avrg(i) = mean(FILTRATION.rate{i});

%% Sediment Flux Model -----

if run_SFM
[SFM_input,SFM_output] = run_SFM_NODM(SFM_input,SFM_output,i,dv_trckr);
end

%% Daily value arrays: -----
if END_DAY
    DV_i = dvi;
    hr_i = 1;
    dv_trckr = dv_trckr + 1;
    END_DAY = false;
else
    hr_i = hr_i + 1;
end
end
%Save output:
save(output_fn1,'CHLA','TSS','BIODEP','FILTRATION','ROMS','HYDRO','VO',...
'model_length_hours','oysterheight','Reef_length','N')

```

## getROMS\_data.m

```
%% Input parameters for ChopROMS_NODM -----

% Coordinates:
f = 'choproms_his_0031.nc'; %reference netCDF file:
coordinates = [38.767807; -76.296817];
lat_input = coordinates(1); lon_input = coordinates(2);

nDepth_nodes = 20; %number of vertical depth nodes
angle = 45; %orientation of major reef axis from true north;
num_ROMS_files = 60; %Number of total ROMS netCDF files being used

%% Locate reef on chopROMS grid -----
[lat_loc, lon_loc, gridsizes] = Locate_ChopROMS_NODM(f,lat_input,lon_input);

%% Import chopROMS output: -----

% Time parameters:
Time_chopROMS_NODM

% Oceanographic/environmental parameters:
ChopROMS_NODM

%Average chopROMS values by hour and determine current direction:
Hourly_Averaged_Values_NODM

save netCDF_input.mat
```

### setupSFM.m

```
function [input, output, primeOutput] = setupSFM_NODM
    %% Build structure comprised of SFM input variables: -----
    fclose('all');
    input = load('netCDF_input.mat','year_of_sim','intg_day_of_ts',...
                'hour_of_ts','numdays','unique_days',...
                'model_length_hours','TEMP_avrg','SAL_avrg','depth');
    load('sfminput.mat','cims','sedinput','sfmconinput',...
        'sfmolwctvfinput','fluxzilla');
    adj_jsorp = 0.25;
    yrprimed = 15; %# of years for priming SFM

    % For input.CIMS data:
    for i = 1:size(cims,2)
        if strcmp(cims(i).station,'MARCTRL')
            input.CIMS = cims(i);
        end
    end

    % For Fluxilla data:
    for i = 1:size(fluxzilla,2)
        if strcmp(fluxzilla(i).station,'MARCTRL')
            input.FLUX = fluxzilla(i);
        end
    end

    clear('cims','fluxzilla');
    %% Initialize input structures:

    sed = sedinput(3);
    input.sfmcon = sfmconinput(4);
    olwc = sfmolwctvfinput(6);

    %% Prime the model by building up N&C stocks in the sediment -----

    % Get overlying water column (OLWC) data:
    input.adj_jsorp = adj_jsorp;
    abbrev = sprintf('%s_%s',input.CIMS.station,'cims');
    olwc.abbrev = abbrev;
    olwc.yrprimed = yrprimed;
    olwc.descrip = 'primed';

    [olwc] = createolwdepflux_prime(olwc,input);
    input.olwc_inputName = olwc.inputname;
    olwc.jsorsi = olwc.jsorsi*1.4;

    %Make the OLWC file:
    if exist(olwc.inputname,'file') == 2
        delete(olwc.inputname)
    end
    createsfmolwctvf_alg(olwc);

    % Make the sediment input file:
    if exist('sed.inp','file') == 2
        delete('sed.inp')
    end
end
```

```

createsedininput(sed);

%Get numbers and names of variables:
varNames.olwc = fieldnames(olwc);
nVars.olwc = size(fieldnames(olwc),1);
varNames.sed = fieldnames(sed);
nVars.sed = size(fieldnames(sed),1);

%Make reference olwc struct:
input.olwc_ref = cell2struct(cell(nVars.olwc,1),varNames.olwc);

%Save values from priming:
primeOutput.olwc = olwc;
primeOutput.sed_input = sed;

%% Initialize SFM input/output structures -----
%Make a variable that keeps track of hourly overlying water column values:
output = struct;
output.olwc = struct;
input.olwc = struct;
input.isn.olwc = false(nVars.olwc,1);
for i = 1:nVars.olwc
    if isnumeric(olwc.(varNames.olwc{i}))
        input.isn.olwc(i) = true;
        input.olwc.(varNames.olwc{i}) = nan(input.numdays,1);
        output.olwc.(varNames.olwc{i}) = nan(input.numdays,1);
    else
        input.olwc.(varNames.olwc{i}) = cell(input.numdays,1);
        output.olwc.(varNames.olwc{i}) = cell(input.numdays,1);
    end
end

%Make a variable that keeps track of hourly sediment concentrations: ---
input.isn.sed = false(nVars.sed,1);
for i = 1:nVars.sed
    if isnumeric(sed.(varNames.sed{i}))
        input.isn.sed(i) = true;
        output.sed.(varNames.sed{i}) = nan(input.numdays,1);
    else
        output.sed.(varNames.sed{i}) = cell(input.numdays,1);
    end
end

%% Generate SFM control file: -----

input.sfmcon.holwc = round(input.depth);
input.sfmcon.olwcfilename = sprintf('%solwc-tv.inp',input.CIMS.station);
input.sfmcon.inputname = sprintf('%s.inp',input.CIMS.station);
input.sfmcon.abbrev = [input.CIMS.station,'cims'];
input.sfmcon.time = yrprimed*365;

%Make control file:
if exist(input.sfmcon.inputname,'file') == 2
    delete(input.sfmcon.inputname)
end
createsfmcontrol(input.sfmcon);

```

```

%% Run SFM -----

% The following runs the SFM executable:
runSFM = sprintf('sfm_w_poc_lim.exe < %s outfile',input.sfmcon.inputname);
system(runSFM);

% This parses the output into a structure
[sfmoutput] = parseoutput(olwc);

varNames.sfmout = fieldnames(sfmoutput);
nVars.sfmout = length(varNames.sfmout);

%% Create sed.inp for first model timestep from the primed sfm output:

%Locate the latest timestep in the SFM output that :
[Yend, ~, ~] = datevec(sfmoutput.time(end,1));
[~, cMM, cDD] = datevec(datenum(input.year_of_sim,1,...
    input.intg_day_of_ts(1)));
nearest_dn = datenum(Yend,cMM,cDD);
if ismember(nearest_dn,sfmoutput.time)
    near_dn_ind = (sfmoutput.time == nearest_dn);
else
    near_dn_ind = (sfmoutput.time == datenum(Yend-1,cMM,cDD));
end
temp_sed_inp = sfmoutput;
for i=1:nVars.sfmout
    temp_sed_inp.(varNames.sfmout{i}) =
sfmoutput.(varNames.sfmout{i})(near_dn_ind);
end

%Set current sediment concentrations to the output from SFM:
unitConv_outVars = {'pop1r','pop2r','pop3r','pon1r','pon2r','pon3r',...
    'poc1r','poc2r','poc3r','psiavr'};
unitConv_sedVars = {'pop1','pop2','pop3','pon1','pon2','pon3',...
    'poc1','poc2','poc3','posi'};
nameConv_outVars = {'po4l','po4t2','nh4l','nh4t2','no3l','no3t2',...
    'hs1','hst2','sil','sit2','ch4l','ch42'};
nameConv_sedVars = {'po4t1','po4t2','nh4t1','nh4t2','no3t1','no3t2',...
    'h2st1','h2st2','sit1','sit2','methane1','methane2'};
ucovL = length(unitConv_outVars);
SedOut_allConv = [unitConv_outVars, nameConv_outVars;...
    unitConv_sedVars, nameConv_sedVars];
m2 = 0.36;
for i=1:size(SedOut_allConv(2))
    if i <= ucovL
        sed.(SedOut_allConv{2,i}) = temp_sed_inp.(SedOut_allConv{1,i})...
            *1e6*m2; %converts from mg/g to mg/m3
            %for PON/POC/POP
    else
        sed.(SedOut_allConv{2,i}) = temp_sed_inp.(SedOut_allConv{1,i});
    end
end
primeOutput.sed = sed;
input.SedOut = SedOut_allConv;
input.ucovL = ucovL;
input.sed = sed;

```

```

%% Create additional output structures: -----
%To track output from SFM:
output.sfmout = struct;
input.isn.sfmout = false(nVars.sfmout,1);
for i = 1:nVars.sfmout
    if isnumeric(sfmoutput.(varNames.sfmout{i}))
        input.isn.sfmout(i) = true;
        output.sfmout.(varNames.sfmout{i}) = nan(input.numdays,1);
    else
        output.sfmout.(varNames.sfmout{i}) = cell(input.numdays,1);
    end
end
primeOutput.sfmoutput = sfmoutput;

%Also, save variable info to input structure for future use:
input.varNames = varNames;
input.nVars = nVars;

%% Calculate OLWC values for each timestep in the model: -----

[input] = initialize_OLWC(input);

rmvFields = {'CIMS', 'FLUX'};
input = rmfield(input,rmvFields);

end

```

## initialize\_NODM.m

```
%% Model Initialization

% This script initializes the various cell arrays, vectors, and matrices
% that form the spatially- and temporally-discretized model domain.
% Starting boundary conditions and various static parameters are also defined
% here.

% The "Modify:...." section header indicates groups of variables that can be
% modified, if need be.
% All other variable definitions should remain unaltered.

AA = nan(model_length_hours,1);
BB = cell(model_length_hours,1);
CC = nan(numdays,1);
DD = cell(numdays,1);

%% Reef parameters and boundary conditions (some values can be modified)--

% Modify:.....
fraction = 1916543;% chlorophyll (mg/cm^3) to TSS (mg/L) conversion factor
% ---> current value based on Eyes on the Bay data for Harris Creek
dx = 10;% preliminary boxsize for Chla adv-diffusion grid and biodeposit
% sublayer (cm)
outBD = 7.04e-4;% ambient upstream [biodeposit] (mgBD/cm3)
% Starting concentrations of biodeposits in sublayer:
starting_BDL_S1_m2 = 0;% S1 = Active biodeposit layer (mg/m^2)
starting_BDL_S2_m2 = 0;% S2 = Inactive/decayed biodeposit layer (mg/m^2)

L = Reef_length*100;% length of reef(cm)
if any(oysterheight)
    g = 8e-5*(oysterheight*10)^2.175;
else
    oysterheight=( (g/0.00008)^(1/2.175) )/10;% cm from DW=0.00008*H^2.175
    %where H is in mm
end

%% Oyster geometry -----
VO = struct;
if oysters_include == 1
    % Modify: .....
    angle_of_elevation = 60;% vertical orientation of oysters on the reef (0-
90 deg).
    %0 deg = parallel with the substrate
    %Shao and Yang '05 parameters:
    n = 0.1;
    a = 6;
    bs = 5;
    c = 0.37;
    % .....

    % Calculate oyster shape/geometry for use in stress partitioning
    % equations:
    [eta_bio,s_bio,b_bio,roughness_SA,Af,As,...
    total_allow_density,lambda_bio,aerial_a] = ...
```



```

        = Virtual_Oyster_Reef(oysterheight,angle_of_elevation,N);
close all
F = 1e4; %F is the reference area of a unit of reef (1 m2)(1e4 cm^2)
% Approximations:
% aerial_a = s_bio*b_bio;
% Af = b_bio*eta_bio;
% As = s_bio*eta_bio;
LAMBDA = (N*Af)/F; %roughness density --> frontal-area index
ETA = (N*aerial_a)/F;
LAMBDA_e = (LAMBDA/(1-ETA)^n)*exp(-(a*LAMBDA)/(1-ETA)^n);
VO.eta_bio = eta_bio; VO.s_bio = s_bio; VO.b_bio = b_bio;
VO.roughness_SA = roughness_SA;
VO.total_allow_density = total_allow_density;
VO.lambda_bio = lambda_bio;
end

%% [Chla] and DO from data: -----

% Chl-a and DO concentrations are determined from empirical data
% 'chla_avrgs' = daily averages of Chl-a concentrations (ug/L)
% 'DO_avrgs' = daily averages of dissolved oxygen concentrations (mg/L)

hours_of_day = AA; utx = 1;
for i = 1:numdays
    hours_of_day(utx:(utx+23)) = 0:23;
    utx = utx + 24;
end
day_fraction = hours_of_day/24;

%Chla from upper bay:
chla_avrgs = zeros(model_length_hours,1);
load UHC
for i = 1:model_length_hours
    mm = day_month_match(intg_day_of_ts(i),2);
    days_b4 = sum(month_num_of_days(1:mm-1));
    d_o_m = intg_day_of_ts(i)-days_b4;
    if any(UHC.m == mm & UHC.d==d_o_m)==1
        cday_vals = UHC.value(UHC.m==mm & UHC.d==d_o_m &
UHC.hour==hours_of_day(i));
        cday_vals = cday_vals(isnan(cday_vals)==0);
    end
    chla_avrgs(i) = mean(cday_vals);
end

%DO from upper bay
DO_avrgs = zeros(model_length_hours,1);
load UHC_DO
for i = 1:model_length_hours
    mm = day_month_match(intg_day_of_ts(i),2);
    days_b4 = sum(month_num_of_days(1:mm-1));
    d_o_m = intg_day_of_ts(i)-days_b4;
    if any(UHC_DO.m == mm & UHC_DO.d==d_o_m)==1
        cday_vals = UHC_DO.value(UHC_DO.m==mm & UHC_DO.d==d_o_m...
& UHC_DO.hour==hours_of_day(i));
        cday_vals = cday_vals(isnan(cday_vals)==0);
    end
    DO_avrgs(i) = mean(cday_vals);
end

```

```

end
clear mm d_o_m cday_vals

%% Oyster filtration (some values can be modified) -----

% Modify: .....
% Particle size distribution:
% part_size_distr = [column 1]: particle size classes (um) [column 1]
%                   [column 2]: size distribution (% of total seston
%                   comprised of each size class)
% part_size_distr = [1.73 .57 .506; 2.18 .782 .518; 2.74 .831 .622;...
%                   3.46 .961 .735; 4.35 .1 .743; 5.48 .934 .86;...
%                   6.91 .931 .72; 9.97 1 1; 100 0 0]
%
% (Palmer and Williams 1980)
% See: Palmer and Williams 1980, Winter 1978, Riisgard 1988, Mohlenberg and
% Riisgard 1978
% for info on size-specific particle retention efficiency in oysters
% Note: part_size_distr = [7 1] ensures a 100% retention efficiency (default
% setting)
part_size_distr = [7 1]; %this size ensures a 100% retention efficiency
% .....

% Maximum filtration rate (m^2)
% --> this is an allometric, size/weight based formula
Frmx = 0.17*(g^0.75); % (m^3 oyster^-1 day^-1) (Ehrich and Harris 2015)
Frmx = Frmx*N/24; % (m^3 m^-2 hr^-1)

%Track difference between upstream and downstream Chl-a concentrations
FILTRATION.upstreamCHLA = nan(20,model_length_hours);
FILTRATION.downstreamCHLA = nan(20,model_length_hours);

%% Spatial partitioning of model domain / General hydrodynamics:.....

% Conversions:
z1_cm = z1.*100; %convert vertical grid cell centerpoints from meters to cm
depth_cm = depth*100; %in cm
deltad_cm = deltad*100; % in cm
ubar = abs(VEL_avrg.*360000); %cm/hr
sed_zo = 0.002;
if oysters_include == 1
    z0 = eta_bio/30;
else
    z0 = sed_zo;
end

% Depth-specific velocity:
ustar = zeros(1,model_length_hours);
u=cell(nDepth_nodes,1);
for i=1:model_length_hours %**
    % ustar(i)=ubar(i)*(2*depth_cm-(z0))/(5*(z0+depth_cm*(log(depth_cm/z0)-
    1))); %u*
    ustar(i)=2*ubar(i)*(depth_cm-(z0))/(5*(z0+depth_cm*(log(depth_cm/z0)-
    1))); %u*
for z=1:nDepth_nodes
    u{z}(i)=(ustar(i)/0.4)*log(z1_cm(z)/z0); %cm/hr
end

```

```

end
% Vertical turbulent diffusivity:
K=BB;
for i=1:model_length_hours
    K{i}=nan(size(z1_cm));
end
dkdz = BB;
for i = 1:model_length_hours
    dkdz{i}=nan(size(z1_cm));
end
for i=1:model_length_hours
for z=1:nDepth_nodes
    K{i}(z)=0.4*ustar(i)*z1_cm(z)*(1-(z1_cm(z)/depth_cm));
    dkdz{i}(z)=0.4*ustar(i)*(1-2*(z1_cm(z)/depth_cm));
end
end

%Stability Criteria (spatial partitioning in the horizontal dimension):
dz=deltad_cm;
us_max=(max(abs(ustar))/0.4)*log((depth_cm*0.5)/z0);
us_min=(min(abs(ustar))/0.4)*log((depth_cm*0.5)/z0);
Ks_max=0.4*max(abs(ustar))*z1_cm(nDepth_nodes)*(1-((depth_cm*0.5)/depth_cm));
Ks_min=0.4*min(abs(ustar))*z1_cm(nDepth_nodes)*(1-((depth_cm*0.5)/depth_cm));
dcs_max=((dz^2)*us_max)/(5*Ks_max);
dcs_min=((dz^2)*us_min)/(5*Ks_min);
if dcs_min<dx
    dx=dcs_min;
end
if dcs_max<dx
    dx=dcs_max;
end
% disp(dx);

%Make horizontal grid cells:
Boxnum=ceil(L/dx);
X = zeros(1,Boxnum);
for x=2:Boxnum %gridcell position from leading edge of reef
    X(1)=dx*0.5;
    X(x)=X(x-1)+dx;
end

%% The biodeposit sublayer: (some values can be modified)-----

% Modify: .....
starting_BDL_S1_m2 = 0; %starting concentrations of biodepositis in the S1
layer
starting_BDL_S2_m2 = 0; %starting concentrations of biodeposits in the S2
layer
S1_decay = -0.064; % recently-produced biodeposit decay rate
% .....

% Freshly deposited biodeposit sublayer (S1):
biodep_rate = nan(1,Boxnum);
BD_layer_S1_m2 = BB;
for i = 1:model_length_hours
    BD_layer_S1_m2{i} = zeros(1,Boxnum);
end

```

```

% Decayed biodeposit sublayer (S2):
BD_layer_S2_m2 = BB;
for i = 1:model_length_hours
    BD_layer_S2_m2{i} = zeros(1,Boxnum);
end

%% Biodeposit Transport (some values can be modified) -----

% Modify: .....
tau_crit = 0.05; %critical shear stress for suspension
Cr = 0.3;        %isolated roughness area drag element
ref_height = z1(3); %Reference height for calculating logarithmic velocity
profiles
transport_trckr = 1;
.....

% Keep record of shear stress and friction velocities:
hydroVars = {'susp_indicator','ustar_grain','ustar_total','tau_grain',...
             'tau_total','tau_unobstr','Cd','zo_bio'};
HYDRO = struct;
for v = 1:length(hydroVars)
    HYDRO.(hydroVars{v}) = AA;
end

% Biodeposit roughness height
if oysters_include == 1
    oysterheight_m = oysterheight / 100;
    ESD = (266.67*oysterheight)-117.74; %in microns
    ESD_m = ESD*1e-6;
    ws = (0.0334*ESD^0.8153)/1e3; %m/s
    k_grain = 2 * ESD_m/100; %cm
    zo_grain_m = 2.5*ESD_m/30;
    zo_grain = zo_grain_m/100; %cm
end

% Aerial reef coverage
if oysters_include == 1
    VO.perc_oyster = (aerial_a*N)/F; % percent aerial area covered by oysters
    VO.perc_sed = 1 - VO.perc_oyster;
    VO.sediment_SA = 1-(1*VO.perc_oyster); % m^2
    VO.oyster_SA = roughness_SA * N / F; % total 3D surface area of oysters
    % contained in a m^2
    VO.total_SA_per_m2 = VO.oyster_SA +1;
    VO.BD_dilution_factor = 1/VO.total_SA_per_m2;
end

% Organic matter from biodeposits going to SFM
OM_to_SFM = {'PON_to_SFM','POC_to_SFM','POP_to_SFM'};
massX = [4.8 34.8 0.58];
for i = 1:3
    SFM_output.(OM_to_SFM{i}) = BB;
    for j = 1:model_length_hours
        SFM_output.(OM_to_SFM{i}){j} = zeros(1,Boxnum);
    end
    SFM_input.(OM_to_SFM{i}) = zeros(1,Boxnum);
end

```

```

% Deposition/Suspension
susp_indicator_SFM = AA; %record when suspension occurs
BD_suspension = BB;
bottom_perc_total = BB;
REEF_Deposition = BB;
RAAdjSed_Deposition = BB;
BD_input_all = BB;
botperctot_tracker = BB;

%% Initialize Grid-Specific SFM variables:
%%%%%%%%%%%%%%%%%%%%%%%%%%%%%%%%%%%%%%%%%%%%%%%%%%%%%%%%%%%%%%%%%%%%%%%%

% if run_SFM && SFM_resolution == 1
%     sfmolwctvfinpnt_gs_array = cell(1,Boxnum);
%     olwcind = length(sfmolwctvfinpnt); %locate current row
%     temp_sfmol = sfmolwctvfinpnt(olwcind);
%     temp_sfmol(2).time = []; %create new row
%     sedinpnt_gs_array = cell(1,Boxnum);
%     OLWC_Final = cell(1,Boxnum);
%     SFMOutput_Final = cell(1,Boxnum);
%     Sed_Input_Final = cell(1,Boxnum);
%     for i = 1:Boxnum
%         sfmolwctvfinpnt_gs_array{i} = temp_sfmol(2);
%         OLWC_Final{i} = olwc_fields';
%         SFMOutput_Final{i} = SFMout_fieldnames';
%         Sed_Input_Final{i} = sedinp_fields';
%         sedinpnt_gs_array{i} = sedinpnt(sedinpntind);
%     end
%     olwc_plchd = 2;
%     sfmoF_plchd = 2;
%     sif_plchd = 2;
% end

%% Create cell arrays to record model output:
%%%%%%%%%%%%%%%%%%%%%%%%%%%%%%%%%%%%%%%%%%%%%%%%%%%%%%%%%%%%%%%%%%%%%%%%

% Biodeposition
BIODEP.conc = BB; %records concentration of biodeposits in the active layer
(AFTER transport)
BIODEP.flux = BB; % tracks biodeposits produced per m2 (mg m^-2 h^-1) (BEFORE
transport)
BIODEP.toSed = BB;

% Filtration and Water Column
FILTRATION.rate = BB; %final filtration rate (m^3 oyster^-1 hr^-1)
TSS = BB; %records [TSS] across the reef at each timesetp
CHLA = BB; %records [Chla] across the reef at each timestep

%(Reef-wide averages)
FILTRATION.rate_avrg = AA;

% ROMS variables
ROMS.sal = SAL_avrg;
ROMS.vel = VEL_avrg;
ROMS.temp = TEMP_avrg;
ROMS.rho = RHO_avrg;

```

```

ROMS.visc = MU_avrg;
ROMS.currentDir = UX_dir_switch_hourly;
ROMS.DO = DO_avrgs;
ROMS.dNodes = z1;
ROMS.depth = depth;

%% Set up daily value tracking:
dvi = struct; %empty reference strucutre for DVi initialization
END_DAY = false;
dv_trckr = 1;
hr_i = 1;

%Temporary arrays (for the summation of hourly values):
dvi_vn = {'sal','temp','DO'};
for i = 1:length(dvi_vn)
    dvi.(dvi_vn{i}) = nan(24,1);
end
dvi_vn = {'conc','flux','toSed'};
for i = 1:length(dvi_vn)
    dvi.(dvi_vn{i}) = zeros(24,Boxnum);
end
% for i = 1:3
%     dvi.(OM_to_SFM{i}) = zeros(24,Boxnum);
% end
DVi = dvi; %temporary structure for recording daily values

%Output arrays:
ROMS.sal_daily = CC;
ROMS.temp_daily = CC;
ROMS.DO_daily = CC;
BIODEP.conc_daily = DD;
BIODEP.flux_daily = DD;
BIODEP.toSed_daily = DD;

%% Create names for .mat file output:
fntxt = sprintf('RL%d_N%d_SZ%d_%s',Reef_length,N,oysterheight,...
    datestr(clock,'mmmdd'));
output_fn1 = fullfile(dir_1,[sprintf('output_%s',fntxt) '.mat']);

```

## Virtual\_Oyster\_Reef.m

```

Function [eta_bio,s_bio,b_bio,roughness_SA,Af,As,...
        total_allow_density,lambda_bio,aerial_a,lmw] = ...
        Virtual_Oyster_Reef(oysterheight,angle_of_elevation,N)

%% Virtual Oyster Reef -----
% This function calculates all oyster shape/spacing parameters:
surface_rugosity = 0;
texture_overlay = 0;
warning('off','MATLAB:singularMatrix');

%% Calculate size dimensions of the oysters - relations from empirical study

max_width = 0.6355*oysterheight+0.8709;
loc_max_width = 0.8218*oysterheight-1.8657;
        %location of region of maximum shell width (as measured
        %from the hinge)as a percentage of the total shell length;
L_curv_anterior = oysterheight - loc_max_width;
S_w_to_tW = 0.44;
s_x = S_w_to_tW * max_width;
l_x = max_width-s_x;
hinge_dx = 0.05*oysterheight;
LXEM_dist = 0.09*oysterheight; %distance of long_x elliptical maxima from
        % semiminor lattitudinal axis
loc_max_height = (-0.0316*oysterheight+0.666)*oysterheight;
max_height = 0.1418*oysterheight+2.1789;
H_of_l_valve = 0.2*max_height;

%% Plot shell shape -----

%% First draw 2D oyster shape over the xy plane (b.e.v.)

xy_center_x = 5; xy_center_y = 10; %center of oyster's lat and long axis
rep_interp = 100;

%Hinge_dx
hinge_dx_x = linspace(xy_center_x-hinge_dx,xy_center_x,rep_interp);
hinge_dx_y = repelem(xy_center_y-loc_max_width,rep_interp);

%Short_x posterior diagonal (sxpdx) from hinge to area of maximum width:
sxpdx_x = linspace(xy_center_x-s_x,xy_center_x-hinge_dx,rep_interp);
sxpdx_y = linspace(xy_center_y,xy_center_y-loc_max_width);
sxpdx_slope = -(loc_max_width/(s_x-hinge_dx));
sxpdx_int = sxpdx_y(rep_interp)-(sxpdx_slope*sxpdx_x(rep_interp));

%Short_x anterior curved portion (sxac) from area of maximum width:
sxac_x = linspace(xy_center_x-s_x,xy_center_x,rep_interp);
sxac_y = zeros(1,rep_interp);
for i=1:rep_interp %use standard equation for an ellipse to solve for sxac_y
    sxac_y(i)= sqrt(abs(L_curv_anterior^2-(L_curv_anterior^2*(sxac_x(i)-
xy_center_x)^2/s_x^2)))+xy_center_y;
end

%Long_x anterior curved portion (sxac) from area of maximum width:
lxac_x = linspace(xy_center_x,xy_center_x+l_x,rep_interp);
lxac_y = zeros(1,rep_interp);

```

```

for i=1:rep_interp %use standard equation for an ellipse to solve for sxac_y
    lxac_y(1,i) = (sqrt(abs((1-((lxac_x(i)-
xy_center_x)^2/l_x^2))*L_curv_anterior^2)))+ xy_center_y;
end

%Long_x posterior parabolic/curved portion (lxpc):
dx_LXEM = 0.3;
lxpc_li_x = xy_center_x;
lxpc_li_y = xy_center_y+loc_max_width-(2*LXEM_dist);
lxpc_ri_x = xy_center_x;
lxpc_ri_y = xy_center_y-loc_max_width;
lxpc_m_x = xy_center_x+l_x+dx_LXEM;
lxpc_m_y = xy_center_y-LXEM_dist;
%Using equation x = a*y^2+b*y+c:
A = [lxpc_li_y^2 lxpc_li_y 1;. % lxpc_li_x =lxpc_li_y^2(a)+lxpc_li_y(b)+c
     lxpc_ri_y^2 lxpc_ri_y 1;. % lxpc_ri_x = lxpc_ri_y^2(a)+lxpc_ri_y(b)+c
     lxpc_m_y^2 lxpc_m_y 1]; % lxpc_m_x = lxpc_m_y^2(a)+lxpc_m_y(b)+c
B = [lxpc_li_x; lxpc_ri_x; lxpc_m_x];
X = A\B; %X holds the coefficients (a,b,c) of the parabola
lxpc_y = linspace(xy_center_y-LXEM_dist,xy_center_y-
loc_max_width,rep_interp);
lxpc_x = zeros(1,rep_interp);
for i=1:rep_interp
    lxpc_x(1,i)=(X(1)*lxpc_y(i)^2)+(X(2)*lxpc_y(i))+X(3);
end

%sxac to lxpc connector (stlc):
stlc_x = linspace(xy_center_x+l_x,xy_center_x+l_x+dx_LXEM);
stlc_y = linspace(xy_center_y,xy_center_y-LXEM_dist);
stlc_slope = -LXEM_dist/dx_LXEM;
stlc_int = stlc_y(rep_interp)-(stlc_x(rep_interp)*stlc_slope);

% Construct 2D xy-coordinate grid for virtual oyster (vo):
vo_x = [hinge_dx_x fliplr(sxpd_x) sxac_x lxac_x stlc_x lxpc_x];
vo_y = [hinge_dx_y fliplr(sxpd_y) sxac_y lxac_y stlc_y lxpc_y];
% test = plot(vo_x,vo_y,'b','linewidth',2); xlim([0 10]); ylim([0 16]); axis
equal;
% xlabel('X');ylabel('Y');zlabel('Z');

%% Create a matrix of points contained within the oyster outline: -----

vo_x_right = [lxac_x stlc_x lxpc_x];
vo_y_right = [lxac_y stlc_y lxpc_y];
flip_voyr = fliplr(vo_y_right);

vo_x_left = nan(1,length(vo_y_right));
vo_y_left = vo_y_right;
for i = 1:length(vo_y_left)
    if vo_y_left(i)>= xy_center_y %sxac
        vo_x_left(i) = -sqrt(abs(s_x^2-(s_x^2*...
            (vo_y_left(i)-xy_center_y)^2/L_curv_anterior^2)))...
            + xy_center_x;
    else %sxp
        vo_x_left(i) = (vo_y_left(i)-sxp_int)/sxp_slope;
    end
end
end

```



```

% plot(vo_x_left,vo_y_left,vo_x_right,vo_y_right)

rep_interp2 = 100;
xi = nan(length(vo_y_right),rep_interp2);
for i =1:length(vo_y_right)
    xi(i,:) = linspace(vo_x_left(i),vo_x_right(i),rep_interp2);
end
yi = nan(length(vo_y_right),rep_interp2);
for i=1:length(vo_y_right)
    yi(i,:)= repelem(vo_y_right(i),rep_interp2);
end

%% Next draw 3D oyster shape in vertical planes (xz and yz):-----

%Create left valve:

% In the yz plane:
y_max_h = xy_center_y-loc_max_width+loc_max_height;
yz_a = (xy_center_y+L_curv_anterior-y_max_h);
yz_b = (max_height-H_of_l_valve);
yz_a2 = loc_max_height;

zi_yz = nan(length(vo_y_right),rep_interp2);
for i=1:length(vo_y_right)
    if yi(i,1)<= y_max_h
        for j = 1:rep_interp2
            zi_yz(i,j)= sqrt(abs((1 - (yi(i,j)-y_max_h)^2/yz_a2^2) *
yz_b^2)) + H_of_l_valve;
        end
    else
        for j = 1:rep_interp2
            zi_yz(i,j)= sqrt(abs((1 - (yi(i,j)-y_max_h)^2/yz_a^2) * yz_b^2))
+ H_of_l_valve;
        end
    end
end
% figure();surf(xi,yi,zi_yz);shading interp;axis equal;zlim([0 5]);

% In the x_z plane:

zi_xz = nan(length(vo_y_right),rep_interp2);
for i=1:length(vo_y_right)
    xz_li_x = vo_x_left(i);
    xz_li_z = H_of_l_valve;
    xz_ri_x = vo_x_right(i);
    xz_ri_z = H_of_l_valve;
    xz_m_x = xi(i,floor(rep_interp2/2));
    xz_m_z = zi_yz(i,1);

    A = [xz_li_x^2 xz_li_x 1;xz_ri_x^2 xz_ri_x 1;xz_m_x^2 xz_m_x 1];
    B = [xz_li_z; xz_ri_z; xz_m_z];
    X = A\B;
    for j=1:rep_interp2
        zi_xz(i,j)=(X(1)*xi(i,j)^2)+(X(2)*xi(i,j))+X(3);
    end
end

```

```

for i=1:length(vo_y_right)
    for j=1:rep_interp2
        if zi_xz(i,j)>max_height
            zi_xz(i,j)=max_height;
        end
    end
end

[loc_long_axis_r, loc_long_axis_c] = find(zi_xz == max(max(zi_xz)));

if surface_rugosity==1
    %Add some surface rugosity:
    z_rows = 1:length(vo_y_right); z_col = 1:rep_interp2;
    row_select = datasample(z_rows,1000);
    col_select = datasample(z_col, 50);
    col_select = repmat(col_select,1,20);
    rand_zi = rand(1,1000)*0.09;
    neg_select = [1 -1]; neg_select=repmat(neg_select,1,500);
    for i = 1:1000
        zi_xz(row_select(i),col_select(i))=
zi_xz(row_select(i),col_select(i))+rand_zi(i)*neg_select(i);
    end
end

figure();
Lvalve_surf = surf(xi,yi,zi_xz);shading interp; axis equal;zlim([0 5]);
hold on;
zi_flat = repelem(H_of_l_valve,length(vo_y_right));
zi_flat = repmat(zi_flat',1,rep_interp2);

[loc_Lv_hpr_r loc_Lv_hpr_c] = find(zi_xz == max(max(zi_xz)));
xlabel('X');ylabel('Y');zlabel('Z');
Lvalve_x = Lvalve_surf.XData;
Lvalve_y = Lvalve_surf.YData;
Lvalve_z = Lvalve_surf.ZData;

%% Create right valve: -----

y_max_h = xy_center_y-loc_max_width+loc_max_height;
yz_a = xy_center_y+L_curv_anterior-y_max_h;
yz_b = H_of_l_valve;
yz_a2 = xy_center_y-loc_max_width;

zi_yz_rv = nan(length(vo_y_right),rep_interp2);
for i=1:length(vo_y_right)
    if yi(i,1)<= y_max_h
        for j = 1:rep_interp2
            zi_yz_rv(i,j)= sqrt(abs((1 - (yi(i,j)-y_max_h)^2/yz_a^2)...
                * yz_b^2));
        end
    else
        for j = 1:rep_interp2
            zi_yz_rv(i,j)= sqrt(abs((1 - (yi(i,j)-y_max_h)^2/yz_a^2)...
                * yz_b^2));
        end
    end
end
end

```

```

zi_yz_rv = -zi_yz_rv+zi_flat;

zi_xz_rv = nan(length(vo_y_right),rep_interp2);
for i=1:length(vo_y_right)
    xz_li_x = vo_x_left(i);
    xz_li_z = H_of_l_valve;
    xz_ri_x = vo_x_right(i);
    xz_ri_z = H_of_l_valve;
    xz_m_x = xi(i,floor(rep_interp2/2));
    xz_m_z = zi_yz_rv(i,1);

    A = [xz_li_x^2 xz_li_x 1;xz_ri_x^2 xz_ri_x 1;xz_m_x^2 xz_m_x 1];
    B = [xz_li_z; xz_ri_z; xz_m_z];
    X = A\B;
    for j=1:rep_interp2
        zi_xz_rv(i,j)=(X(1)*xi(i,j)^2)+(X(2)*xi(i,j))+X(3);
    end
end

Rvalve_surf = surf(xi,yi,zi_xz_rv); shading interp; axis equal; hold on;
Rvalve_x = Rvalve_surf.XData;
Rvalve_y = Rvalve_surf.YData;
Rvalve_z =Rvalve_surf.ZData;

%% Vertical Orientation -----

direction = [1 0 0];
origin = [xy_center_x xy_center_y-loc_max_width 0];
max_z_lims =
sind(angle_of_elevation)*(oysterheight+H_of_l_valve)+H_of_l_valve;
rotate(Lvalve_surf,direction,angle_of_elevation,origin); zlim([0
max_z_lims]); hold on;
min_rot_z = min(min(Lvalve_surf.ZData));
rotate(Rvalve_surf,direction,angle_of_elevation,origin); hold on;
% xlabel = 'x';ylabel='y';
Lvalve_X_rot = Lvalve_surf.XData; Lvalve_Y_rot = Lvalve_surf.YData;
Lvalve_Z_rot = Lvalve_surf.ZData;
Rvalve_X_rot = Rvalve_surf.XData; Rvalve_Y_rot = Rvalve_surf.YData;
Rvalve_Z_rot = Rvalve_surf.ZData;

%% Af --> projected surface area normal to the flow -----

% Ventral portion:
if angle_of_elevation > 4
    Rvalve_xzproj = nan(length(Rvalve_X_rot)-1,1);
    for i = 1:length(Rvalve_X_rot)-1
        xz_base_a = Rvalve_X_rot(i,rep_interp2)-Rvalve_X_rot(i,1);
        xz_base_b = Rvalve_X_rot(i+1,rep_interp2)-Rvalve_X_rot(i+1,1);
        xz_zdiff = abs(Rvalve_Z_rot(i+1,1)-Rvalve_Z_rot(i,1));
        Rvalve_xzproj(i) = (xz_base_a+xz_base_b)/2 * xz_zdiff;
    end
else
    min_dz = min(min(Rvalve_Z_rot)); %min height of the oyster at its
                                     %current angle of elevation
    [loc_min_dz_r, loc_min_dz_c] = find(Rvalve_Z_rot==min_dz);
    Rvalve_xzproj = nan(loc_min_dz_r-1,1);
    for i = 1:loc_min_dz_r-1

```

```

        xz_base_a = Rvalve_X_rot(i,rep_interp2)-Rvalve_X_rot(i,1);
        xz_base_b = Rvalve_X_rot(i+1,rep_interp2)-Rvalve_X_rot(i+1,1);
        xz_zdiff = abs(Rvalve_Z_rot(i+1,1)-Rvalve_Z_rot(i,1));
        Rvalve_xzproj(i) = (xz_base_a+xz_base_b)/2 * xz_zdiff;
    end
end
Rvalve_xzproj(isnan(Rvalve_xzproj)) = 0;
xz_proj_area_ventral = sum(Rvalve_xzproj);

% Dorsal portion:
if angle_of_elevation < 90
    max_dz = max(max(Lvalve_Z_rot)); %max height of the oyster at its
                                     %current angle of elevation
    %max_dy = max(max(Lvalve_Y_rot)); %leading edge of the oyster (frontal
                                     % apex) in the y direction
    Lvalve_Z_rot(isnan(Lvalve_Z_rot)) = 0;
    hvp_i = 1;
    while 1
        H_of_ventral_portion = max(Lvalve_Z_rot(hvp_i,:));
        %height of uppermost point where the left and right valves
        %(dorsal and ventral sides) meet
        if hvp_i == size(Lvalve_Z_rot,1)
            break
        else
            if H_of_ventral_portion == 0
                hvp_i = hvp_i + 1;
            else
                break
            end
        end
    end
end
[loc_max_dz_r, loc_max_dz_c] = find(Lvalve_Z_rot==max_dz);
y_at_lmxdz = Lvalve_Y_rot(loc_max_dz_r(1), loc_max_dz_c(1));
%x_at_lmxdz = Lvalve_X_rot(loc_max_dz_r(1),loc_max_dz_c(1));
for i = 1:length(vo_y_right)-1
    if y_at_lmxdz<=Lvalve_Y_rot(i,rep_interp2) &&...
        y_at_lmxdz>=Lvalve_Y_rot(i+1,rep_interp2)
        %values of Lvalve_Y_rot(i,1) and Lvalve_Y_rot(i,rep_interp2)
        % approx the same
        loc_yz_int_y_lmxdz = i;
        %loc_yz_int_y_lmxdz is the row # in Lvalve_Y_rot whose endpoints
        %(col #=1orrep_interp2)are directly below the location of the
        %max height of the oyster (at its current angle of elevation)
    end
end
yzint_at_lmxdz_x1 = Lvalve_X_rot(loc_yz_int_y_lmxdz,rep_interp2);
                                     %ends of the dorsal parabola
yzint_at_lmxdz_x2 = Lvalve_X_rot(loc_yz_int_y_lmxdz,1);
diff_x1x2 = abs(yzint_at_lmxdz_x1 - yzint_at_lmxdz_x2);
yzint_at_lmxdz_z = Lvalve_Z_rot(loc_yz_int_y_lmxdz,rep_interp2);
xz_li_x = 0; xz_li_z = 0; % pretend parabola intercepts the origin
xz_ri_x = diff_x1x2; xz_ri_z = 0;
xz_m_x = diff_x1x2/2; xz_m_z = max_dz-yzint_at_lmxdz_z;
A = [xz_li_x^2 xz_li_x 1;xz_ri_x^2 xz_ri_x 1;xz_m_x^2 xz_m_x 1];
B = [xz_li_z; xz_ri_z; xz_m_z];
X = A\B;
int_yz_array = linspace(0,diff_x1x2,rep_interp2);

```

```

int_yz = zeros(1,100);
for i=1:rep_interp2
    x = int_yz_array;
    int_yz(1,i) = (1/3)*X(1)*x(i)^3+(1/2)*X(2)*x(i)^2+X(3)*x(i);
end
y_definite_int_apex = int_yz(1,rep_interp2);
xz_m_z2 = H_of_ventral_portion-yzint_at_lmxdz_z;
A = [xz_li_x^2 xz_li_x 1; xz_ri_x^2 xz_ri_x 1; xz_m_x^2 xz_m_x 1];
B = [xz_li_z; xz_ri_z; xz_m_z2];
X = A\B;
int_yz_array = linspace(0,diff_x1x2, rep_interp2);
int_yz = zeros(1,rep_interp2);
for i =1:100
    x = int_yz_array;
    int_yz(1,i) = (1/3)*X(1)*x(i)^3+(1/2)*X(2)*x(i)^2+X(3)*x(i);
end
y_definite_int_values = int_yz(1,rep_interp2);
xz_proj_area_dorsal = y_definite_int_apex-y_definite_int_values;
else
    xz_proj_area_dorsal = 0;
end
xz_proj_area = xz_proj_area_ventral + xz_proj_area_dorsal;

% Note: the parabola being used to calculate the area of the dorsal portion
% does not exactly fit the actual curvature of shell (the dorsal, windward
% portion is actually composed of a parabola and a part of an ellipse);
% however, this approximation is used because the shape is essentially a
parabola

%% Windward wetted surface area -----

% Ventral portion:
min_dz = min(min(Rvalve_Z_rot)); %min height of the oyster at its current
                                %angle of elevation
[loc_min_dz_r, loc_min_dz_c] = find(Rvalve_Z_rot==min_dz);
y_at_lmxdz = Lvalve_Y_rot(loc_min_dz_r(1), loc_min_dz_c(1));
yzint_at_lmxdz_x1 = min(min(Rvalve_X_rot)); %ends of the dorsal parabola
yzint_at_lmxdz_x2 = max(max(Rvalve_X_rot));
windw_dorsal_x = nan(size(Rvalve_X_rot));
windw_dorsal_y = nan(size(Rvalve_X_rot));
windw_dorsal_z = nan(size(Rvalve_X_rot));
for i =1:length(Rvalve_X_rot)
    for j = 1:rep_interp2
        if Rvalve_Y_rot(i,j)>= y_at_lmxdz
            if Rvalve_X_rot(i,j)<= yzint_at_lmxdz_x2 &&
Rvalve_X_rot(i,j)>=yzint_at_lmxdz_x1
                windw_dorsal_x(i,j) = Rvalve_X_rot(i,j);
                windw_dorsal_y(i,j) = Rvalve_Y_rot(i,j);
                windw_dorsal_z(i,j) = Rvalve_Z_rot(i,j);
            end
        end
    end
end
end

%Find how many rows in windw_dorsal have at least one value
an_plchd = 0;
for i=1:length(Rvalve_X_rot)

```

```

any_nan = any(double(isnan(windw_dorsal_x(i,:)))==0);
if any_nan==1
    an_plchd = an_plchd+1;
end
end
Rvalve_SA = nan(an_plchd,1);
lvsa_plchd = 1;
for i =1:length(Rvalve_X_rot)
    Rvalve_SA_tri = 0; Rvalve_SA_trap = 0;
    for j = 1:rep_interp2-1 %find xz distance between 2 neighboring x values
        if isnan(windw_dorsal_x(i,j+1))==0 && isnan(windw_dorsal_x(i,j))==0
            Rvalve_xzdist_b1 = ...
                sqrt((abs(Rvalve_z(i,j+1)-Rvalve_z(i,j)))^2 ...
                    + (abs(Rvalve_x(i,j+1)-Rvalve_x(i,j)))^2);
        end
        if i<length(Rvalve_X_rot)
            Rvalve_ydiffSA = abs(Rvalve_y(i+1,1)-Rvalve_y(i,1));
            if isnan(windw_dorsal_x(i,j+1))==0 ...
                && isnan(windw_dorsal_x(i,j))==0
                %Find surface area of triangle/trapezoidal units:
                if isnan(windw_dorsal_x(i+1,j+1))==0 ...
                    && isnan(windw_dorsal_x(i,j))==1 %triangle
                    Rvalve_SA_tri = Rvalve_SA_tri + 0.5*Lvalve_xz_dist_b1*...
                        Rvalve_ydiffSA;
                end
                if isnan(windw_dorsal_x(i+1,j+1))==0 ...
                    && isnan(windw_dorsal_x(i,j))==0 %trapezoid
                    Rvalve_xzdist_b2 = ...
                        sqrt((abs(Rvalve_z(i+1,j+1)-...
                            Rvalve_z(i+1,j)))^2 + (abs(Rvalve_x(i+1,j+1)-...
                                Rvalve_x(i+1,j)))^2);
                    Rvalve_trap_bases = ...
                        (Rvalve_xzdist_b1+Rvalve_xzdist_b2)/2;
                    Rvalve_SA_trap = ...
                        Rvalve_SA_trap + Rvalve_trap_bases*Rvalve_ydiffSA;
                end
            end
        end
    end
    Rvalve_SA(lvsa_plchd) = Rvalve_SA_tri+Rvalve_SA_trap;
    lvsa_plchd = lvsa_plchd+1;
end
windwet_SA_Rvalve = sum(Rvalve_SA);

% Dorsal portion:
if angle_of_elevation == 90
    windwet_SA_Lvalve = 0;
else
    windw_dorsal_x = nan(size(Lvalve_X_rot));
    windw_dorsal_y = nan(size(Lvalve_X_rot));
    windw_dorsal_z = nan(size(Lvalve_X_rot));
    for i =1:size(Lvalve_X_rot,1)
        for j = 1:rep_interp2
            if Lvalve_Z_rot(i,j)>=yzint_at_lmxdz_z
                if Lvalve_Y_rot(i,j)>= y_at_lmxdz
                    if Lvalve_X_rot(i,j)>= yzint_at_lmxdz_x2 &&
Lvalve_X_rot(i,j)<=yzint_at_lmxdz_x1

```

```

        windw_dorsal_x(i,j) = Lvalve_X_rot(i,j);
        windw_dorsal_y(i,j) = Lvalve_Y_rot(i,j);
        windw_dorsal_z(i,j) = Lvalve_Z_rot(i,j);
    end
end
end
end
end
% check_wdx = isnan(windw_dorsal_x); check_wdy = isnan(windw_dorsal_y);
% check_wdz = isnan(windw_dorsal_z);
% x_z_comp = unique(check_wdx==check_wdz)
% x_y_comp = unique(check_wdx==check_wdy)
% y_z_comp = unique(check_wdy==check_wdz)
%Find how many rows in windw_dorsal have at least one value
an_plchd = 0;
for i=1:length(Lvalve_X_rot)
    any_nan = any(double(isnan(windw_dorsal_x(i,:)))==0);
    if any_nan==1
        an_plchd = an_plchd+1;
    end
end
Lvalve_SA = nan(an_plchd,1);
lvsa_plchd = 1;
for i =1:length(Lvalve_X_rot)
    Lvalve_SA_tri = 0; Lvalve_SA_trap = 0;
    for j = 1:rep_interp2-1
        %find xz distance between 2 neighboring x valvues
        if isnan(windw_dorsal_x(i,j+1))==0 ...
            && isnan(windw_dorsal_x(i,j))==0
            Lvalve_xzdist_b1 =...
                sqrt((abs(Lvalve_z(i,j+1)-Lvalve_z(i,j)))^2 ...
                    + (abs(Lvalve_x(i,j+1)-Lvalve_x(i,j)))^2);
        end
        if i<length(Lvalve_X_rot)
            Lvalve_ydiffSA = abs(Lvalve_y(i+1,1)-Lvalve_y(i,1));
            if isnan(windw_dorsal_x(i,j+1))==0 ...
                && isnan(windw_dorsal_x(i,j))==0
                %Find surface area of triangle/trapezoidal units:
                if isnan(windw_dorsal_x(i+1,j+1))==0 ...
                    && isnan(windw_dorsal_x(i,j))==1 %triangle
                    Lvalve_SA_tri = Lvalve_SA_tri + 0.5 * ...
                        Lvavle_xz_dist_b1 * Lvalve_ydiffSA;
                end
                if isnan(windw_dorsal_x(i+1,j+1))==0...
                    && isnan(windw_dorsal_x(i,j))==0 %trapezoid
                    Lvalve_xzdist_b2 = ...
                        sqrt((abs(Lvalve_z(i+1,j+1)...
                            - Lvalve_z(i+1,j)))^2 +
                            (abs(Lvalve_x(i+1,j+1)...
                                -Lvalve_x(i+1,j)))^2);
                    Lvalve_trap_bases = ...
                        (Lvalve_xzdist_b1+Lvalve_xzdist_b2)/2;
                    Lvalve_SA_trap = ...
                        Lvalve_SA_trap+Lvalve_trap_bases*Lvalve_ydiffSA;
                end
            end
        end
    end
end
end

```

```

        end
        Lvalve_SA(lvsa_plchd) = Lvalve_SA_tri+Lvalve_SA_trap;
        lvsa_plchd = lvsa_plchd+1;
    end
    windwet_SA_Lvalve = sum(Lvalve_SA);
end

windwet_SA = windwet_SA_Rvalve + windwet_SA_Lvalve;

%% Aerial surface area (xy projected area)

xy_y_diff = nan(length(Lvalve_Y_rot)-1,1);
for i = 1:length(Lvalve_Y_rot)-1 %find spacing between rows in y-direction
    xy_y_diff(i) = abs(Lvalve_Y_rot(i+1,1)-Lvalve_Y_rot(i,1));
end
xy_trap_area = nan(length(Lvalve_Y_rot)-1,1);
for i = 1:length(Lvalve_Y_rot)-1 %Find trapzoidal area of each segment (A =
(a+b)/2*h)
    xy_trap_a = Lvalve_X_rot(i,rep_interp2)-Lvalve_X_rot(i,1);
    xy_trap_b = Lvalve_X_rot(i+1,rep_interp2)-Lvalve_X_rot(i+1,1);
    xy_trap_area(i) = (xy_trap_a+xy_trap_b)/2*xy_y_diff(i);
end
xy_trap_area(isnan(xy_trap_area)==1)=0;
xy_proj_area = sum(xy_trap_area);

%% Total surface area (total wetted SA)

% Right valve
Rvalve_xzdist = nan(length(Rvalve_y),rep_interp2-1);
for i = 1:length(Rvalve_y) %find xz distance between 2 neighboring x valves
    for j = 1:rep_interp2-1
        Rvalve_xzdist(i,j) = sqrt((abs(Rvalve_z(i,j+1)-Rvalve_z(i,j)))^2 ...
            + (abs(Rvalve_x(i,j+1)-Rvalve_x(i,j)))^2);
    end
end
Rvalve_ydiffSA = nan(rep_interp2-1,1); %find spacing between rows in y-
direction
for i = 1:length(Rvalve_y)-1
    Rvalve_ydiffSA(i) = abs(Rvalve_y(i+1,1)-Rvalve_y(i,1));
end
Rvalve_SA = nan(length(Rvalve_ydiffSA),rep_interp2-1); %A = (a+b)/2*h
rvsa_plchd = 1;
for i = 1:length(Rvalve_ydiffSA) %find area of trapazoid
    for j = 1:rep_interp2-1
        Rvalve_trap_bases = (Rvalve_xzdist(rvsa_plchd+1,j) ...
            + Rvalve_xzdist(rvsa_plchd,j))/2;
        Rvalve_SA(i,j) = Rvalve_trap_bases*Rvalve_ydiffSA(i);
    end
    rvsa_plchd = rvsa_plchd+1;
end

% Left valve
Lvalve_xzdist = nan(length(Lvalve_y),rep_interp2-1);
for i = 1:length(Lvalve_y) %find xz distance between 2 neighboring x valves
    for j = 1:rep_interp2-1
        Lvalve_xzdist(i,j) = sqrt((abs(Lvalve_z(i,j+1)-Lvalve_z(i,j)))^2...
            + (abs(Lvalve_x(i,j+1)-Lvalve_x(i,j)))^2);
    end
end

```



```

    end
end
Lvalve_ydiffSA = nan(rep_interp2-1,1); %find spacing between rows in
                                     %y-direction
for i = 1:length(Lvalve_y)-1
    Lvalve_ydiffSA(i) = abs(Lvalve_y(i+1,1)-Lvalve_y(i,1));
end
Lvalve_SA = nan(length(Lvalve_ydiffSA),rep_interp2-1); %A = (a+b)/2*h
rvsa_plchd = 1;
for i = 1:length(Lvalve_ydiffSA) %find area of trapazoid
    for j = 1:rep_interp2-1
        Lvalve_trap_bases =
(Lvalve_xzdist(rvsa_plchd+1,j)+Lvalve_xzdist(rvsa_plchd,j))/2;
        Lvalve_SA(i,j) = Lvalve_trap_bases*Lvalve_ydiffSA(i);
    end
    rvsa_plchd = rvsa_plchd+1;
end
roughness_SA = sum(nansum(Rvalve_SA))+sum(nansum(Lvalve_SA));

%% Spacing -----

length_y = (max(max(Lvalve_Y_rot)))-(min(min(Lvalve_Y_rot)));
width_x = (max(max(Lvalve_X_rot)))-(min(min(Lvalve_X_rot)));
H_of_DorsHigh = Lvalve_Z_rot(loc_Lv_hpr_r, loc_Lv_hpr_c);
%area of virtual oyster:
vo_ideal_area = length_y*width_x;
%length of side of sqr oyster with the same area as the virtual oyster
voi_side = sqrt(vo_ideal_area);
%find number of evenly distributed units in N
Nsqr = round(sqrt(N));
% Nsqr = sqrt(N);
%Space between Nsqr equidistant sqr oysters
lambda_bio = (100-(voi_side*Nsqr))/(Nsqr+1)+voi_side/2;
% lambda_bio = (100-(voi_side*Nsqr))/(Nsqr+1)+voi_side;
% if lambda_bio<0
%     errordlg('The given oyster density is not possible, please adjust');
% end

if any(Rvalve_z(:)>H_of_DorsHigh(1,1))
    i = 1;
    plchd = max(max(Rvalve_Z_rot));
    while plchd > H_of_DorsHigh
        plchd = Rvalve_Z_rot(i,loc_Lv_hpr_c);
        i = i+1;
    end
    matching_rv_hodh_y = Rvalve_Y_rot(i-2,loc_Lv_hpr_c)-
(min(min(Lvalve_Y_rot)));
    num_vo_in_yaxis = floor((100-length_y)/matching_rv_hodh_y(1,1));
    num_vo_in_xaxis = floor(100/width_x);
else
    num_vo_in_yaxis = floor(100/length_y);
    num_vo_in_xaxis = floor(100/width_x);
end
total_allow_density = num_vo_in_yaxis*num_vo_in_xaxis;

% if total_allow_density < N

```

```

%      errordlg('The given number of oysters m^-2 (N) may be unrealistic for
oysters of this size');
% else
%      msgbox({'The chosen oyster density is reasonable'}, 'Density');
% end

%% Create biogenic roughness parameters

eta_bio = max(max(Lvalve_surf.ZData)); %height of roughness element
s_bio = (max(max(Lvalve_surf.YData)))-(min(min(Lvalve_surf.YData)));
% s = streamise length of the roughness elements (parallel to flow)
b_bio = (max(max(Lvalve_surf.XData)))-(min(min(Lvalve_surf.XData)));
% b_bio = spanwise length of roughness elements (transverse to flow)
Af = xz_proj_area; %projected surface area normal to flow
As = windwet_SA;
aerial_a = xy_proj_area;
lmw = loc_max_width;

end

```

## Biodeposit\_Suspension.m

```

%% Biodeposit Suspension
% This is used to determine whether biodeposit suspension occurs during a
% given timestep (i.e the shear stress acting on the interstitial sediments
% is > than the critical shear stress)

%% Biodeposit Suspension
%% Calculate shear stress between oysters

if oysters_include == 0
    ustar_grain = VEL_avrg(i)/((1/0.4)*log(ref_height/sed_zo));
    ustar_total = ustar_grain;
    tau_total = RHO_avrg(i)*ustar_grain^2;
    tau_s = tau_total;
    tau_unobstr = tau_total;
    Cd = ustar_total^2/VEL_avrg(i)^2;
    zo_bio = NaN;
    if tau_s >= tau_crit
        HYDRO.susp_indicator(i) = 1;
    else
        HYDRO.susp_indicator(i) = 0;
    end
else
    kin_visc = ROMS.visc(i)/RHO_avrg(i);
    ustar_grain = VEL_avrg(i)/((1/0.4)*log(ref_height/zo_grain_m));
    tau_unobstr = RHO_avrg(i)*ustar_grain^2;
    Cg = ustar_grain^2/VEL_avrg(i)^2;
    if LAMBDA <= 0.1
        zo_bio = 0.5*eta_bio*LAMBDA;%height of roughness element (Letau 1967)
        zo_bio_m = zo_bio/100;
        ustar_total = VEL_avrg(i)/((1/0.4)*log(ref_height/zo_bio_m));
        Cd = ustar_total^2/VEL_avrg(i)^2;
        tau_total = RHO_avrg(i)*ustar_total^2;
        BETA = Cr/Cg;
        ts_tt = 1/(1+(LAMBDA/BETA)); %ratio of ground surface drag to total
                                   % drag
        tau_s = ts_tt*tau_total; %shear stress on intervening ground surface
    else
        if LAMBDA <= 0.25
            zo_bio = eta_bio*(1.6*LAMBDA*(1-1.67*ETA));
        else
            zo_bio = 5*eta_bio/30; %Styles
        end
        zo_bio_m = zo_bio/100;
        ustar_total = VEL_avrg(i)/((1/0.4)*log(ref_height/zo_bio_m));
        Cd = ustar_total^2/VEL_avrg(i)^2;
        BETA = Cr/Cg;
        tau_total = RHO_avrg(i)*ustar_total^2;
        ts_tt = (1-((BETA*LAMBDA_e)/(1+BETA*LAMBDA_e)))*exp(-bs*ETA);
        ts = ts_tt*tau_total;
        tau_s = ts;
    end
end

%Record: -----
HYDRO.ustar_grain(i) = ustar_grain;

```

```

HYDRO.ustar_total(i) = ustar_total;
HYDRO.tau_grain(i) = tau_s; %tau_grain; JEREMY Switched
HYDRO.tau_total(i) = tau_total;
HYDRO.tau_unobstr(i) = tau_unobstr;
HYDRO.Cd(i) = Cd;
HYDRO.zo_bio(i) = zo_bio;

%% Resuspension and the growth/decay of the biodeposit sublayers

if BD_AdvD_include
    if tau_s >= tau_crit %suspension occurs
        %'BD_suspension' serves as the input to the transport adv-diffusion
        % matrices
        if i == 1
            BD_suspension{i} = starting_BDL_S1_m2 + BD_input_inst_m2(1,:);
                                % ( mg m^-2 hr^-1)
        else
            BD_suspension{i} = BD_layer_S1_m2{i-1} + BD_input_inst_m2(1,:);
        end
        HYDRO.susp_indicator(i) = 1; % for use in createlowdepflux.m
    else %suspension does not occur (deposition directly to S1)
        if i == 1
            BD_layer_S1_m2{i}(1,:) = ...
                (starting_BDL_S1_m2 + BD_input_inst_m2(1,:)) * exp(S1_decay);
            BD_layer_S2_m2{i}(1,:) = ...
                ((starting_BDL_S1_m2 + BD_input_inst_m2(1,:)) ...
                * (1 - exp(S1_decay))) + starting_BDL_S2_m2;
        else
            BD_layer_S1_m2{i}(1,:) = (BD_layer_S1_m2{i-1}(1,:) + ...
                BD_input_inst_m2(1,:)) * exp(S1_decay);
            BD_layer_S2_m2{i}(1,:) = ((BD_layer_S1_m2{i-1}(1,:) + ...
                BD_input_inst_m2(1,:)) * (1 - exp(S1_decay))) ...
                + BD_layer_S2_m2{i-1}(1,:);
        end
        BD_suspension{i} = zeros(1, Boxnum);
        HYDRO.susp_indicator(i) = 0;
    end
end

%% Biodeposit Transport (Advection-Diffusion equations)

if BD_AdvD_include
    if tau_s >= tau_crit %suspension occurs

        tt_perc = transport_trckr/i;
        fprintf('Calculating transport....[ %d/%d  (%.3g%%)] \n', ...
            transport_trckr, i, tt_perc);
        transport_trckr = transport_trckr + 1;

        Biodeposit_Transport

        %Update biodeposit sublayer:
        if i == 1
            BD_layer_S1_m2{i}(1,:) =
                (starting_BDL_S1_m2 + REEF_Deposition{i}(1,:)) * exp(S1_decay);
            BD_layer_S2_m2{i}(1,:) = REEF_Deposition{i}(1,:) * (1 -
                exp(S1_decay)) + starting_BDL_S2_m2;
        end
    end
end

```

```

        else
            BD_layer_S1_m2{i}(1,:) = REEF_Deposition{i}(1,:)*exp(S1_decay);
            BD_layer_S2_m2{i}(1,:) = REEF_Deposition{i}(1,:)*(1-
exp(S1_decay)) ...
            + BD_layer_S2_m2{i-1}(1,:);
        end
        BIODEP.toSed{i} = REEF_Deposition{i};
    else
        BIODEP.toSed{i} = BD_input_inst_m2;
    end
else
    BIODEP.toSed{i} = BD_input_inst_m2;
end

%% Update output structures:

%Hourly:
BIODEP.flux{i} = BD_input_inst_m2;
BIODEP.conc{i} = BD_layer_S1_m2{i};
BIODEP.rate{i} = biodep_rate;

%Daily:
DVi.conc(hr_i,:) = BIODEP.conc{i}(1,:);
DVi.toSed(hr_i,:) = BIODEP.toSed{i};
DVi.flux(hr_i,:) = BIODEP.flux{i};
%Daily output:
if END_DAY
    BIODEP.conc_daily{dv_trckr} = sum(DVi.conc);
    BIODEP.flux_daily{dv_trckr} = sum(DVi.flux);
    BIODEP.toSed_daily{dv_trckr} = sum(DVi.toSed);
    percComp = (dv_trckr/numdays)*100;
    fprintf('%s=%d - %d/%d
(%.3g%%)\n', 'N', N_array(msni), dv_trckr, numdays, percComp);
end

```

## Biodeposit\_Transport.m

```

%% Setup

num_iterations = 100;
u_cm_sec = VEL_avrg(i)*100;
if u_cm_sec <= 30
    dx_BDT = 30;
else
    dx_BDT = ceil(u_cm_sec/10)*10;
end
nD_nodes_BDT = 40;
dz_BDT = depth_cm/nD_nodes_BDT;
z1_BDT = dz_BDT:dz_BDT:depth_cm;
dt = 1; %timestep in seconds

% Velocity values:
ubar = ones(1,num_iterations)*u_cm_sec;
ws_ts = ws*100; %cm/s
ustar_BDT = zeros(1,num_iterations);
u1_BDT=cell(nD_nodes_BDT,1);
for ib=1:num_iterations %**
    ustar_BDT(ib)=2*ubar(ib)*(depth_cm-
(z0))/(5*(z0+depth_cm*(log(depth_cm/z0)-1))); %u*
    for z=1:nD_nodes_BDT
        u1_BDT{z}(ib)=(ustar_BDT(ib)/0.4)*log(z1_BDT(z)/z0); %cm/hr
    end
end

% Find vertical diffusivity values:
K_BDT=cell(num_iterations,1);
for ib=1:num_iterations
    K_BDT{ib}=nan(size(z1_BDT));
end
dkdz_BDT = cell(num_iterations,1);
for ib = 1:num_iterations
    dkdz_BDT{ib}=nan(size(z1_BDT));
end
for ib=1:num_iterations
    for z=1:nD_nodes_BDT
        K_BDT{ib}(z)=0.4*ustar_BDT(ib)*z1_BDT(z)*(1-(z1_BDT(z)/depth_cm));
        dkdz_BDT{ib}(z)=0.4*ustar_BDT(ib)*(1-2*(z1_BDT(z)/depth_cm));
    end
end

%Make horizontal grid cells:
Boxnum_BDT = ceil(Reef_length*100/dx_BDT); %Mindy rounded up 2/4/2021
BD_dim = nD_nodes_BDT*Boxnum_BDT;

%% Create index arrays

bd_x_ind = zeros(nD_nodes_BDT,Boxnum_BDT);
bd_z_ind = zeros(nD_nodes_BDT,Boxnum_BDT);
for ib = 1:Boxnum_BDT
    bd_x_ind(:,ib) = ib;
end

```

```

for j_BDT = 1:nD_nodes_BDT
    bd_z_ind(j_BDT,:) = j_BDT;
end
bd_x_ind = reshape(bd_x_ind,[BD_dim,1]);
bd_z_ind = reshape(bd_z_ind,[BD_dim,1]);

%% Create matix of boundary condition indeces:

boundC = zeros(nD_nodes_BDT,Boxnum_BDT);
boundC(1,1) = 1;
for ib = 2:Boxnum_BDT-1
    boundC(1,ib) = 2;
end
boundC(1,Boxnum_BDT) = 3;
for ib = 2:nD_nodes_BDT-1
    boundC(ib,Boxnum_BDT) = 4;
end
boundC(nD_nodes_BDT,Boxnum_BDT) = 5;
for ib = 2:Boxnum_BDT-1
    boundC(nD_nodes_BDT,ib) = 6;
end
boundC(nD_nodes_BDT,1) = 7;
for ib = 2:nD_nodes_BDT-1
    boundC(ib,1) = 8;
end
bound_index = reshape(boundC,[BD_dim,1]);

%% Time-domain matrix

if UX_dir_switch_hourly(i) == 1
    BD_susp_prime = BD_suspension{i};
else
    BD_susp_prime = fliplr(BD_suspension{i});
end
%Re-arrange BD_suspension to fit dimensions of BD adv-diff grid
dx_in_dxBDT = dx_BDT/dx; % # of model BD_sublayer gridcells in one BD adv-
diff gridcell
BD_susp = zeros(1,Boxnum_BDT);
bds_plchd = 1;
for nz = 1:Boxnum_BDT/2
    BD_susp(nz) = mean(BD_susp_prime(bds_plchd:bds_plchd+dx_in_dxBDT-1));
    bds_plchd = bds_plchd + dx_in_dxBDT;
end

Biodeposits = cell(num_iterations,1);
BD = zeros(nD_nodes_BDT,Boxnum_BDT);
A = zeros(BD_dim); %The coefficient matrix

for ni = 1:num_iterations

    if ni == 1
        BD_input = zeros(nD_nodes_BDT,Boxnum_BDT);
        % BD_input(nD_nodes_BDT - nD_nodes_BDT/4,:) = BD_susp;
        BD_input(nD_nodes_BDT/2,:) = BD_susp;
    else
        BD_input = zeros(nD_nodes_BDT,Boxnum_BDT);
    end
end

```

```

end

%Add input matrix to existing biodeposit concentrations:
if ni == 1
    BD = BD + BD_input;
else
    BD = Biodeposits{ni-1}+BD_input;
end
BD_n = reshape(BD, [BD_dim,1]);

%Calculate next time step:
for ib = 1:BD_dim
    if ws_ts + dkdz_BDT{ni}(bd_z_ind(ib)) < 0
        gamma = 0;
    else
        gamma = 1;
    end

    ab = dt*(K_BDT{ni}(bd_z_ind(ib))/dz_BDT^2 +
dkdz_BDT{ni}(bd_z_ind(ib))/dz_BDT*gamma + ws_ts/dz_BDT*gamma);
    bb = dt*(-2*K_BDT{ni}(bd_z_ind(ib))/dz_BDT^2 +
dkdz_BDT{ni}(bd_z_ind(ib))/dz_BDT*((1-gamma)-gamma)...
    + ws_ts/dz_BDT*((1-gamma)-gamma)) - 1;
    cb = dt*(K_BDT{ni}(bd_z_ind(ib))/dz_BDT^2 -
dkdz_BDT{ni}(bd_z_ind(ib))/dz_BDT*(1-gamma) - ws_ts/dz_BDT*(1-gamma));
    if bound_index(ib) == 1 || bound_index(ib) == 8 || bound_index(ib) ==
7
        rb = -BD_n(ib) +
dt*u1_BDT{bd_z_ind(ib)}(ni)/dx_BDT*(BD(bd_z_ind(ib),bd_x_ind(ib))-outBD);
    else
        rb = -BD_n(ib) +
dt*u1_BDT{bd_z_ind(ib)}(ni)/dx_BDT*(BD(bd_z_ind(ib),bd_x_ind(ib))-
BD(bd_z_ind(ib),bd_x_ind(ib)-1));
    end

    %Fill matrices A and BD_n:
    A(ib,ib) = bb;
    switch bound_index(ib)
        case 0 %interior nodes
            A(ib,ib+1) = ab;
            A(ib,ib-1) = cb;
            BD_n(ib) = rb;
        case 1 %bottom left corner
            A(ib,ib+1) = ab;
            BD_n(ib) = rb - cb*BD_n(ib);
        case 2 %bottom row
            A(ib,ib+1) = ab;
            BD_n(ib) = rb - cb*BD_n(ib);
        case 3 %bottom right corner
            A(ib,ib+1) = ab;
            BD_n(ib) = rb - cb*BD_n(ib);
        case 4 %right column
            A(ib,ib+1) = ab;
            A(ib,ib-1) = cb;
            BD_n(ib) = rb;
        case 5 %top right corner
            A(ib,ib-1) = cb;

```



```

        BD_n(ib) = rb - ab*0;
    case 6 %top row
        A(ib,ib-1) = cb;
        BD_n(ib) = rb - ab*0;
    case 7 %top left corner
        A(ib,ib-1) = cb;
        BD_n(ib) = rb - ab*0;
    case 8 %left column
        A(ib,ib+1) = ab;
        A(ib,ib-1) = cb;
        BD_n(ib) = rb;
    end
end
A = sparse(A);
BDn_plus = A\BD_n;
BDn_plus(BDn_plus<0) = 0;
Biodeposits{ni} = reshape(BDn_plus,[nD_nodes_BDT,Boxnum_BDT]);
end

%% Find deposition profile:
starting_sum = sum(BD_susp)/num_iterations;
bottom_dep_perc = zeros(num_iterations,Boxnum_BDT);
for nj = 1:num_iterations
    inst_sum_BDT = sum(sum(Biodeposits{nj}));
    bottom_dep_perc(nj,:) = (Biodeposits{nj}(1,:)./inst_sum_BDT)*...
        (inst_sum_BDT/starting_sum);
end
bdp_summed = sum(bottom_dep_perc);

total_int = trapz(1:Boxnum_BDT,bdp_summed);
bottom_perc_total= bdp_summed./total_int;
botperc_tot_tracker{i} = bottom_perc_total;

%% Connect deposition profile to the BD sublayer:

rd_plchd = 1;
perc = nan(1,Boxnum*2);
for nj = 1:Boxnum_BDT
    pv = bottom_perc_total(nj)/(dx_in_dxBDT*2);
    perc(rd_plchd:rd_plchd+(dx_in_dxBDT*2)-1) = ones(1,dx_in_dxBDT*2)*pv;

    rd_plchd = rd_plchd + dx_in_dxBDT*2;
end
deposition = perc*sum(BD_susp_prime);

if UX_dir_switch_hourly(i) == 1
    REEF_Deposition{i} = deposition(1:Boxnum);
    RAdjSed_Deposition{i} = deposition(Boxnum+1:Boxnum*2);
else
    REEF_Deposition{i} = fliplr(deposition(1:Boxnum));
    RAdj_Deposition{i} = fliplr(deposition(Boxnum+1:Boxnum*2));
end

```

### runSFM.m

```
function [input,output] = run_SFM_NODM(input,output,dv_trckr)

% This script connects the filtration and biodeposition models to SFM
varNames = input.varNames;
nVars = input.nVars;
model_dn =
datenum([input.year_of_sim,1,input.intg_day_of_ts(dv_trckr),0,0,0]);
model_ds = datestr(model_dn,'mm/dd/yy');

% Delete existing files:
% files2remove = {input.sfmcon.inputname; 'sed.inp';
input.olwc_inputName;...
%         'outfile'; 'RCAF14'; 'RCAF14.txt'; 'RCAFICSED'}};
% for f2r = 1:length(files2remove)
%     if exist(files2remove{f2r},'file') == 2
%         delete(files2remove{f2r})
%     end
% end

%% Create OLWC file::

%Use the olwc concentrations calculated in setup_SFM_NODM in order to
% build the hourly olwc input structure.
%Incorporate POC/PON/POP from the biodeposit layer:
olwc = input.olwc_ref;
for v = 1:nVars.olwc
    if input.isn.olwc(v)
        vi = input.olwc.(varNames.olwc{v})(dv_trckr);
    else
        vi = input.olwc.(varNames.olwc{v}){dv_trckr};
    end
    if strcmp(varNames.olwc{v},'jpoc')
        olwc.jpoc = vi + mean(input.POC_to_SFM);
    elseif strcmp(varNames.olwc{v},'jpon')
        olwc.jpon = vi + mean(input.PON_to_SFM);
    elseif strcmp(varNames.olwc{v},'jpop')
        olwc.jpop = vi + mean(input.POP_to_SFM);
    else
        olwc.(varNames.olwc{v}) = vi;
    end

    %Update output structure:
    if input.isn.olwc(v)
        output.olwc.(varNames.olwc{v})(dv_trckr) = ...
            olwc.(varNames.olwc{v});
    else
        output.olwc.(varNames.olwc{v}){dv_trckr} = ...
            olwc.(varNames.olwc{v});
    end
end

% Make the file:
createsfmolwctvf_alg(olwc);

%% Create sed input file:
```

```

input.sed.sedtemp = output.olwc.temp(dv_trckr);
input.sed.descript = model_ds;

createsedinput(input.sed);

%Save to output structure:
for k = 1:nVars.sed
    ki = input.sed.(varNames.sed{k});
    if isempty(ki)
        output.sed.(varNames.sed{k})(dv_trckr) = nan;
    else
        if input.isn.sed(k)
            svL = length(ki);
            if svL > 1
                if dv_trckr == 1
                    output.sed.(varNames.sed{k}) = nan(input.numdays,svL);
                end
                output.sed.(varNames.sed{k})(dv_trckr,:) = ki;
            else
                output.sed.(varNames.sed{k})(dv_trckr) = ki;
            end
        else
            output.sed.(varNames.sed{k}){dv_trckr} = ki;
        end
    end
end

%% Make control file:
input.sfmcon.time = 1;
% input.sfmcon.descrip = model_ds;
createsfmcontrol(input.sfmcon);

%% Run model

% This line actually runs the model:
runSFM = sprintf('sfm_w_poc_lim.exe < %s >
outfile',input.sfmcon.inputname);
system(runSFM);

% Parse the text output into a structure:
[sfmoutput] = parseoutput(olwc);

%% Save output
for k = 1:nVars.sfmout
    if input.isn.sfmout(k)
        output.sfmout.(varNames.sfmout{k})(dv_trckr) = ...
            sfmoutput.(varNames.sfmout{k});
    else
        output.sfmout.(varNames.sfmout{k}){dv_trckr} = ...
            sfmoutput.(varNames.sfmout{k});
    end
end

%% Convert units in the sfm output to match sed.inp

m2 = 0.36;
for k=1:size(input.SedOut(2))

```

```

if k <= input.ucovL
    input.sed.(input.SedOut{2,k}) = ...
                                sfmoutput.(input.SedOut{1,k})*1e6*m2;
                                %converts from mg/g to mg/m3 for PON/POC/POP
else
    input.sed.(input.SedOut{2,k}) = sfmoutput.(input.SedOut{1,k});
end
end
end

```

## initialize\_OLWC.m

```
function [input] = initialize_OLWC(input)

% This script connects the filtration and biodeposition models to SFM:
cims = input.CIMS;
varNames = input.varNames;

%% Build olwc structure using averaged daily values from the cims data: -----
for i = 1:input.numdays
    model_dn = datenum([input.year_of_sim,1,input.unique_days(i),0,0,0]);
    model_ds = datestr(model_dn,'mm/dd/yy');

    %Get index of cims values from the same days as the current model
    %timestep:
    [~,MM, DD] = datevec(model_dn);
    [Ystart,~] = datevec(cims.datetimei(1,1));
    [Yend,~] = datevec(cims.datetimei(end,1));
    nYrs = Yend - Ystart +1;
    dn_allYrs = datenum([(Ystart:Yend)', repelem(MM,nYrs,1), ...
        repelem(DD,nYrs,1)]);
    [cday_indx,~] = ismember(cims.datetimei,dn_allYrs);

    %Create input structure that will be used to create olwctcf file:
    olwc = input.olwc_ref;
    olwc_vars = ...
        {'jpoc', 'jpon', 'jpop', 'jsorp', 'jsorsi', 'po4', 'nh4', 'no23', 'si'};
    cims_vars = ...
        {'JdepC', 'JdepN', 'JdepP', 'JdepPsorp', 'JdepSi', 'po4i', 'nh4i', 'no23i', 'sii'};
    for v = 1:length(olwc_vars)
        if strcmp(olwc_vars{v}, 'jsorp')
            olwc.(olwc_vars{v}) = olwc.jpoc * (input.adj_jsorp);
        else
            vi = mean(cims.(cims_vars{v}))(cday_indx), 'omitnan');
            if strcmp(olwc_vars{v}, 'jsorsi')
                olwc.(olwc_vars{v}) = vi * 1.4;
            else
                olwc.(olwc_vars{v}) = vi;
            end
        end
    end

end

olwc.inputname = input.olwc_inputName;
olwc.sal = NaN;
olwc.temp = NaN;
olwc.time = model_dn;
olwc.do = NaN;
olwc.abbrev = cims.station;
olwc.descrip = model_ds;
olwc.yrprimed = 1;
olwc.realtime = model_dn;

%Save to output structure:
for k = 1:input.nVars.olwc
    if input.isn.olwc(k)
```

```
        input.olwc.(varNames.olwc{k})(i) = olwc.(varNames.olwc{k});  
    else  
        input.olwc.(varNames.olwc{k}){i} = olwc.(varNames.olwc{k});  
    end  
end  
end
```

### chopROMS\_NODM.m

```
%% Imports ChopROMS variables into NODM workspace:
% Retrieve the depth, mainstream (depth-averaged) velocity, depth-specific
% velocity, temperature, and salinity values from the netCDF files. Each
% array element corresponds to a chopROMS model timestep
%(duration = 10 minutes).

%% Depth and S-nodes:
% Note: many of the commands/calaculations are only here in case the user
% chooses to use a# of depthnodes that besides the default 20 for the Chl-a
% advection-diffusion grid

%Retrieve the water depth at the reef location that is given by chopROMS.
bathymetry = nc_varget(f, 'h');
depth = bathymetry(lat_loc, lon_loc);
clear bathymetry

s = nc_varget(f, 's_rho');
n_nodes = length(s); % number of ROMS depth nodes
deltad = depth/nDepth_nodes; %height increment of depth node
s_nodes_depths = (s.*depth)*-1; %array of s-nodes dpeths from surface
                                %Note: first enry is the bottomost s-node

z1 = zeros(nDepth_nodes,1);
z1(1) = 0.5*deltad;
for i = 2:nDepth_nodes %z1 = the array of the centerpoints of gridcells
    z1(i) = z1(i-1)+deltad; %z1 = the height above the bottom
end

                                %Note: s_nodes_depths and z1 should reflect
                                %the same information, but their contents
                                %should be inverses of eachother
z2 = depth - z1; %Match z1 to s_nodes_depth (should == s_node_depths)
s_nodes = zeros(nDepth_nodes,1);
k = nan(n_nodes,1);
%s_nodes = array holding teh s-grid locations of z1 values

for w = 1:(nDepth_nodes)
    for i = 1:(n_nodes)
        k(i) = abs(s_nodes_depths(i)-z2(w));
    end
    [M,I] = min(k);
    s_nodes(w) = I;
    if length(I) > 1
        error = errordlg('manual allocation of nodes is neccessary');
    end
end

%% Retrieve varabiles from chopROMS output for entire oyster growing season:
cROMS_vars = cell(6,1);
for i = 1:6
    cROMS_vars{i} = cell(num_ROMS_files,1);
end

for i =1:num_ROMS_files
    if i<10
        cROMS_fname = 'choproms_his_000';
```

```

else
    cROMS_fname = 'choproms_his_00';
end
j = num2str(i);
cROMS_fext = '.nc';
f_i = [cROMS_fname j cROMS_fext];

%% Velocity
u_velocity = nc_varget(f_i, 'u');
UVEL_i = cell(nDepth_nodes, 1);
for n = 1:nDepth_nodes
    UVEL_i{n} = squeeze(u_velocity(:, s_nodes(n), lat_loc, lon_loc));
end
cROMS_vars{1}{i} = UVEL_i;
clear('u_velocity', 'UVEL_i');

v_velocity = nc_varget(f_i, 'v');
VVEL_i = cell(nDepth_nodes, 1);
for n = 1:nDepth_nodes
    VVEL_i{n} = squeeze(v_velocity(:, s_nodes(n), lat_loc, lon_loc));
end
cROMS_vars{2}{i} = VVEL_i;
clear('v_velocity', 'VVEL_i');

%Find mainstream velocity:
UBAR_ROMS_U = nc_varget(f_i, 'ubar');
cROMS_vars{3}{i} = squeeze(UBAR_ROMS_U(:, lat_loc, lon_loc));
clear('UBAR_ROMS_U');

VBAR_ROMS_V = nc_varget(f_i, 'vbar');
cROMS_vars{4}{i} = squeeze(VBAR_ROMS_V(:, lat_loc, lon_loc));
clear('VBAR_ROMS_V');
%UBAR and VBAR are given in meters/second

%% Salinity, Temperature, and Density
dds_loc = 2;

salinity = nc_varget(f_i, 'salt');
cROMS_vars{5}{i} = squeeze(salinity(:, dds_loc, lat_loc, lon_loc));
clear('salinity');

temperature = nc_varget(f_i, 'temp');
cROMS_vars{6}{i} = squeeze(temperature(:, dds_loc, lat_loc, lon_loc));
clear('temperature');

end

%% start-time adjustment: -----

% This section applies the minute time restructuring described in
Time_chopROMS_NODM.m

UVEL = cell(num_ROMS_files, 1);
VVEL = cell(num_ROMS_files, 1);
UBAR = cell(num_ROMS_files, 1);
VBAR = cell(num_ROMS_files, 1);
TEMP = cell(num_ROMS_files, 1);

```



```

SAL = cell(num_ROMS_files,1);

final_cROMS_vars = {UVEL VVEL UBAR VBAR TEMP SAL};

for i = 1:length(final_cROMS_vars)
    if i < 3 %UVEL and VVEL
        final_cROMS_vars{i} = cell(num_ROMS_files,1);
        for j = 1:num_ROMS_files
            for k = 1:nDepth_nodes
                if k ==1
                    final_cROMS_vars{i}{j} = cell(nDepth_nodes,1);
                end
                if j==1
                    final_cROMS_vars{i}{j}{k} = ...
                        cROMS_vars{i}{j}{k}(1:length(cROMS_vars{i}{j}{k})-1);
                else
                    last_ts = ...
                        cROMS_vars{i}{j-1}{k}(length(cROMS_vars{i}{j-1}{k}));
                    final_cROMS_vars{i}{j}{k} = ...
                        [last_ts; cROMS_vars{i}{j}{k}(1:length(cROMS_vars{i}{j}{k})-1)];
                end
            end
        end
    else
        for j = 1:num_ROMS_files
            if j==1
                final_cROMS_vars{i}{j} = ...
                    cROMS_vars{i}{j}(1:length(cROMS_vars{i}{j})-1);
            else
                last_ts = cROMS_vars{i}{j-1}(length(cROMS_vars{i}{j-1}));
                final_cROMS_vars{i}{j} = ...
                    [last_ts;cROMS_vars{i}{j}(1:length(cROMS_vars{i}{j})-1)];
            end
        end
    end
end

UVEL = final_cROMS_vars{1}; VVEL = final_cROMS_vars{2};
UBAR = final_cROMS_vars{3}; VBAR = final_cROMS_vars{4};
TEMP = final_cROMS_vars{5}; SAL = final_cROMS_vars{6};
clear('cROMS_vars'); clear('final_cROMS_vars');

%% Create a single matrix for each variable -----

UVEL_cROMS = nan(nDepth_nodes,length(ocean_time));
VVEL_cROMS = nan(nDepth_nodes,length(ocean_time));
UBAR_cROMS = nan(length(ocean_time),1);
VBAR_cROMS = nan(length(ocean_time),1);
TEMP_cROMS = nan(length(ocean_time),1);
SAL_cROMS = nan(length(ocean_time),1);

ats_plchd = 1;
for i =1:num_ROMS_files
    for j = 1:nDepth_nodes
        UVEL_cROMS(j,ats_plchd:nts_inFiles_summed(i)) =
            UVEL{i}{j}(1:nts_inFiles_STA(i));
        VVEL_cROMS(j,ats_plchd:nts_inFiles_summed(i)) = ...

```

```

VEL{i}{j}(1:nts_inFiles_STA(i));
    end
    UBAR_cROMS(ats_plchd:nts_inFiles_summed(i)) = ...
UBAR{i}(1:nts_inFiles_STA(i));
    VBAR_cROMS(ats_plchd:nts_inFiles_summed(i)) = ...
VBAR{i}(1:nts_inFiles_STA(i));
    TEMP_cROMS(ats_plchd:nts_inFiles_summed(i)) = ...
TEMP{i}(1:nts_inFiles_STA(i));
    SAL_cROMS(ats_plchd:nts_inFiles_summed(i)) = ...
SAL{i}(1:nts_inFiles_STA(i));
    ats_plchd = nts_inFiles_summed(i)+1;
end

%% Find along-channel velocity -----

% Note: rot2xy is used to transform the velocity components from true north
% so that u- and
% v- are oriented towards teh major axis of the reef.
% --> ex: if the major axis of the reef in question is oriented in a
% straight east-west direction, then a 90 angle of transformation should be
% entered as an input to the
%     rot2xy fucntion.

% depth-integrated
VEL_AC = cell(num_ROMS_files,1);
for i=1:num_ROMS_files
    VEL_AC{i} = (rot2xy(UBAR{i},VBAR{i},angle))';
end
VEL_AC_all_ts = (rot2xy(UBAR_cROMS,VBAR_cROMS,angle))';

% depth-specific
UX = cell(num_ROMS_files,1);
for i=1:num_ROMS_files
    UX{i} = nan(nDepth_nodes,nts_inFiles_STA(i));
    for j = 1:nDepth_nodes
        UX{i}(j,:) = rot2xy(UVEL{i}{j},VVEL{i}{j},angle);
    end
end
UX_all_ts = rot2xy(UVEL_cROMS,VVEL_cROMS,angle);

%% Find velocity oriented to true north-----
% depth-integrated
VEL_0 = cell(num_ROMS_files,1);
for i=1:num_ROMS_files
    VEL_0{i} = (rot2xy(UBAR{i},VBAR{i},0))';
end
VEL_0_all_ts = (rot2xy(UBAR_cROMS,VBAR_cROMS,0))';

% depth-specific
UX_0 = cell(num_ROMS_files,1);
for i=1:num_ROMS_files
    UX_0{i} = nan(nDepth_nodes,nts_inFiles_STA(i));
    for j = 1:nDepth_nodes
        UX_0{i}(j,:) = rot2xy(UVEL{i}{j},VVEL{i}{j},0);
    end
end
UX_0_all_ts = rot2xy(UVEL_cROMS,VVEL_cROMS,0);

```

## References

- Asmus, R. M., & Asmus, H. (1991). Mussel beds: limiting or promoting phytoplankton?. *Journal of Experimental Marine Biology and Ecology*, 148(2), 215-232.
- Beck, M. W., Brumbaugh, R. D., Airoidi, L., Carranza, A., Coen, L. D., Crawford, C., ... & Guo, X. (2011). Oyster reefs at risk and recommendations for conservation, restoration, and management. *Bioscience*, 61(2), 107-116.
- Bernard, F. R. (1974). Particle sorting and labial palp function in the Pacific oyster *Crassostrea gigas* (Thunberg, 1795). *The Biological Bulletin*, 146(1), 1-10.
- Butman, C. A., Fréchette, M., Geyer, W. R., & Starczak, V. R. (1994). Flume experiments on food supply to the blue mussel *Mytilus edulis* L. as a function of boundary-layerflow. *Limnology and oceanography*, 39(7), 1755-1768.
- Carmichael, R. H., Walton, W., & Clark, H. (2012). Bivalve-enhanced nitrogen removal from coastal estuaries. *Canadian journal of fisheries and aquatic sciences*, 69(7), 1131-1149.
- Chanson, H. (2004). *Environmental hydraulics for open channel flows*. Elsevier.
- Coen, L. D., & Luckenbach, M. W. (2000). Developing success criteria and goals for evaluating oyster reef restoration: ecological function or resource exploitation?. *Ecological engineering*, 15(3-4), 323-343.
- Coen, L. D., Brumbaugh, R. D., Bushek, D., Grizzle, R., Luckenbach, M. W., Posey, M. H., ... & Tolley, S. G. (2007). Ecosystem services related to oyster restoration. *Marine Ecology Progress Series*, 341, 303-307.
- Cornwell, J. C., J. M. Rose, M. L. Kellogg, M. Luckenbach, S. Bricker, K. Paynter, C. Moore, M. Parker, L. Sanford, W. Wolinski, A. Lacatell, L. Fegley, K. Hudson, J. Reichert-Nguyen, E. French, and W. Slacum. 2016. Panel Recommendations on the Oyster BMP Nutrient and Suspended Sediment Reduction Effectiveness Determination Decision Framework and Nitrogen and Phosphorus Assimilation in Oyster Tissue Reduction Effectiveness for Oyster Aquaculture Practices.
- Damas, D. (1935). Le role des organisms dans la formation des vascs marines. *Ann. Soc. Geol. Belg.* 58: 143-152.
- Dame, R. F., & Patten, B. C. (1981). Analysis of energy flows in an intertidal oyster reef. *Marine Ecology Progress Series*, 5(2), 115-124.
- Dame, R. F. (1999). Oyster reefs as components in estuarine nutrient cycling: Incidental or regulating. *Oyster reef habitat restoration: a synopsis and synthesis of approaches*. Edited by MW Luckenbach, R. Mann and JA Wesson. Virginia Institute of Marine Science Press, Gloucester Point, 267-280.

- Dame, R., & Libes, S. (1993). Oyster reefs and nutrient retention in tidal creeks. *Journal of Experimental Marine Biology and Ecology*, 171(2), 251-258.
- Dame, R. F., Zingmark, R. G., & Haskin, E. (1984). Oyster reefs as processors of estuarine materials. *Journal of Experimental Marine Biology and Ecology*, 83(3), 239-247.
- Dame, R. F., Spurrier, J. D., & Wolaver, T. G. (1989). Carbon, nitrogen and phosphorus processing by an oyster reef. *Marine Ecology Progress Series*, 249-256.
- Dame, R. F., Spurrier, J. D., & Zingmark, R. G. (1992). In situ metabolism of an oyster reef. *Journal of Experimental Marine Biology and Ecology*, 164(2), 147-159.
- Deslous-Paoli, J. M., Lannou, A. M., Geairon, P., Bougrier, S., Raillard, O., & Héral, M. (1992). Effects of the feeding behavior of *Crassostrea gigas* (Bivalve Molluscs) on biosedimentation of natural particulate matter. *Hydrobiologia*, 231(2), 85-91.
- Doering, P. H., Oviatt, C. A., & Kelly, J. R. (1986). The effects of the filter-feeding clam *Mercenaria mercenaria* on carbon cycling in experimental marine mesocosms. *Journal of Marine Research*, 44(4), 839-861.
- Ehrich, M. K., & Harris, L. A. (2015). A review of existing eastern oyster filtration rate models. *Ecological Modelling*, 297, 201-212.
- Forsyth, M. K. (2014). *Investigations of the effects of oyster allometry and reef morphology on filtration rate and particle capture using numerical models* (Doctoral dissertation, University of Maryland, College Park).
- Frechette, M., Butman, C. A., & Geyer, W. R. (1989). The importance of boundary-layer flows in supplying phytoplankton to the benthic suspension feeder, *Mytilus edulis* L. *Limnology and oceanography*, 34(1), 19-36.
- Gibbs, M., Funnell, G., Pickmere, S., Norkko, A., & Hewitt, J. (2005). Benthic nutrient fluxes along an estuarine gradient: Influence of the pinnid bivalve *Atrina zelandica* in summer. *Marine Ecology Progress Series*, 288, 151-164.
- Giles, H., & Pilditch, C. A. (2004). Effects of diet on sinking rates and erosion thresholds of mussel *Perna canaliculus* biodeposits. *Marine Ecology Progress Series*, 282, 205-219.
- Giles, H., & Pilditch, C. A. (2006). Effects of mussel (*Perna canaliculus*) biodeposit decomposition on benthic respiration and nutrient fluxes. *Marine Biology*, 150(2), 261-271.
- Gutiérrez, J. L., Jones, C. G., Strayer, D. L., & Iribarne, O. O. (2003). Mollusks as ecosystem engineers: the role of shell production in aquatic habitats. *Oikos*, 101(1), 79-90.
- Haven, D. S., & Morales-Alamo, R. (1966). Aspects of biodeposition by oysters and other invertebrate filter feeders 1. *Limnology and Oceanography*, 11(4), 487-498.

- Haven, D. S., & Morales-Alamo, R. (1970). Filtration of particles from suspension by the American oyster *Crassostrea virginica*. *The Biological Bulletin*, 139(2), 248-264.
- Higgins, C. B., Tobias, C., Piehler, M. F., Smyth, A. R., Dame, R. F., Stephenson, K., & Brown, B. L. (2013). Effect of aquacultured oyster biodeposition on sediment N<sub>2</sub> production in Chesapeake Bay. *Marine Ecology Progress Series*, 473, 7-27.
- Henriksen, K., & Kemp, W. M. (1988). Nitrogen cycling in coastal marine environments.
- Hoellein, T. J., & Zarnoch, C. B. (2014). Effect of eastern oysters (*Crassostrea virginica*) on sediment carbon and nitrogen dynamics in an urban estuary. *Ecological Applications*, 24(2), 271-286.
- Holyoke, R. R. (2008). *Biodeposition and biogeochemical processes in shallow, mesohaline sediments of Chesapeake Bay*. University of Maryland, College Park.
- Humphries, A. T., Ayvazian, S. G., Carey, J. C., Hancock, B. T., Grabbert, S., Cobb, D., ... & Fulweiler, R. W. (2016). Directly measured denitrification reveals oyster aquaculture and restored oyster reefs remove nitrogen at comparable high rates. *Frontiers in Marine Science*, 3, 74.
- Jansen, H. M., Verdegem, M. C. J., Strand, Ø., & Smaal, A. C. (2012). Seasonal variation in mineralization rates (CNP-Si) of mussel *Mytilus edulis* biodeposits. *Marine biology*, 159(7), 1567-1580.
- Jordan, S. J. (1987). *Sedimentation and remineralization associated with biodeposition by the American oyster Crassostrea virginica (Gmelin)* (Doctoral dissertation, University of Maryland, College Park).
- Kaspar, H. F., Asher, R. A., & Boyer, I. C. (1985). Microbial nitrogen transformations in sediments and inorganic nitrogen fluxes across the sediment/water interface on the South Island West Coast, New Zealand. *Estuarine, Coastal and Shelf Science*, 21(2), 245-255.
- Kautsky, N., & Evans, S. (1987). Role of biodeposition by *Mytilus edulis* in the circulation of matter and nutrients in a Baltic coastal ecosystem. *Marine Ecology Progress Series*, 201-212.
- Kellogg, M. L., Cornwell, J. C., Owens, M. S., & Paynter, K. T. (2013). Denitrification and nutrient assimilation on a restored oyster reef. *Marine Ecology Progress Series*, 480, 1-19.
- Kemp, W. M., Sampou, P., Caffrey, J., Mayer, M., Henriksen, K., & Boynton, W. R. (1990). Ammonium recycling versus denitrification in Chesapeake Bay sediments. *Limnology and Oceanography*, 35(7), 1545-1563.

Kemp, W. M., Boynton, W. R., Adolf, J. E., Boesch, D. F., Boicourt, W. C., Brush, G., ... & Stevenson, J. C. (2005). Eutrophication of Chesapeake Bay: historical trends and ecological interactions. *Marine ecology progress series*, 303, 1-29.

Kennedy, V. S., Newell, R. I., & Eble, A. F. (Eds.). (1996). *The eastern oyster: Crassostrea virginica*. University of Maryland Sea Grant College.

Kristensen, E. 1988. Benthic fauna and biogeochemical processes in marine sediments: microbial activities and fluxes, p. 207-249. In T. H. Blackburn and J. Sørensen [eds.], *Nitrogen Cycling in Coastal Marine Environments*. John Wiley & Sons.

Kundu, P., and I. Cohen (2008), *Fluid Mechanics*, Elsevier, San Diego, Calif.

Loosanoff, V. L., & Engle, J. B. (1947). Feeding of oysters in relation to density of microorganisms. *Science*, 105(2723), 260-261.

Lund, E. J. (1957). Self-silting by the oyster and its significance for sedimentation geology. *Publ Inst Mar Sci Univ Texas*, 4, 320-327.

Muschenheim, D. K., & Newell, C. R. (1992). Utilization of seston flux over a mussel bed. *Marine Ecology Progress Series*, 131-136.

Nelson, K. A., Leonard, L. A., Posey, M. H., Alphin, T. D., & Mallin, M. A. (2004). Using transplanted oyster (*Crassostrea virginica*) beds to improve water quality in small tidal creeks: a pilot study. *Journal of Experimental Marine Biology and Ecology*, 298(2), 347-368.

Newell, R. I. and Jordan, S.J. 1983. Preferential ingestion of organic material by the American oyster *Crassostrea virginica*. *Marine Ecology Progress Series*, 13(1), 47-53.

Newell, R. I. (1988). Ecological changes in Chesapeake Bay: are they the result of overharvesting the American oyster, *Crassostrea virginica*. *Understanding the estuary: advances in Chesapeake Bay research*, 129, 536-546.

Newell, R. I., Cornwell, J. C., & Owens, M. S. (2002). Influence of simulated bivalve biodeposition and microphytobenthos on sediment nitrogen dynamics: a laboratory study. *Limnology and Oceanography*, 47(5), 1367-1379.

Newell, R. I., & Koch, E. W. (2004). Modeling seagrass density and distribution in response to changes in turbidity stemming from bivalve filtration and seagrass sediment stabilization. *Estuaries*, 27(5), 793-806.

Newell, R. I. (2004). Ecosystem influences of natural and cultivated populations of suspension-feeding bivalve molluscs: a review. *Journal of Shellfish research*, 23(1), 51-62.

- Newell, R. I., Fisher, T. R., Holyoke, R. R., & Cornwell, J. C. (2005). Influence of eastern oysters on nitrogen and phosphorus regeneration in Chesapeake Bay, USA. In *The comparative roles of suspension-feeders in ecosystems* (pp. 93-120). Springer, Dordrecht.
- Owens, M. S. (2009). *Nitrogen cycling and controls on denitrification in mesohaline sediments of Chesapeake Bay*. University of Maryland, College Park.
- O'Riordan, C. A., Monismith, S. G., & Koseff, J. R. (1995). The effect of bivalve excurrent jet dynamics on mass transfer in a benthic boundary layer. *Limnology and Oceanography*, 40(2), 330-344.
- Petersen, J. K. and others 2014. Mussels as a tool for mitigation of nutrients in the marine environment. *Marine Pollution Bulletin* 82: 137-143.
- Riisgård, H. U. (1988). Efficiency of particle retention and filtration rate in 6 species of Northeast American bivalves. *Marine ecology progress series*. Oldendorf, 45(3), 217-223.
- Piehl, M. F., & Smyth, A. R. (2011). Habitat-specific distinctions in estuarine denitrification affect both ecosystem function and services. *Ecosphere*, 2(1), 1-17.
- Porter, E. T., Cornwell, J. C., & Sanford, L. P. (2004). Effect of oysters *Crassostrea virginica* and bottom shear velocity on benthic-pelagic coupling and estuarine water quality. *Marine Ecology Progress Series*, 271, 61-75.
- Rodney, W. S., & Paynter, K. T. (2006). Comparisons of macrofaunal assemblages on restored and non-restored oyster reefs in mesohaline regions of Chesapeake Bay in Maryland. *Journal of Experimental Marine Biology and Ecology*, 335(1), 39-51.
- Rothschild, B. J., Ault, J. S., Gouletquer, P., & Héral, M. (1994). Decline of the Chesapeake Bay oyster population: a century of habitat destruction and overfishing. *Marine Ecology Progress Series*, 29-39.
- Seitzinger, S. P. (1988). Denitrification in freshwater and coastal marine ecosystems: ecological and geochemical significance. *Limnology and oceanography*, 33(4part2), 702-724.
- Shao, Y., & Yang, Y. (2005). A scheme for drag partition over rough surfaces. *Atmospheric Environment*, 39(38), 7351-7361.
- Silvester, N. R., & Sleight, M. A. (1984). Hydrodynamic aspects of particle capture by *Mytilus*. *Journal of the Marine Biological Association of the United Kingdom*, 64(4), 859-879.
- Sundbäck, K., & Miles, A. (2002). Role of microphytobenthos and denitrification for nutrient turnover in embayments with floating macroalgal mats: a spring situation. *Aquatic Microbial Ecology*, 30(1), 91-101.
- Tenore, K. R., & Dunstan, W. M. (1973). Comparison of feeding and biodeposition of three bivalves at different food levels. *Marine Biology*, 21(3), 190-195.

Tenore, K. R., Cammen, L., Findlay, S. E.G., and Phillips, N. 1982. Perspectives in factors controlling detritus mineralization depending on detritus source. *Journal of Marine Research*, 40, 473-90.

Ward, J. E., Newell, R. I., Thompson, R. J., & MacDonald, B. A. (1994). In vivo studies of suspension-feeding processes in the eastern oyster, *Crassostrea virginica* (Gmelin). *The Biological Bulletin*, 186(2), 221-240.

Welsh, D. T., & Castadelli, G. (2004). Bacterial nitrification activity directly associated with isolated benthic marine animals. *Marine Biology*, 144(5), 1029-1037.

Widdows, J., Brinsley, M. D., Bowley, N., & Barrett, C. (1998). A benthic annular flume for in situ measurement of suspension feeding/biodeposition rates and erosion potential of intertidal cohesive sediments. *Estuarine, Coastal and Shelf Science*, 46(1), 27-38.

Wilberg, M. J., Livings, M. E., Barkman, J. S., Morris, B. T., & Robinson, J. M. (2011). Overfishing, disease, habitat loss, and potential extirpation of oysters in upper Chesapeake Bay. *Marine Ecology Progress Series*, 436, 131-144.

Wright, L. D., Gammisch, R. A., & Byrne, R. J. (1990). Hydraulic roughness and mobility of three oyster-bed artificial substrate materials. *Journal of Coastal Research*, 867-878.



